A Study on the Potential of *Stenotrophomonas koreensis* and *Bacillus rigiliprofundi* to Ameliorate the Toxicity of Industrial Dyes Malachite Green and Remazol Brilliant Blue R

A thesis submitted by

SHREYA BISWAS

for the degree of
Doctor of Philosophy (Science)

Department of Lifescience & Biotechnology
Faculty of Science
Jadavpur University
Kolkata 700032
India

2022

A Study on the Potential of *Stenotrophomonas koreensis* and *Bacillus rigiliprofundi* to Ameliorate the Toxicity of Industrial Dyes Malachite Green and Remazol Brilliant Blue R

Thesis submitted by

Shreya Biswas
(Registration no: 248/16/Life Sc./25)

for the degree of
Doctor of Philosophy
(Science)

Department of Lifescience & Biotechnology
Faculty of Science
Jadavpur University
Kolkata 700032
India

2022

CERTIFICATE FROM THE SUPERVISOR

This is to certify that the thesis entitled "A STUDY ON THE POTENTIAL OF *Stenotrophomonas koreensis* AND *Bacillus rigiliprofundi* TO AMELIORATE THE TOXICITY OF INDUSTRIAL DYES MALACHITE GREEN AND REMAZOL BRILLIANT BLUE R" Submitted by Smt....SHREYA BISWAS....who got her name registered on 8th DECEMBER, 2016 for the award of Ph. D. (Science) degree of Jadavpur University, is absolutely based upon her own work under the supervision of DR. PIYALI BASAK and that neither this thesis nor any part of it has been submitted for either any degree / diploma or any other academic award anywhere before.

(DR. PIYALI BASAK)
22.03.2022

DECLARATION

I hereby declare that all the work presented in the thesis titled "A STUDY ON THE POTENTIAL OF *Stenotrophomonas koreensis* AND *Bacillus rigiliprofundi* TO AMELIORATE THE TOXICITY OF INDUSTRIAL DYES MALACHITE GREEN AND REMAZOL BRILLIANT BLUE R" is my original work. I have cited all the resources that I have used for the purpose of this thesis.

Shreya Biswas

22.03.2022

(SHREYA BISWAS)

ACKNOWLEDGEMENTS

Dedicated to Ma and Baba

CONTENTS

Chapter 0

Aims and Objectives, Framework of the study & Abstract

AIMS AND OBJECTIVES

- Isolation and identification of the bacteria capable of decolorising industrial dyes

- Optimisation of the physical and chemical parameters for dye decolorisation

- Assessment of toxicity of the decolorised product

FRAMEWORK OF THE STUDY

Isolation, Selection and identification bacteria capable of dye decolorisation ■ Selection of strains based on their dye degradation ability : qualitative and quantitative ■ Subsequent identification of the selected strains by morphological, biochemical, cultural and 16S rDNA sequencing	Article published in Journal of the Indian Chemical Society, Elsevier
Studies on malachite green decolorisation by the strain Stenotrophomonas koreensis ■ Batch decolorisation experiments ■ Biodegradation analysis (Confirmation of degradation): (i) TLC [(a) butanol: acetic acid (4:1:2 v/v), (b) propanol, (c) n propanol: ethyl acetate: acetic acid: water (6:1:1:2 v/v)]; (ii) UV-Vis; (iii) HPLC; (iv) FTIR ■ Optimisation of operational parameters temperature, pH, inoculum concentration by Response Surface Methodology and effect of media components N and C for malachite green decolorisation ■ Investigation of potential of *Stenotrophomonas* to degrade dyes other than MG ■ Immobilisation of the bacterium: production, characterisation and use of the biobeads for decolorisation of malachite green ■ Decolorisation of MG by the bacterium in presence of different heavy metals ■ Kinetics of malachite green decolorisation by *S.koreensis* ■ Determination of the enzymes responsible for the decolorisation process ■ Assessment of toxicity of malachite green before and after degradation walking through the key levels of ecosystem: (i) Aquatic toxicity: (a) Algae growth inhibition test and chlorophyll production assay using *Anabaena flos-aque* , (b) *Daphnia* acute immobilisation test, (c) growth inhibition of aquatic plant using *Lemna minor* ; (d) toxicity using zebra fish *Danio rerio* (ii) Phytotoxicity using important crop plants : (a) wheat, (b) pulse ; (iii) Cytotoxicity using (a) human skin cells and (b)cancer cells (MTT assay and DAPI imaging); (iv) Toxicity studies on beneficial soil bacterium : (a) *B.subtilis*, (b) *B.pumilus*; (v) Earthworm (*Eisenia fetida*) acute toxicity test; (vi) Blood/serum biochemistry and histopathology using mice (*Mus musculus*); (vii) Genotoxicity using Allium cepa root tips	Book chapter published in the Utilisation and Management of Bioresources, Springer Article under review in the Bioremediation Journal, Taylor and Francis Article published in Plant Science Today, Horizon Publications Manuscript to be communicated
Studies on Remazol Brilliant Blue R decolorisation by the strain Bacillus rigiliprofundi ■ Remazol Brilliant Blue dye decolorisation by the selected bacterial strain ■ Characterisation of bacteria before and after dye adsorption ■ Adsorption kinetics: (i) pseudo-first order, (ii) Pseudo-second-order ■ Toxicity estimation of RBBR before and after bacterial treatment	Article published in the journal Microbiology, Springer

ABSTRACT

Malachite green is a textile dye that has long been used in aquaculture as an antiprotozoal and antifungal agent. It is basic in nature and its chloride and oxalate forms are readily soluble in water. The dye is mutagenic, carcinogenic, teratogenic, and impedes plant growth severely. *Stenotrophomonas koreensis* was isolated from a textile effluent and employed to biologically degrade the recalcitrant toxic dye malachite green. Chromatographic and Spectroscopic analysis confirmed the degradation of the dye. In the absence of any supplements or media, *S.koreensis* decolorized 98% malachite green in 4h. The highest degradation of up to 98.78 % was obtained at pH 6, temperature 45^0C and inoculum size 6.36 ml using RSM within one hour. 98.6% decolorization was achieved within 2.5 h of the addition of soymeal extract or peptone. The strain also decolorized the azo dye methyl orange up to 96%. *S.koreensis* was immobilized into reusable PVA-sodium alginate beads to facilitate easier handling, which showed 95.49% decolorization. One of the most promising features of this strain is that even in the presence of heavy metals, *S.koreensis* actively degraded the dye. *S.koreensis* biodegraded malachite green following the first-order reaction kinetics. The enzymes responsible for the malachite green degradation were tyrosinase, malachite green reductase, and NADH-DCIP reductase. Several and detailed ecotoxicological studies were performed in compliance with Organisation for Economic Co-operation and Development (OECD) guidelines to ensure that the products obtained after the bio-degradation were safe for release in the ecosystem. Aquatic toxicity was estimated by exposing photosynthetic cyanobacteria *Anabaena flos-aque*, small crustacean zooplankton *Daphnia magna*, floating aquatic macrophyte *Lemna minor* and zebrafish *Danio rerio* to the dye and the degradation product. Since malachite green can also potentially contaminate land through aquaculture run-offs, textile and tannery effluents; some important land organisms were also tested for toxicity. Beneficial soil bacteria *Bacillus subtilis* and *Bacillus pumilus*, earthworm *Eisenia fetida*, important crop plants *Triticum aestivum* and *Lens culinaris* and model vertebrate *Mus musculus* were also exposed to the dye and the degradation product to evaluate the reduction of toxicity after the bacterial dye degradation process. Genotoxicity of dye and degradation product was evaluated using root tip cells of *Allium cepa*. MTT assays of malachite green and its biodegraded product were conducted using Human cell lines HaCat and HepG2. Results indicated that the degradation product was significantly safer than malachite green. Remazol Brilliant Blue

R (RBBR), a common precursor of other dyes and a toxic organo-pollutant, is an extensively used anthraquinone dye in the textile industry. In this study, bioadsorption of RBBR by the bacterial strain *Bacillus rigiliprofundi* was investigated. The effects of various physical parameters on dye adsorption were studied. The kinetics and isotherm of adsorption were analysed. The bacterial adsorbent was characterized by Fourier Transform Infrared Spectroscopy (FTIR) and Scanning Electron Microscopy (SEM). Phytotoxicity and cytotoxicity was evaluated before and after the adsorptive removal of the dye. Upto 80% RBBR was adsorbed and removed by the bacteria in ten days. The optimum conditions for biosorption were pH 5.5, adsorbent dosage 30mg, initial dye concentration 25 mg/L and temperature 40ºC. The adsorption followed pseudo-first order kinetics and fitted appropriately to the Langmuir model. This is the first report on adsorptive decolorisation of the highly recalcitrant RBBR by the strain *Bacillus rigiliprofundi*.

Chapter 1
General Introduction and Review of Literature

GENERAL INTRODUCTION

Colors play a significant role in our everyday lives, and dyes have found their use from fabric to food since time immemorial. In ancient times, natural dyes were made from flowers, fruits, and lichens. From the latter half of the nineteenth century, toxic synthetic dyes started being manufactured since they generated huge revenues and were easier to manufacture [Nagendrappa, G., 2010]. In recent times, synthetic dyes cover most of all dyes and are relentlessly and unnecessarily used, from coloring fancy cakes to regular medicines. When dyes come in contact with the eyes or skin, they can cause serious injury. If ingested through food, and dyes can cause harm indirectly. Industries that use dyes, like textiles, tanneries, or printing presses, let out effluents loaded with untreated concentrated dyes. These toxic dyes initially affect aquatic life but eventually reach all other strata of the environment. Dyes are one of the major harmful components of effluents of several different industries [Lellis et al., 2019]. Leather, textile, printing, food processing are the most rigorous users of dyes [Slama et al., 2021] and also some of the greatest contributors of coloured effluents. Every passing day new dyes are synthesized and marketed for commercial use. Coloured wastewater when let out in waterbodies surrounding these industries causes exponential environmental deterioration [Sarayu and Sandhya 2012]. Since light penetration is obstructed by coloured discharges, it hinders the photosynthesis of aquatic plants [Pandey et al., 2017]. Dyes can broadly be divided into these classes according to KirkOthmer, (1984): Acid dyes, basic dyes, direct dyes, fluorescent dyes, reactive dyes, sulphurous dyes, vat dyes and dye-precursors. In recent times, dyes are more familiarly classified according to the Colour Index published by the *Society of Dyers and Colourists*. Not only are there different types of dyes, but the dying process itself varies, like exhaust dying, continuous dying, printing etc. [Clark, 2021]. Pollution caused by dyes is one of the most serious concerns in the present day scenario. Effluents containing dyes from industries, especially leather, textile and printing industries, when let out into the water bodies cause hindrance in photosynthesis of the aquatic flora, damaging the water ecosystem. Around 10% of the industrial dyes used, enters the ecosystem through these effluents [Zollinger, 1987] annually discharging over 50,000 tons of dye, consisting toxic substances, into the environment [Tan et al., 2018]. Throughout the last decade, the continuous rise in the use of reactive dyes has been witnessed, mainly due to the increased utilization of cellulose fibers in the textile

industry [Benkhaya et al., 2020]. Most of the dyes, currently used are synthetic xenobiotics, having conjugated molecules and doesn't get easily degraded [Unuofin et al., 2019]. For the removal of dyes, biosorption is an emerging approach [Elgarahy et al., 2021]. Effluents loaded with dyes can be efficiently treated with activated carbon, but activated carbon being considerably costly, is not a commercially feasible option [Kumar et al., 2016]. Some dyes even resist biodegradation by conventional activated sludge treatments [Ceretta et al., 2021]. A few techniques like chemical precipitation, electrocoagulation, elimination by adsorption etc. are currently in use. But these techniques are also mostly incapable of completely eliminating the toxic colorants. Instead, they just transform them from one form to another, which may again be toxic leading to requirement of further treatment [Amin et al., 2020]. Methods like flocculation, ozonation, photo-oxidation, froth floatation, ion exchange etc. are less efficient in terms of cost, quality, applicability and may produce wastes which are not environmentally safe to dispose [Rajasulochana and Preethy, 2016]. Sometimes, conjugated approaches are employed for obtaining better results in terms of quality and time [Ledakowicz and Paździor, 2021]. Biological treatment methods for elimination of dye, are advantageous over modern physical and chemical techniques in terms of efficiency, cost effectiveness, low-maintenance, etc. Biodecolorisation, or the biological removal of color or dye from wastewater, can be accomplished through one of the two processes: adsorption or degradation. This study attempts to curate, utilize, and provide some fundamental information regarding two such microorganism that can degrade or adsorb and overcome the toxicity of dyes in industrial effluents.

REVIEW OF LITERATURE

Of all the major life-forms that has been on the face of earth, mankind has been here for the shortest span of time, but the damage they have caused is incredible and outrageous. Almost everything that humans do, from sustenance to pleasure, from production of food crops to manufacturing air-conditioners or life-saving drugs, there is potential to cause pollution. Addition of colors can make the dull look bright, the old look new and the unattractive look attractive. Synthetic dyes which are mostly used to serve this purpose pose extreme levels of toxicity to the environment. The industries which use dye in their products, generate a huge amount of dye-loaded wastewater. Nearly 200,000 tons of dyes are let out into the environment through effluents annually as a result of low adsorption

of the dyes onto the dying materials due to inefficient dying techniques [Andrade-Guel et al., 2021]. Remediation of dye-pollution by bacteria has been thoroughly studied since the process is efficient and cost effective [Mohapatra et al., 2020; Desai et al., 2020; Chen et al., 2021]. Malachite green is a highly toxic and recalcitrant triphenylmethane dye used in a wide array of industries. Apart from its use as a traditional colorant of fabric, leather, and paper, it is used as an antifungal and antibacterial agent in aquaculture. Due to its easy availability and low cost, it is even applied to green vegetables to make them appear fresher. Malachite green can be attributed to numerous health hazards. Developmental abnormalities, mutations, and cancers result from prolonged exposure to the dye [Srivastava et al. 2004]. Numerous toxicological investigations of the dye have revealed that it can irritate test mammals' eyes and mucous membranes [Sudova et al., 2007]. It is also, a tested mutagen [Mittelstaedt et al., 2004]. However, several world agencies that work for pollution control have made it mandatory to remediate the dye-containing effluents before being released outside. Malachite green has a complex structure that allows it to withstand sunlight, biological activity, and various degradative environmental conditions, making it resistant to degradation. The dye's recalcitrant nature allows it to circumvent standard wastewater treatment techniques, allowing it to persist in the environment [Barapatre & Jha 2020].

It is widely acknowledged that biological remediation is a better alternative than chemical or physical treatments, mainly because of the secondary pollutants generated by the latter two. Decolorization of malachite green has been studied by many authors previously. Jasińska et al, (2012) decolorized 97.4% of the dye with *Myrothecium roridum* IM 6482 in 96 h. Du et al. (2011) reported 90-97% degradation of malachite green by *Pseudomonas sp.* strain DY1 in 24h. Laccase enzyme from the *Trichoderma asperellum* strain demonstrated excellent malachite green degradation (97.18%) in 98.58 minutes [Shanmugam et al., 2017]. A comprehensive compilation on previously reported strains degrading malachite green is presented in Table 1. *S.koreensis* till now had remained untapped for its potential to degrade malachite green. The bacterium was first reported from compost near Daejeon city in South Korea [Yang et al. 2006]. Another strain, *Stenotrophomonas maltophilia,* was isolated from soil contaminated with effluent from a wine industry. Extracellular laccase was produced by this strain and resulted in partial decolorization of certain dyes like methylene blue (53%), methyl green (71%), methyl orange (48%) in 48hr [Galai et al. 2009]. It is often seen that industries that use

dyes let out heavy metals through their effluents. Since chromium is used extensively in chrome-tanning leather and is required for collagen cross-linking, tannery effluents are high in hazardous hexavalent chromium. Apart from chromium, run-offs from leather-processing industries also contain other heavy metals like cadmium, cobalt, lead, arsenic, nickel, selenium, etc. [Lofrano et al. 2016]. Production of color pigments requires heavy metals like lead, chromium, cadmium, etc.[Halimoon & Yin 2010]. Hence effluents from textiles also contain significant concentrations of these heavy metals. Bacteria are vulnerable to heavy metals. Their presence in the medium inhibits bacterial growth. Earlier, heavy metals were used as antimicrobial agents [Hobman & Crossman 2015]. Studies have consistently shown that metals in general, including heavy metals, are highly effective against bacteria that form biofilms [Teitzel & Parsek 2003; Harrison et al. 2004]. Heavy metals are "oligodynamic" meaning, a small amount of heavy metal can show significant activity. In bacteria, heavy metals bind to enzyme proteins to kill them or suppress the functionality of the enzymes they produce. From these facts, it is clear that for microbial remediation of dyes from tannery and textile effluents, it should be an essential criterion for the microorganism to be tolerant to high concentrations of heavy metals.

Patil et al. (2012) reported *S.koreensis* to produce surfactants capable of abatement of heavy metals. In the present study, we check the dye-decolorizing ability of *S.koreensis* in the presence of various concentrations of these heavy metals. Several enzymes present in bacteriaand fungi are involved in the biodegradation of dyes. Lignolytic enzymes like laccase, manganese peroxidase, lignin peroxidase, etc., break the azo groups of azo dyes to yield compounds that contain a lesser number of benzene rings, for example, sodium naphthalene sulfonate and cycloheptadienylium [Asses et al., 2018]. In addition to the lignolytic enzymes, some enzymes are specific for triphenylmethane dye degradation, such as triphenylmethane reductase and malachite green reductase. The products formed this way are significantly lessertoxic than the original dye [Asses et al.,2018; Wanyonyi et al., 2017; Liu et al., 2020].

Nature has conceived a plethora of potent instruments in microorganisms that can be used for human welfare. Only degradation of any toxic dye does not fulfil the ecological requirement: a few studies suggest that the dye degradation products are more hazardous than the dyes themselves [Mishal and Gawai, 2018; Saini et al., 2018]. Toxicity

assessment of the end product obtained after any degradation process is crucial to validate the process's safety. The use of an array of bioassays with organisms from several ecological ranks allows for a more accurate assessment of the environmental impact of a toxic compound introduced into a given ecosystem.

Photosynthetic bacteria is believed to play the crucial role of oxygenation of the earth's atmosphere, when the earliest traces of life appeared and has since then formed the foundation of the aquatic ecosystem, which is the cyanobacteria [Sánchez-Baracaldo and Cardona, 2020]. The blue-green algae *Anabaena flos-aque* was chosen for our study. Zooplanktons feed on the aquatic algae and forms the connecting link for the transfer of energy between the primary photosynthetic producer organisms, ie, the algae and the larger vertebrates like fish [Sterner, 2009; Lomartire et al., 2021]. Higher photosynthetic macrophytes like duckweeds (*Lemna minor*) also play significant roles in the water ecosystem. Not only do they provide a habitat for the small amphibians, but also acts as a food source for certain aquatic birds and fish [Cao et al., 2018]. Malachite green has the ability to pollute not only water, but also land (industrial run-offs often contaminate adjoining land areas). Bacteria residing in the soil are responsible for nutrient recycling, and plays particularly important roles in the carbon, nitrogen, sulphur and phosphorous replenishment [Msimbira and Smith, 2020]. They are also involved in production of plant growth hormones [Prasad et al., 2021]. Earthworms (*Eisenia fetida*) lie above bacteria in soil ecosystem. Although they might appear insignificant and unattractive, earthworms have the potential to modify the physical and chemical properties of the soil, thereby influencing the life of other soil organisms [Bhadauria and Saxena, 2010]. Chemical modification of soil include better availability of essential nutrients like phosphorus and nitrogen to plants after being digested and excreted out into the soil by earthworms in the form of "earthworm cast". In terms of physical modification, earthworms dig up tightly packed soils to allow air circulation, which in turn leads to better interaction of oxygen with bacteria and promotes their growth [Lu et al., 2021]. Dyes are known to have negative impact on the germination of plants [Matpang et al., 2017; Rajashekar et al., 2021; Rahman et al., 2018]. There can be significant and direct occupational exposure of malachite green to persons working in textiles, tanneries or aquaculture farms [Okafoagu et al., 2017; Singh and Chadha, 2016]. Effluents from these industries may run off into rivers or even into the urban water- supplies thereby causing non-point-source pollution. Consumption of coloured green vegetables and fish treated

with malachite green for a prolonged period may also lead to direct exposure of the toxicant to human beings. Given the constantly expanding dye industries, determining the toxicity of textile dyes to the ecosystem is critical in determining the best course of action for future environmental safety concerns. The dye production industry has raised awareness about numerous environmental challenges, and products with the least environmental impact are being manufactured and promoted. The evaluation of the impacts of textile dyes on the ecosystem, on the other hand, will pique the users' interest in adopting an appropriate treatment technology.

Table 1.1 Comparison of malachite green decolorising ability of *Stenotrophomonas koreensis* with other strains in their corresponding chemically optimised media

Sl. No.	Microorganisms	Medium	Incubation time (h)	Initial Dye concentration (mg/L)	% Decolorisation	Reference
1.	*Kocuria rosea*	Nutrient Broth medium	5	50	100	Parshetti et al. (2006)
2.	*Klebsiella aerogenes S27*	Distilled water	8	100	100	Shang et al (2019)
3.	*Tenacibaculum sp. HMG1*	2216E liquid medium	12	20	98.8	Qu et al. (2018))
4.	*Myrothecium roridum IM 6482*	Czapek-Dox	96	10	97.4	Jasińska et al (2012)
5.	*Deinococcus radiodurans R1*	Tryptone Glucose Yeast	0.5	200	97.2	Lv G.Y. et al (2013)
6.	*Trichoderma asperellum (isolated laccase enzyme)*	Distilled water	1.643	122.66	97.18	Shanmugam et al. (2017)

7.	*Micrococcus sp. BD15*	1g/L urea and 0.9g/L yeast extract in distilled water	1	100	96.9	Du et al (2012)
8.	*Ochrobactrum sp JN214485*	Minimal Salt Medium	48	50	96.2	Vijayalakshmidevi et al. (2014)
9.	*Cyathus bulleri*	Maltose Mineral Salt Medium	48	30	96.2	Vasdev et al (1995)
10.	*Irpex lacteus F17* *(isolated manganese peroxidase enzyme)*	50 mM sodium malonate buffer	1	200	96	Yang et al. (2016)
11.	*Bacilllus cereus DC11*	M9 synthetic medium	4	19	96	Deng et al (2008)
12.	*Penicillium ochrochloron*	Czapek doxbroth	14	50	93	Shedbalakar et al (2011)
13.	*Exiguobacterium sp. MG2*	Water	2	2500	93	Wang et al. (2012)
14.	*Pseudomonas sp. YB2*	Synthetic medium consisting of NaCl 1.0 g, NH4Cl 1.0 g, KH2PO4 0.5 g,	24	1500	90.4	Tao et al. (2017)

		K2HPO4 1.5 g, MgSO4·7H2O 0.01 g, and C6H12O6 50 g				
15.	*Pseudomonas sp. strain DY1*	Luria Bertani medium	24	100-1000	90.3-97.2	Du et al (2011)
16.	*Pseudomonas sp. MDB1*	Mineral Salt Medium and 0.1% yeast extract	12	10	>90	Lin et al (2009)
17.	*Aeromonas hydrophila*	M9 synthetic medium containing 0.1% (w/v) yeast extract	10	50	>90	Ren et al (2006)
18.	*Brevibacillus laterosporus MTCC 2298*	Mineral Salt Medium	3	100	87	Gomare et al (2009)
19.	*Pandoraea pulmonicola YC32*	Distilled water	3.5	50	85.2	Chen et al (2009)
20.	*Saccharomyces cerevisiae MTCC 463*	Distilled water	7	100	85	Jadhav et al (2006)
21.	*Cunninghamella elegans*	Water	24	19.70	85	Cha et al (2001)

			(54 μM)		
22.	*Citrobacter sp*	Luria Bertani medium	1	36.49 (100 μM)	84	An et al. (2002)
23.	*Sphingomonas paucimobilis*	Mineral Salt Medium	4	50	82.49	Ayed et al (2009)
24.	*Cosmarium sp.*	Modified Bold's Basal medium	3.5	10	74	Daneshvar (2007)
25.	*Shewanella decolorationis NTOU1*	Phosphate-buffered basal medium (with 20mM formate and 20mM ferric citrate)	1	100	66.1	Chen et al (2010)
26.	*Aspergillus flavus*	Optimized Kirk's basalmedium	144	150	100	Barapatre et al. (2017)
27.	*Aspergillus flavus*	Potato Dextrose Broth	168	0.1g/100ml medium	83	Subramanian et al. (2014)
28.	*Streptomyces chrestomyceticus S20*	1% glucose and yeast extract	96	300	99	Vignesh et al. (2020)
29.	*Bacillus thuringiensis RUN1*	Nutrient broth	6	40	84.17	Olukanni et al. (2013)
30.	*Penicillium simplicissimum*	Nutrient Broth	336	100	54	Chen et al. (2015)

31.	*Staphylococcus epidermidis*	Mineral Salt Medium	12	700ppm	90	Ayed et al. (2010)
32.	*Fomes fomentarius*	Potato Dextrose Broth	168	100	30	Jayasinghe et al. (2008)
33.	*Lenzites elegans WDP2*	Glucose, acetic acid, micronutrients	24	50	96	Rai et al. (2007)
34.	*Sporotrichum pulverulentumvarsha*	1% Glucose	24	50	99	Vaidya et al. (2008)
35.	*Pseudomonasveronii JW3-6*	Water	168	50	93.5	Song et al. (2010)
36.	*Stenotrophomonas maltophila*	Mineral Salt Broth	28	100	97	Alaya et al. (2021)
37.	***Stentotrophomonas koreensis***	**Water**	**4**	**100**	**98**	**The present study**
		1g/L soymeal extract or peptone	**2.5**	**100**	**98.05**	

Remazol Brilliant Blue R is a highly recalcitrant and toxic dye extensively used as a synthetic colorant in textile and tanneries. Although biological remediation of RBBR is more favorable than non-biological (physical or chemical) processes in terms of production cost, maintenance and ecological sustainability, reports of bacteria-mediated removal of RBBR are rare. Most of the studies regarding the removal of RBBR report the use of specially functionalized materials whose production involves complex processing

steps. Additional processing often leads to elevated production costs (Saputra et al., 2017). Only a few RBBR degrading strains of fungi have been reported to date, which may be due to the highly recalcitrant nature of the dye. A comparison of maximum monolayer adsorption capacities of RBBR dye on various adsorbents is presented in Table 1.2.

Table 1.2 Comparison of *B. rigiliprofundi* as an adsorbent with other previously reported matrices and organisms

Adsorbent	Maximum monolayer adsorption capacity q_m (mgg^{-1})	Reference
Amino-functionalised organosilane	21.3	Saputra et al., 2017
Cross-linked chitosan-glyoxal/kaolin clay composite	447.1	Jawad et al., 2021
Polyaniline/chitosan	303.03	Mahanta et al., 2009
Diethyl triamine functionalized magnetic macro-reticular hybrid material	0.153 mmol g^{-1}	Elwakeel et al., 2016
Polyaniline doped p-Toluene sulfonic acid	28.27	Janaki et al., 2012
Fly ash	135.70	Kara et al., 2007
Polyaniline camphor sulfonic acid	42.00	Janaki et al., 2012
Borax cross-linked Jhingan gum hydrogel	9.884	Mate & Mishra, 2020
Magnetic chitosan-glutaraldehyde/zinc oxide/Fe3O4 nanocomposite	176.6	Reghioua et al., 2021
Macroporous polystyrene resin	208.33	Ozturk & Silah, 2020
Pinang frond based activated carbon	43.8	Ahmad et al., 2014
Periwinkle shell activated carbon	312.64	Bello & Ahmad, 2011
Pomegranate Peel Activated Carbon	370.86	Ahmad et al.,2014
Water hyacinth root powder	83.33	Kulkarni et al., 2018
Trichoderma koningiopsis	0.951	Syafiuddin & Fulazzaky, 2021
Yeast	127.6	Barreda-Reyes et al., 2015
Scenedesmus quadricauda	45.7	Ergene et al., 2009
Bacillus rigiliprofundi	**57.803**	**The present study**

REFERENCES

Ahmad MA, Puad NA, Bello OS. Kinetic, equilibrium and thermodynamic studies of syntheticdye removal using pomegranate peel activated carbon prepared by microwave-induced KOH activation. Water Resour. Ind. 2014; vol.6: pp18-35.

Ahmad, M. A., Herawan, S. G., & Yusof, A. A. Equilibrium, kinetics, and thermodynamics of Remazol Brilliant Blue R dye adsorption onto activated carbon prepared from pinang frond.2014. International Scholarly Research Notices

Alaya, V., Kodi, R. K., Ninganna, E., Gowda, B., & Shivanna, M. B. (2021). Decolorization of Malachite green dye by Stenotrophomonas maltophilia a compost bacterium. *Bulletin of theNational Research Centre*, *45*(1), 1-13.

Amin, S., Rastogi, R.P., Chaubey, M.G., Jain, K., Divecha, J., Desai, C. and Madamwar, D., 2020. Degradation and toxicity analysis of a reactive textile diazo dye-Direct Red 81 by newly isolated Bacillus sp. DMS2. *Frontiers in microbiology*, *11*, p.2280.
An, S. Y., Min, S. K., Cha, I. H., Choi, Y. L., Cho, Y. S., Kim, C. H., & Lee, Y. C. (2002).

and leucomalachite green in female Big Blue B6C3F1 mice. Mutat Res Genet Toxicol EnvironMutagen. 561:127-138

Andrade-Guel, M., Ávila-Orta, C.A., Cabello-Alvarado, C., Cadenas-Pliego, G., Esparza- González, S.C., Pérez-Alvarez, M. and Quiñones-Jurado, Z.V., 2021. Non-Woven Fabrics Based on Nanocomposite Nylon 6/ZnO Obtained by Ultrasound-Assisted Extrusion for Improved Antimicrobial and Adsorption Methylene Blue Dye Properties. *Polymers*, *13*(11), p.1888.

Asses, N., Ayed, L., Hkiri, N., & Hamdi, M. (2018). Congo red decolorization and detoxification by Aspergillus niger: removal mechanisms and dye degradation pathway. *BioMed research international*, *2018*.

Ayed, L., Chaieb, K., Cheref, A., & Bakhrouf, A. (2009). Biodegradation of

triphenylmethanedye Malachite Green by Sphingomonas paucimobilis. *World Journal of Microbiology and Biotechnology*, *25*(4), 705-711.

Ayed, L., Chaieb, K., Cheref, A., & Bakhrouf, A. (2010). Biodegradation and decolorization of triphenylmethane dyes by Staphylococcus epidermidis. *Desalination*, *260*(1-3), 137-146.

Barapatre, A., Aadil, K. R., & Jha, H. (2017). Biodegradation of malachite green by the ligninolytic fungus Aspergillus flavus. *CLEAN–Soil, Air, Water*, *45*(4), 1600045.

Barapatre, Anand & Jha, Harit. (2020). Microbial Degradation of Malachite Green In book: MALACHITE GREEN PROPERTIES AND USES Publisher: Nova Science

Publishers, Inc. pp.113-153

Barreda-Reyes, K. L., Ortega-López, J., Ortega-Regules, A. E., Santiago-Santiago, L. A., & Netzahuatl-Muñoz, A. R. Removal of remazol brilliant blue R dye from aqueous solutions using yeast biomass as biosorbent. Rev. cuba. quím. (En línea), 2015. vol. 27(2)

Bello OS, Ahmad MA. Response surface modeling and optimization of remazol brilliant blue reactive dye removal using periwinkle shell-based activated carbon. Sep. Sci. Technol.. 2011;vol. 46(15): pp.2367-79.

Benkhaya, S., M'rabet, S. and El Harfi, A., 2020. A review on classifications, recent synthesis and applications of textile dyes. Inorganic Chemistry Communications, 115, p.107891.

Bhadauria, T. and Saxena, K.G., 2010. Role of earthworms in soil fertility maintenance through the production of biogenic structures. *Applied and environmental soil science*, *2010*.

Biological decolorization of dye solution containing malachite green by Pandoraea pulmonicola YC32 using a batch and continuous system. *Journal of Hazardous Materials*, *172*(2-3), 1439-1445.

Cao, H.X., Fourounjian, P. and Wang, W., 2018. The importance and potential of duckweeds as a model and crop plant for biomass-based applications and beyond. *Handbook of environmental materials management. Springer International Publishing, Cham*, pp.1-16.

Ceretta, M.B., Nercessian, D. and Wolski, E.A., 2021. Current Trends on Role of Biological Treatment in Integrated Treatment Technologies of Textile Wastewater. *Frontiers in Microbiology*, *12*, p.518.

Cha, C. J., Doerge, D. R., & Cerniglia, C. E. (2001). Biotransformation of malachite green by the fungus Cunninghamella elegans. *Applied and environmental microbiology*, *67*(9), 4358- 4360.

Chen, C. H., Chang, C. F., & Liu, S. M. (2010). Partial degradation mechanisms of malachite green and methyl violet B by Shewanella decolorationis NTOU1 under anaerobic conditions. *Journal of Hazardous Materials*, *177*(1-3), 281-289.

Chen, C. Y., Kuo, J. T., Cheng, C. Y., Huang, Y. T., Ho, I. H., & Chung, Y. C. (2009).

Chen, G., An, X., Li, H., Lai, F., Yuan, E., Xia, X. and Zhang, Q., 2021. Detoxification of azo dye Direct Black G by thermophilic Anoxybacillus sp. PDR2 and its application potential in bioremediation. Ecotoxicology and Environmental Safety, 214, p.112084.

Chen, S. H., & Ting, A. S. Y. (2015). Biosorption and biodegradation potential of triphenylmethane dyes by newly discovered Penicillium simplicissimum isolated from indoor wastewater sample. *International Biodeterioration & Biodegradation*, *103*, 1-7.

Clark, M. ed., 2011. Handbook of textile and industrial dyeing: principles, processes and types of dyes. Elsevier., pp. 3-23.

Daneshvar, N., Ayazloo, M., Khataee, A. R., & Pourhassan, M. (2007). Biological decolorization of dye solution containing Malachite Green by microalgae Cosmarium sp. *Bioresource technology*, *98*(6), 1176-1182.

Decolorization of triphenylmethane and azo dyes by Citrobacter sp. *Biotechnology letters*, *24*(12), 1037-1040.

Deng, D., Guo, J., Zeng, G., & Sun, G. (2008). Decolorization of anthraquinone, triphenylmethane and azo dyes by a new isolated Bacillus cereus strain DC11. *International Biodeterioration & Biodegradation*, *62*(3), 263-269.

Desai, C., Jain, K.R., Boopathy, R., van Hullebusch, E.D. and Madamwar, D., 2021. Eco- Sustainable Bioremediation of Textile Dye Wastewaters: Innovative Microbial Treatment Technologies and Mechanistic Insights of Textile Dye Biodegradation. Frontiers in Microbiology, 12.

Du L N, Wang S, Li G, Wang B, Jia X M, Zhao, Y H, Chen Y L (2011). Biodegradation of malachite green by *Pseudomonas sp.* strain DY1 under aerobic condition: characteristics, degradation products, enzyme analysis and phytotoxicity. Ecotoxicology 20:438-446

Du L N, Wang S, Li G, Wang B, Jia X M, Zhao, Y H, Chen Y L (2011). Biodegradation of malachite green by *Pseudomonas sp.* strain DY1 under aerobic condition: characteristics, degradation products, enzyme analysis and phytotoxicity. Ecotoxicology 20:438-446

Du, L. N., Zhao, M., Li, G., Zhao, X. P., & Zhao, Y. H. (2012). Highly efficient decolorization of malachite green by a novel *Micrococcus sp.* strain BD15. Environ Sci Pollut R., 19(7):2898-2907

Elgarahy, A.M., Elwakeel, K.Z., Mohammad, S.H. and Elshoubaky, G.A., 2021. A critical review of biosorption of dyes, heavy metals and metalloids from wastewater as an efficient and green process. *Cleaner Engineering and Technology*, p.100209.

Elwakeel, K. Z., El-Bindary, A. A., Ismail, A., & Morshidy, A. M. Sorptive removal of Remazol Brilliant Blue R from aqueous solution by diethylenetriamine functionalized magnetic macro-reticular hybrid material. Rsc Advances, 2016 vol. 6(27), pp.22395-22410

Ergene, A., Ada, K., Tan, S., & Katırcıoğlu, H.. Removal of Remazol Brilliant Blue R dye from aqueous solutions by adsorption onto immobilized Scenedesmus quadricauda: Equilibrium and kinetic modeling studies. Desalination, 2009 vol. 249(3), pp.1308-1314.

Galai, S., Touhami, Y., & Marzouki, M. N. (2012). Response surface methodology applied to laccases activities exhibited by Stenotrophomonas maltophilia AAP56 in different growth conditions. *BioResources*, *7*(1), 0706-0726.

Gomare, S. S., Parshetti, G. K., & Govindwar, S. P. (2009). Biodegradation of malachite green by Brevibacillus laterosporus MTCC 2298. *Water environment research*, *81*(11), 2329-2336. Halimoon, N., & Yin, R. G. S. (2010). Removal of heavy metals from textile wastewater using zeolite. *Environment Asia*, *3*(2010):124-130

Grayson, M., Kirk, R.E. and Othmer, D.F., 1984. Kirk-Othmer encyclopedia of chemical technology. J. Wiley.

Harrison, J. J., Ceri, H., Stremick, C. A., & Turner, R. J. (2004). Biofilm susceptibility to metal toxicity. Environ. Microbiol. , 6(12): 1220-1227

Hobman, J. L., & Crossman, L. C. (2015). Bacterial antimicrobial metal ion resistance. J. Med. Microbiol., 64(5):471-497

Jadhav, J. P., & Govindwar, S. P. (2006). Biotransformation of malachite green by Saccharomyces cerevisiae MTCC 463. *Yeast*, *23*(4), 315-323.

Janaki V, Oh BT, Shanthi K, Lee KJ, Ramasamy AK, Kamala-Kannan S. Polyaniline/chitosan composite: an eco-friendly polymer for enhanced removal of dyes from aqueous solution. Synth. Met.. 2012; vol. 162(11-12):pp.974-80.

Jasińska A, Różalska S, Bernat P, Paraszkiewicz K, Długoński J (2012). Malachite green decolorization by non-basidiomycete filamentous fungi of *Penicillium pinophilum* and *Myrothecium roridum*. Int Biodeter Biodegr. 73:33-40

Jawad, A. H., Abdulhameed, A. S., Kashi, E., Yaseen, Z. M., ALOthman, Z. A., & Khan,

M. R.. Cross-linked chitosan-glyoxal/kaolin clay composite: Parametric optimization for color removal and COD reduction of remazol brilliant blue R dye. J Polym Environ., 2021 vol. 1-15 Jayasinghe, C., Imtiaj, A., Lee, G. W., Im, K. H., Hur, H., Lee, M. W., ... & Lee, T. S. (2008). Degradation of three aromatic dyes by white rot fungi and the production of ligninolytic enzymes. *Mycobiology*, *36*(2), 114-120.

Kara S, Aydiner C, Demirbas E, Kobya M, Dizge N. Modeling the effects of adsorbent dose and particle size on the adsorption of reactive textile dyes by fly ash. Desalination. 2007; vol. 212(1-3):pp.282-93.

Kulkarni, M. R., Bhagyalakshmi, C., Anand, D., & Herle, R. N. Removal of remazol brilliant blue dye from aqueous solutions using water hyacinth root powder. Desalination WaterTreat., 2018. Vol. 122, pp. 331-338

Kumar, K.V., Ramamurthi, V. and Sivanesan, S., 2016. *Biosorption of malachite green, a cationic dye onto Pithophora sp., a fresh water algae.* Dyes and Pigments, 69(1), pp.102-107.

Ledakowicz, S. and Paździor, K., 2021. Recent achievements in dyes removal focused on advanced oxidation processes integrated with biological methods. *Molecules*, *26*(4), p.870.
Lellis, B., Fávaro-Polonio, C.Z., Pamphile, J.A. and Polonio, J.C., 2019. Effects of textile dyes on health and the environment and bioremediation potential of living organisms. *Biotechnology Research and Innovation*, *3*(2), pp.275-290.

Li, L. T., Hong, Q., Yan, X., Fang, G. H., Ali, S. W., & Li, S. P. (2009). Isolation of a malachite green-degrading Pseudomonas sp. MDB-1 strain and cloning of the tmr2 gene. *Biodegradation*, *20*(6), 769-776.

Lofrano, G., Carotenuto, M., Libralato, G., Domingos, R. F., Markus, A., Dini, L., Gautam RK et al. (2016). Polymer functionalized nanocomposites for metals removal from water and wastewater: an overview. Water Res., 92: 22-37

Lomartire, S., Marques, J.C. and Gonçalves, A.M., 2021. The key role of zooplankton in

ecosystem services: A perspective of interaction between zooplankton and fish recruitment. *Ecological Indicators*, *129*, p.107867.

Lu, Y., Gao, P., Wang, Y., Li, W., Cui, X., Zhou, J., Peng, F. and Dai, L., 2021. Earthworm activity optimized the rhizosphere bacterial community structure and further alleviated the yield loss in continuous cropping lily (Lilium lancifolium Thunb.). *Scientific reports*, *11*(1), pp.1-14.

Lv, G. Y., Cheng, J. H., Chen, X. Y., Zhang, Z. F., & Fan, L. F. (2013). Biological decolorization of malachite green by *Deinococcus radiodurans* R1. Bioresour. Technol, 144:275-280

Mahanta D, Madras G, Radhakrishnan S, Patil S. Adsorption and desorption kinetics of anionicdyes on doped polyaniline. J. Phys. Chem. B. 2009. vol. 113(8):pp. 2293-9.

Mate, C. J., & Mishra, S. Synthesis of borax cross-linked Jhingan gum hydrogel for remediation of Remazol Brilliant Blue R (RBBR) dye from water: adsorption isotherm, kinetic,thermodynamic and biodegradation studies. Int. J. Biol. Macromol, 2020 vol.151, pp.677-690Matpang, P., Sriuttha, M. and Piwpuan, N., 2017. Effects of malachite green on growth and tissue accumulation in pak choy (Brassica chinensis Tsen & Lee). *Agriculture and Natural Resources*, *51*(2), pp.96-102.

Misal, S. A., & Gawai, K. R. (2018). Azoreductase: a key player of xenobiotic metabolism. *Bioresources and Bioprocessing*, *5*(1), 1-9.

Mittal, A., Gupta, V.K., Malviya, A. and Mittal, J., 2008. *Process development for the batch and bulk removal and recovery of a hazardous, water-soluble azo dye (Metanil Yellow) by adsorption over waste materials (Bottom Ash and De-Oiled Soya)*. Journal of Hazardous Materials, 151(2), pp.821-832.

Mittelstaedt RA, Mei N, Webb PJ, Shaddock JG, Dobrovolsky VN, McGarrity LJ, Morris S M, Chen T, Beland FA, Greenlees KJ, Heflich RH (2004). Genotoxicity of malachite green

Mohapatra, R.K., Behera, S.S., Patra, J.K., Thatoi, H. and Parhi, P.K., 2020. Potential

application of bacterial biofilm for bioremediation of toxic heavy metals and dye-contaminated environments. In New and Future Developments in Microbial Biotechnology and Bioengineering: Microbial Biofilms (pp. 267-281). Elsevier.

Msimbira, L.A. and Smith, D.L., 2020. The roles of plant growth promoting microbes in enhancing plant tolerance to acidity and alkalinity stresses. *Frontiers in Sustainable Food Systems*, *4*, p.106.

Nagendrappa, G., 2010. Sir William Henry Perkin: the man and his 'mauve'. *Resonance*, *15*(9), pp.779-793.

Okafoagu, N.C., Oche, M., Awosan, K.J., Abdulmulmuni, H.B., Gana, G.J., Ango, J.T. and Raji, I., 2017. Determinants of knowledge and safety practices of occupational hazards of textile dye workers in Sokoto, Nigeria: a descriptive analytic study. *Journal of public health inAfrica*, *8*(1).

Olukanni, O. D., Adenopo, A., Awotula, A. O., & Osuntoki, A. A. (2013). Biodegradation of malachite green by extracellular laccase producing Bacillus thuringiensis RUN1. *Journal of Basic & Applied Sciences*, *9*, 543.

Ozturk, G., & Silah, H. Adsorptive Removal of Remazol Brilliant Blue R from water by using a macroporous polystyrene resin: isotherm and kinetic studies. Environ. Process, 2020. Vol.7 (2), pp.479-492

Pandey, A., Singh, P. and Iyengar, L., 2007. Bacterial decolorization and degradation of azo dyes. International Biodeterioration & Biodegradation, 59(2), pp.73-84.

Parshetti G, Kalme S, Saratale G, Govindwar S. (2006). Biodegradation of Malachite Green by Kocuria rosea MTCC 1532. Acta Chim. Slov. 53:492-498 http://acta-arhiv.chem-soc.si/53/53-

Patil, S. N., Aglave, B. A., Pethkar, A. V., & Gaikwad, V. B. (2012). Stenotrophomonas koreensis a novel biosurfactant producer for abatement of heavy metals from the environment. Afr. J. Microbiol. Res., 6(24), 5173-5178

Prasad, S., Malav, L.C., Choudhary, J., Kannojiya, S., Kundu, M., Kumar, S. and Yadav, A.N., 2021. Soil microbiomes for healthy nutrient recycling. In *Current Trends in Microbial Biotechnology for Sustainable Agriculture* (pp. 1-21). Springer, Singapore.

Qu, W., Hong, G., & Zhao, J. (2018). Degradation of malachite green dye by Tenacibaculum sp. HMG1 isolated from Pacific deep-sea sediments. *Acta Oceanologica Sinica*, *37*(6), 104- 111.

Rahman, M.A., Rayhan, M.Y.H., Chowdhury, M.A.H., Mohiuddin, K.M. and Chowdhury, M.A.K., 2018. Phytotoxic effect of synthetic dye effluents on seed germination and early growth of red amaranth. *Fundamental and Applied Agriculture*, *3*(2), pp.480-490.

Rai, H. S., Singh, S., Cheema, P. P. S., Bansal, T. K., & Banerjee, U. C. (2007). Decolorization of triphenylmethane dye-bath effluent in an integrated two-stage anaerobic reactor. *Journal ofenvironmental management*, *83*(3), 290-297.

Rajashekar, K.K., Mahadevan, G.D., Neelagund, S.E., Sathynarayana, M., Vijaya, D. and Mulla, S.I., Decolorization of amaranth RI and fast red E azo dyes by thermophilic Geobacillus thermoleovorans KNG 112. *Journal of Chemical Technology & Biotechnology*.

Rajasulochana, P. and Preethy, V., 2016. Comparison on efficiency of various techniques in treatment of waste and sewage water–A comprehensive review. *Resource-Efficient Technologies*, *2*(4), pp.175-184.

Reghioua, A., Barkat, D., Jawad, A. H., Abdulhameed, A. S., Rangabhashiyam, S., Khan, M. R., & ALOthman, Z. A. Magnetic Chitosan-Glutaraldehyde/Zinc Oxide/Fe 3 O 4Nanocomposite: Optimization and Adsorptive Mechanism of Remazol Brilliant Blue R Dye Removal. J. Polym. Environ, 2021. pp. 1-16

Ren, S., Guo, J., Zeng, G., & Sun, G. (2006). Decolorization of triphenylmethane, azo, and anthraquinone dyes by a newly isolated Aeromonas hydrophila strain. *Applied microbiology and biotechnology*, *72*(6), 1316-1321.

Saini, A., Doda, A., & Singh, B. (2018). Recent advances in microbial remediation of textile Azo dyes. *Phytobiont and Ecosystem Restitution*, 45-62.

Sánchez, M. B. (2015). Antibiotic resistance in the opportunistic pathogen Stenotrophomonasmaltophilia. *Frontiers in microbiology*, *6*, 658.

Sánchez-Baracaldo, P. and Cardona, T., 2020. On the origin of oxygenic photosynthesis and Cyanobacteria. *New Phytologist*, *225*(4), pp.1440-1446.

Saputra, O. A., Rachma, A. H., & Handayani, D. S. Adsorption of remazol brilliant blue R using amino-functionalized organosilane in aqueous solution. Indones. J. Chem, 2017 vol. 17(3), pp.343-350

Sarayu, K. and Sandhya, S., 2012. Current technologies for biological treatment of textile wastewater–a review. *Applied biochemistry and biotechnology*, *167*(3), pp.645-661.

Shang, N., Ding, M., Dai, M., Si, H., Li, S., & Zhao, G. (2019). Biodegradation of malachite green by an endophytic bacterium Klebsiella aerogenes S27 involving a novel oxidoreductase. *Applied microbiology and biotechnology*, *103*(5), 2141-2153.

Shanmugam S, Ulaganathan P, Swaminathan K, Sadhasivam S, Wu Y. R. (2017). Enhanced biodegradation and detoxification of malachite green by *Trichoderma asperellum* laccase: degradation pathway and product analysis. Int Biodeter Biodegr.125: 258-268

Shedbalkar, U., & Jadhav, J. P. (2011). Detoxification of malachite green and textile industrial effluent by Penicillium ochrochloron. *Biotechnology and Bioprocess Engineering*, *16*(1), 196. Singh, Z. and Chadha, P., 2016. Textile industry and occupational cancer. *Journal of Occupational Medicine and Toxicology*, *11*(1), pp.1-6.

Slama, H.B., Chenari Bouket, A., Pourhassan, Z., Alenezi, F.N., Silini, A., Cherif-Silini, H., Oszako, T., Luptakova, L., Golińska, P. and Belbahri, L., 2021. Diversity of Synthetic Dyes from Textile Industries, Discharge Impacts and Treatment Methods. *Applied Sciences*, *11*(14), p.6255.

Song, J., Han, G., Wang, Y., Jiang, X., Zhao, D., Li, M., ... & Mu, Y. (2020). Pathway and kinetics of malachite green biodegradation by Pseudomonas veronii. *Scientific reports*, *10*(1),1-11.

Srivastava S, Sinha R, Roy D (2004). Toxicological effects of malachite green. Aquat. Toxicol.66:319-329

Sterner, R.W., 2009. Role of zooplankton in aquatic ecosystems. In *Encyclopedia of inland waters* (pp. 678-688). Elsevier Inc..

Subramanian, T., Ramesh, T., & Kalaiselvam, M. (2014). Degradation of triphenylmethane dye: Malachite green by Aspergillus flavus. *World. J. Pham. Sci*, *3*, 44-50.

Sudova E, Machova J, Svobodova Z, Vesely T (2007). Negative effects of malachite green and possibilities of its replacement in the treatment of fish eggs and fish: a review. Vet Med (Praha)52:527

Syafiuddin, A., & Fulazzaky, M. A. Decolorization kinetics and mass transfer mechanisms of Remazol Brilliant Blue R dye mediated by different fungi. Biotechnol. Rep. 2021. vol. 29, e00573

Tan, I.A.W., Ahmad, A.L. and Hameed, B.H., 2008. Adsorption of basic dye on high-surface-area activated carbon prepared from coconut husk: Equilibrium, kinetic and thermodynamic studies. Journal of hazardous materials, 154(1-3), pp.337-346.

Tao, Y., Wang, F., Meng, L., Guo, Y., Han, M., Li, J., ... & Wang, S. (2017). Biological decolorization and degradation of malachite green by Pseudomonas sp. YB2: process optimization and biodegradation pathway. *Current microbiology*, *74*(10), 1210-1215.

Teitzel, G. M., & Parsek, M. R. (2003). Heavy metal resistance of biofilm and planktonic Pseudomonas aeruginosa. Appl. Environ. Microbiol. , 69(4):2313-2320

Unuofin, J.O., Okoh, A.I. and Nwodo, U.U., 2019. Aptitude of oxidative enzymes for treatment of wastewater pollutants: a laccase perspective. *Molecules*, *24*(11), p.2064.

Vaidya, K., & KONDE, P. U. (2008). Decolorization of malachite green by *Sporotrichum pulverulentumvarsha*. *J Ind Pollut Control*, *24*, 133-137.

Vasdev, K., Kuhad, R. C., & Saxena, R. K. (1995). Decolorization of triphenylmethane dyes by the bird's nest fungus Cyathus bulleri. *Current Microbiology*, *30*(5), 269-272.

Vignesh, A., Manigundan, K., Santhoshkumar, J., Shanmugasundaram, T., Gopikrishnan, V., Radhakrishnan, M., ... & Balagurunathan, R. (2020). Microbial degradation, spectral analysis and toxicological assessment of malachite green by Streptomyces   chrestomyceticus S20. *Bioprocess and biosystems engineering*, *43*(8), 1457-1468.

Vijayalakshmidevi, S. R., & Muthukumar, K. (2014). Biodegradation of malachite green by Ochrobactrum sp. *World Journal of Microbiology and Biotechnology*, *30*(2), 429-437.

Wang, J. A., Gao, F., Liu, Z., Qiao, M., Niu, X., Zhang, K. Q., & Huang, X. (2012). Pathway and molecular mechanisms for malachite green biodegradation in Exiguobacterium sp. MG2. *PLoS One*, *7*(12), e51808.

Wanyonyi, W. C., Onyari, J. M., Shiundu, P. M., & Mulaa, F. J. (2017). Biodegradation and detoxification of malachite green dye using novel enzymes from bacillus cereus strain KM201428: kinetic and metabolite analysis. *Energy Procedia*, *119*, 38-51.

Yang HC, Im WT, Kang MS, Shin DY, Lee ST (2006) *Stenotrophomonas koreensis* sp. nov., isolated from compost in South Korea. Int. J. Syst. Evol. 56:81-84

Yang, X., Zheng, J., Lu, Y., & Jia, R. (2016). Degradation and detoxification of the triphenylmethane dye malachite green catalyzed by crude manganese peroxidase from Irpex lacteus F17. *Environmental Science and Pollution Research*, *23*(10), 9585-9597.

Zollinger H. 1987 Colour chemistry-syntheses, properties and application of organic dyes and pigments. New York: VCH Publishers.

Chapter 2

Isolation, Selection and Identification of the Dye-decolorising Bacterial Strains

INTRODUCTION

Color is the first visible contaminant in the effluents of any industry that uses dye in its products. The presence of harmful organopollutants in the effluent causes the color in the majority of cases. Removal of dyes from industrial wastewater is essential to stop the toxic organopollutants from contaminating water sources as they adversely affect aquatic life and human health. Leather, textile, printing and food processing are the most rigorous users of dyes and also belongs to the list of the greatest contributors of coloured effluents (Biswas et al., 2019; Ardila-Leal et al. 2021). Most of the dyes have complex molecular structures and synthetic origins which give them high stability and thus become difficult to remove and are recalcitrant xenobiotics (Brunel and Dumur, 2020; Mohammed, 2021). Ninety one bacterial strains were isolated from several sources and were subsequently characterised and cultured. Sources like effluents from dye-utilising industries like tanneries and textiles, jute-mills etc. were explored as source of bacteria. Water samples from small local ponds, an urban canal, a river and an estuary were explored. Soil samples drenched in effluents and endophytes from two common aquatic weeds were also investigated. Malachite Green (MG) is a triarylmethane dye. It is available mainly in two forms of salts: hydrochloride and oxalate. Here Malachite Green oxalate has been used. Apart from its widespread use in textile industries, it is also commonly used as a parasiticide in aquaculture since it is capable of preventing fungal attacks and protozoan infections (Yang et al., 2021) Malachite Green has been reported to show high levels of toxicity in both fish and humans on prolonged exposure (Sinha and Jindal, 2020). Mutations, cancers and developmental abnormalities have been attributed to this dye (Alaya et al., 2020). Attempts have been made to decolorise Malachite Green using bacteria *Kocuria rosea* (Parshetti et al., 2016), using fungus *Cunnighamella elegans* (Hussain et al., 2017), and even by some waterborne pathogenic strains of actinobacteria, among many others (Vignesh et al., 2020).

Textile industry is regarded as one of the prime sectors which contibuted enormously in the boost in the GDP of India. But while we celebrate the glory of this industry and its share in the rising economy of our country, we cannot however overlook the fact that, textile again stands as one of the largest polluters of water worldwide, India being no exception. Water pollution poses as a major cause of concern particularly for agricultural crops , since effluents released in the water bodies whose water is used for irrigating

agricultural feilds are often loaded with toxic compounds. One of the most toxic components that are released through these effluents are the dyes. Remazol brilliant blue (RBB) is an anthraquinone dye, widely used in textile industries globally, is a potent toxic organo-pollutant and is frequently used as the precursor of many other dyes (Mechichi et al., 2006). It is one of the most frequently utilized dyes in the textile industry (Ada et al., 2009). *Dichomitus squalens, Trametes trogii* (Eichlerová et al., 2005), *Pleurotus calyptratus* and *Ischnoderma resinosum* have been reported to degrade RBBR (Saratale et al., 2009). In the present study, we have isolated bacteria from several different sources and have tried to explore their potential to decolorise some toxic industrial dyes.

MATERIALS AND METHODS
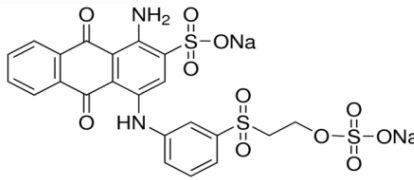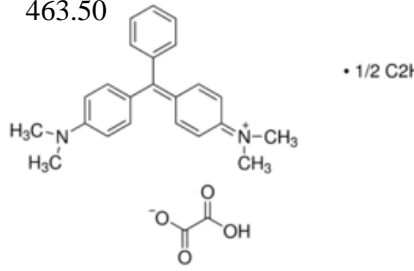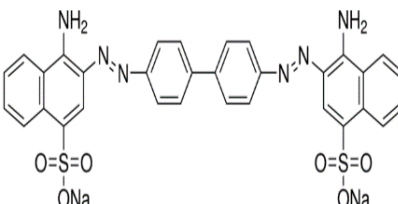
Growth medium
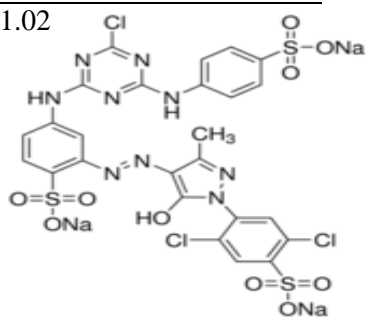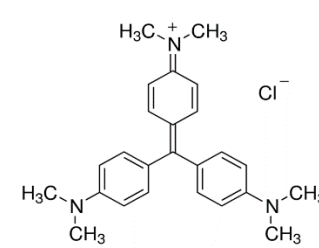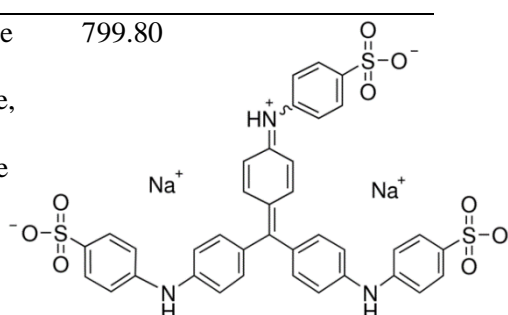
Nutrient broth medium (Composition: Peptone 10g/L, Beef extract 10g/L, Sodium chloride 5g/L; pH adjusted to 7) from Himedia Laboratories and Minimal Salt medium [MSM] (Na2HPO4: 1.8g/L; (NH4)2HPO4: 0.72g/L; K2HPO4: 1.8g/L; MgSO4.7H20: 0.144g/L; FeSO4.7H2O: 0.0072g/L; MnSO4.7H2O: 0.00504g/L; KCL: 0.144g/L; Sucrose: 7.2g/L; pH adjusted to 7) was used for the initial isolation of bacterial strains and all subsequent experiments .

Dyes

All dyes used are of analytical grade and obtained from Sigma-Aldrich. A table of the dyes used in the study is provided below (Table 2.1):

Table 2.1 Overview of the dyes used in the study

Name	CAS No.	Color Index No.	Other names	Molecular Weight (g/mol)	Structure
Remazol Brilliant Blue R	2580-78-1	61200	Reactive Blue 19	626.54	
Malachite Green Oxalate	2437-29-8	42000	N,N,N′,N′ - Tetramethyl-4,4′ - diaminotriphenylcarbenium oxalate, Basic Green 4	463.50	
Congo Red	573-58-0	22120	Congo Red 4B, Cosmos Red, Cotton Red B, Cotton Red C, Direct Red 28, Direct Red R, Direct Red Y	696.7	

Cibacron Yellow	50662-99-2	18972	Reactive yellow 2	831.02	
Crystal Violet	548-62-9	42555	Basic Violet 3, Gentian Violet, Hexamethylpararosaniline chloride, Methyl Violet 10B	407.98	
Methyl Blue	28983-56-4	42780	Acid blue 93, Aniline blue water soluble, Cotton blue, Poirriers blue, Water blue	799.80	

Isolation of bacteria

Effluents were collected aseptically in sterile containers for the isolation of bacteria and were stored in refrigerator at 4ºC for subsequent use. These samples were procured from several different industries in and around Kolkata, including, but not limiting to the ones that use dyes: Textile mill from Gangulibagan, Kolkata [P]; Textile mill from Uluberia, Howrah [Z]; Jeans dying factory, Burrabazar, Kolkata [A], Domestic baatik unit from Madhyamgram, North 24 Parganas [B]; Small printing press from Jadavpur, Kolkata [C]; Three tanneries from Park Circus area, Kolkata [D, W and I]; Tannery from Bhangar, South 24 Parganas [X]; A large dairy industry from Dankuni, Hooghly [F]; and a jute mill from Kamarhati, Kolkata [G]. For enrichment of total population of dye degrading isolates in the samples, 1 mL of the sample was aseptically added to 100 mL of nutrient broth and minimal salt medium. The flasks were incubated in shaking condition at 150 rpm at 28°C for 6 days. The enriched cultures were serially diluted up to 10^{-3} dilution and

the diluted cultures were spread plated aseptically and incubated at 28-30^{0}C for 3 days. Physicochemical characterisation of a few effluents is given below (Tables 2.2, 2.3, 2.4, 2.5):

Table 2.2 Physico-chemical analysis of the effluent W (Tannery from Park Circus Area, Kolkata)

Sl. No.	Parameters	Raw Effluent	Tolerence level as per CPCB*
1	Colour	Brownish	Should be absent
2	Odour	Unpleasant	Should be absent
3	pH	6.1	5.5-9
4	Total solids	12360	≤200
5	Biological Oxygen Demand	96.4	≤100
6	Chemical Oxygen Demand	164	≤250
All parameters were expressed in mg/L except colour, odour and pH CPCB* -Central Pollution Control Board; Environment (Protection) Rules, 1986, Schedule-I			

Table 2.3 Physico-chemical analysis of the effluent X (Tannery from Bhangar, South 24 Parganas)

Sl. No.	Parameters	Raw Effluent	Tolerence level as per CPCB*
1	Colour	Brownish	Should be absent
2	Odour	Unpleasant	Should be absent
3	pH	8.45	5.5-9
4	Total solids	2038	≤200
5	Biological Oxygen Demand	1102.0	≤100
6	Chemical Oxygen Demand	3786.0	≤250
All parameters were expressed in mg/L except colour, odour and pH CPCB* -Central Pollution Control Board; Environment (Protection) Rules, 1986, Schedule-I			

Table 2.4 Physico-chemical analysis of the effluent P (Textile mill from Gangulibagan, Kolkata)

Sl. No.	Parameters	Raw Effluent	Tolerence level as per CPCB*
1	Colour	Greenish	Should be absent
2	Odour	Unpleasant	Should be absent
3	pH	8.9	6.5-8.5
4	Total solids	2451	100
5	Biological Oxygen Demand {3days, at 27°C}	96	≤ 30
6	Chemical Oxygen Demand	310	250
All parameters were expressed in mg/L except colour, odour and pH CPCB* -Central Pollution Control Board ; Environment (Protection) Rules, 1986, Schedule-I			

Table 2.5 Physico-chemical analysis of the effluent Z (Textile mill from Uluberia, Howrah)

Sl. No.	Parameters	Raw Effluent	Tolerence level as per CPCB*
1	Colour	Greenish	Should be absent
2	Odour	Unpleasant	Should be absent
3	pH	8.45	6.5-8.5
4	Total solids	2038	≤ 100
5	Biological Oxygen Demand {3days, at 27°C}	104	≤ 30
6	Chemical Oxygen Demand	290	250
All parameters were expressed in mg/L except colour, odour and pH CPCB* -Central Pollution Control Board ; Environment (Protection) Rules, 1986, Schedule-I			

After analyzing the physiochemical characteristic of effluent it has been observed that there is not much difference in colour and odour, but differences were observed in pH, total solid content, COD and BOD. In case of the effluents from the textile mills, COD and BOD were almost around the Central Pollution Control Board (CPCB) tolerance limit, which may be due to some form of pre-treatment. Figure 2.1 shows places from where effluents were collected in and around Kolkata.
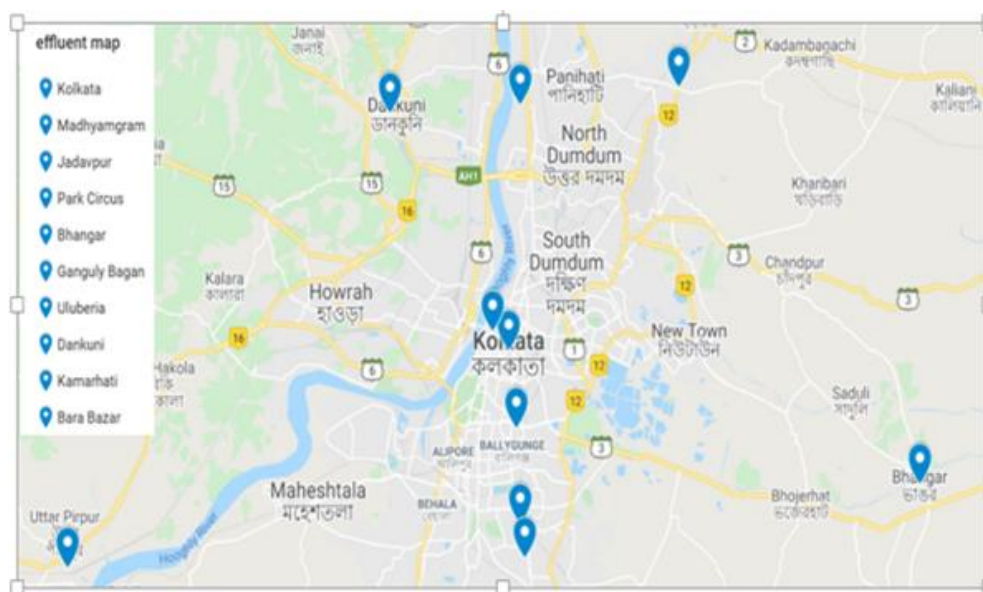
Figure 2.1 Map showing places in and around Kolkata from where effluents were collected

Soil samples drenched by domestic waste-water [soil 1] and soil drenched by dairy effluent [soil 2] were collected. Soil suspensions were made (1 gram soil in 100ml sterile distilled water). Then they were serially diluted upto 10^{-6} dilution and plated on solid nutrient agar and minimal salt medium for isolation of single colonies for pure cultures.

Three natural water sources: A pond from Shantiniketan, Birbhum [Water source 1], River Kopai, Birbhum [Water source 2], The Hugli-Matlah estuary, South 24 Parganas, near Bay of Bengal [Water source 3] and water from an urban sewage canal at Keshtopur, Kolkata were also explored for isolation of dye degrading bacteria. Isolation was done using standard spread plate method. Figure 2.2 gives an overview of places from where natural water samples were collected for the isolation of bacteria.
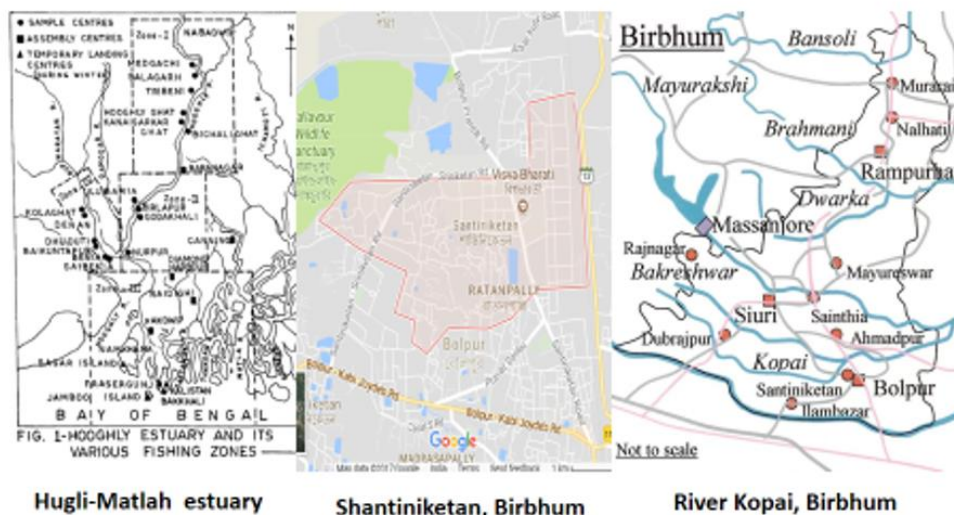
Figure 2.2 Natural water sources for the isolation of bacteria

Bacteria were also isolated from two common aquatic weeds: Water hyacinth (*Eichhornia crassipes*) [Plant 1] and Duck Weed (*Lemna trisulca*) [Plant 2]. The endophytic bacteria used in this study were isolated from different parts of these two healthy growing aquatic weeds. The plant samples were washed under running tap water (pre-treatment) to remove debris and air-dried before being cut into pieces of 5 cm^2 in area. In order to eliminate epiphytic microorganisms surface sterilization was performed. The samples were immersed in 0.5% (v/v) Sodium-hypochlorite for 1 minute, and then washed in sterile distilled water, followed by washing in 70% (v/v) ethanol for 1 minute. Finally, samples were rinsed twice with sterile distilled water for 1 minute each. The surface sterilized samples were blot-dried using sterile filter paper and then aseptically cut into 2 cm^2 in area. The samples were then transferred aseptically onto nutrient agar and minimal salt medium plates and incubated at room temperature for a period of 1 week. The plates were observed daily, and colonies were subcultured individually. Figure 2.3 depicts the protocol for isolation of the endophytes.
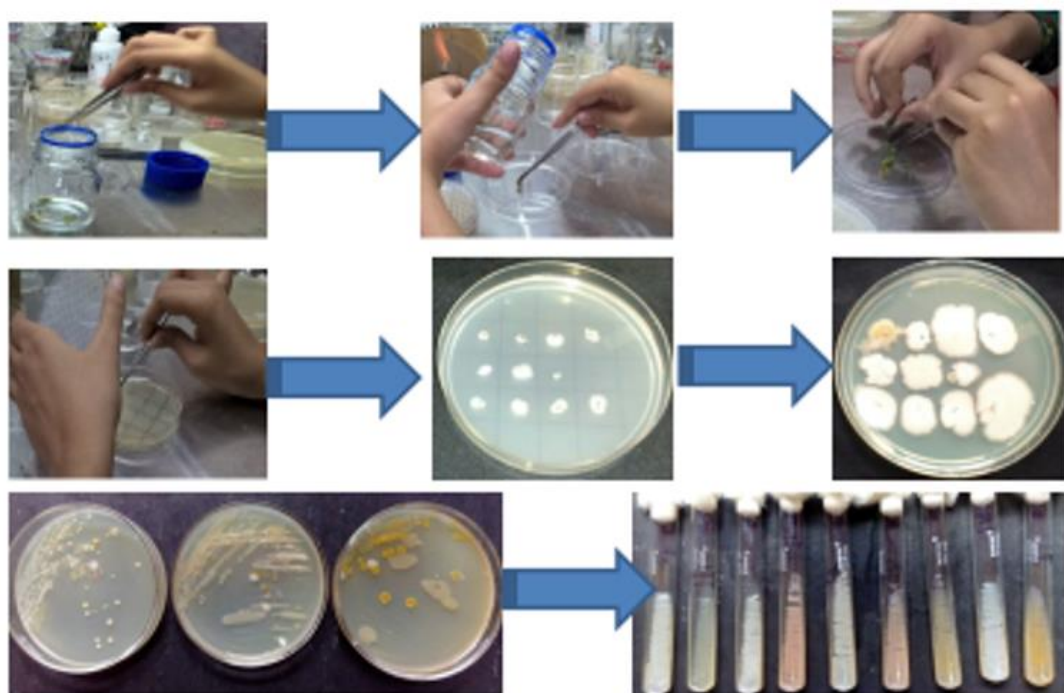
Figure 2.3 Isolation of endophytes from *Eichhornia crassipes* and *Lemna trisulca*

Qualitative decolorisation assay in solid medium

All the isolated strains were inoculated (streaked) into Mineral Salt plates amended with Malachite Green, Remazol Brilliant Blue R, Congo Red, Cibacron Yellow, Crystal Violet, and Methyl Blue. These were incubated at 37˚C for upto 3 days. Strains which had zone of clearance on the otherwise coloured plates were selected as potential dye-degraders. All the selected bacterial strains were maintained as pure cultures at 4˚C and used for further quantitative studies.

Quantitative decolorisation assay in liquid medium

All the selected strains isolated by qualitative analysis were individually inoculated into 5 ml of the minimum salt medium. In conical flaks of 500 ml capacity, 300ml of minimal salt medium each amended with the dyes (20 mg/L) were prepared. 1 mL of the previously prepared liquid culture (grown upto an optical density of 1 at 600nm) of the chosen strains was used to inoculate each flask. These flasks were incubated at 37°C for 7 days and the colour change was noted at regular intervals using UV-Vis spectrophotometer (Agilent Cary 60). In order to compare the decolorisation ability of

the different selected strains, the percentage degradation of dye was calculated and compared to the corresponding control. 10 mL of each dye-containing culture (from the conical flaks) were centrifuged at 10,000 rpm for 15 min to pellet out the bacterial biomass. Absorbance of the supernatant of the centrifuged samples was recorded at respective absorbance maxima of the dyes. All assays were performed in triplicate. Uninoculated dye-less medium was used as blank and results were compared with uninoculated dye-amended controls.

The decolorisation efficiency of different isolates was expressed according to the following formula (Equation 2.1):

$$\textbf{Percentage decolorisation} = \frac{\textbf{Initial absorbance} - \textbf{Final absorbance}}{\textbf{Initial absorbance}} \textbf{ X 100}$$

Equation 2.1

Identification of the selected bacterial isolates

The selected bacterial strains were identified using 16S rDNA sequencing and their morphological, biochemical and cultural characteristics were also studied.

Genetic identification of the bacteria through 16S rDNA sequencing

All of the six selected strains of bacteria were identified genetically by analysing their 16S rDNA. For this, the culture were provided to Xcelris, India. The identification was carried out in three major steps, as described below.

Isolation of genomic DNA

Cells grown in nutrient broth were pelleted out at 10,000rpm for 5min and the supernatant was discarded. Then they were resuspended in TE (Tris-EDTA) buffer and their OD (600nm) was adjusted to 1 with TE buffer (10mM Tris; 1 mM EDTA, pH 8.0). The cell suspension (740 µL) was transferred to a centrifuge tube and 20 µL lysozyme (100 mg/ml) was mixed with it and incubated for 30 min at 37ºC. Next, 40 µL of 10%

SDS (Sodium dodecyl Sulphate) was added to it. Aliquot of 8 µL Proteinase K (10mg/ml) was also added. This mixture was incubated at 56 ºC for 3h. Addition of 100 µL 5M NaCl was made. NaCl/CTAB (Cetyltrimethylammonium bromide) (100 µL) was added and the mixture was heated at 65 ºC and incubated for 10 min. A 24:1 mixture of chloroform: isoamyl alcohol (0.5ml) was added. This was centrifuged at room temperature for 10 min at 10000rpm. The aqueous phase was transferred into a microcentrifuge tube and 0.5ml of phenol: chloroform: isoamyl alcohol (25:24:1) was mixed. This was again centrifuged at 10000rpm for 10 min and the aqueous phase was again transferred to a clean microcentrifuge tube. This process was repeated once more with 0.5ml chloroform: isoamyl alcohol (24:1). 400 µL of the aqueous phase was transferred to a microcentrifuge tube and 240 µL ice-cold isopropanol was added and incubated at -20 ºC for 2hr. Then this was centrifuged at 10000rpm for 15 min at 4 ºC. The pellet thus obtained was washed with cold 70% ethanol and this was centrifuged at 10000rpm for 5min. The supernatant was discarded and the pellet was kept to dry at room temperature. Next, the pellet was resuspended in 170 µL of DNase-free water. For ethanol precipitation of the DNA, 3M sodium acetate (1/10 volume) and 2.5 volumes of 100% ethanol was also added and the mixture was centrifuged down. It was placed in -20 ºC overnight. Next day, supernatant was carefully poured off and the pellet was washed in cold 70% ethanol. This was again centrifuged down at 4 ºC for 5min. The ethanol on top was pipetted out carefully and pellet was vacuum dried for 5min, without the application of any heat. Finally the pellet was resuspended in 100 µl of TE buffer. The purity of the DNA was measured 260nm/280nm absorbance ratio.

Visualisation of the isolated DNA by agarose gel electrophoresis

50 ml TAE buffer was mixed with 0.5 g agarose and was then heated until completely melted. Then 2 µl Ethidium bromide was added to the gel after the temperature reaches 60°C, to facilitate visualization of DNA after electrophoresis. The solution was then poured into a casting tray containing a sample comb and allowed to solidify at room temperature. The comb was removed after the gel solidified, with sufficient care not to rip the bottom of the wells. The gel is then inserted horizontally into the electrophoresis chamber and just covered with buffer. DNA mixed with loading buffer were then loaded into the wells. The lid and power leads were placed on the apparatus, and a current was

applied. After DNA had migrated upto 2/3rd distance, as indicated by the movement of gel loading dye, the power supply was stopped. The gel was then taken out of the buffer.

PCR amplification of the 16S rDNA

Isolated DNA was amplified with 16S rRNA specific primers using Veriti® 99 well thermal cycler (Model No. 9902). A single discrete PCR amplicon band was obtained. The PCR cycle can be divided into the following steps: DNA was denatured for 2 min at 94°C prior to amplification and after amplification an extension step (7 min at 72°C) was undertaken. There were 28 cycles consisting of- denaturation at 94°C for 30 sec, primer annealing for 1 min at 45°C and extension at 72°C for 1 min. The samples were held at 4°C until analysis.

Visualisation of the 16S rDNA by agarose gel electrophoresis

The PCR amplified DNA was then observed by gel electrophoresis (performed according to protocol mentioned above) on a 1.5% agarose gel. The PCR product was excised from the agarose gel with the help of Agarose Gel DNA Purification Spin Kit from HiMedia.

Sequencing

Sanger Sequencing was performed with the PCR amplicons. Bi-directional DNA sequencing reaction of the PCR amplicons were carried out specific primers using BDT v3.1 Cycle sequencing kit on ABI 3730xl Genetic Analyzer. Consensus sequences of 16S rDNA was generated from forward and reverse sequence data using aligner software.

Phylogenetic analysis and sequence alignment

The 16S rDNA sequence was used to carry out BLAST using the NCBI Genbank database, and corresponding sequences of homologous strains were obtained. Based on maximum identity score, sequences were selected and aligned using the multiple alignment software program ClustalW. The neighbor-joining method (Saitou and Nei 1987) was employed to determine the strain's evolutionary history. In the bootstrap test (2000 replicates), the percentage of replicate trees in which the related taxa grouped was

shown next to the branches [Felsenstein 1985]. The evolutionary distances were computed using the Maximum Composite Likelihood method [Tamura et al. 2004]. The evolutionary analyzes were conducted, and the phylogenetic tree was constructed using MEGA6 [Tamura et al. 2013].

Morphological, biochemical and cultural characterisation of the strains

- **Morphological characterisation of the strains**

  ➢ **Colony morphology**

Materials

Nutrient agar ((peptone: 10 g/L, beef extract 10 g/L, sodium chloride 5g/L, agar aagar 2 %, PH 7.3±0.1), Petri plates, glass spreader

Method

Sterile nutrient agar plates were prepared and 0.1 ml culture was evenly spread with a sterile glass spreader. Plates were incubated at 37ºC for 72 hours and the colony characteristics were observed.

  ➢ **Determination of size and shape**

Materials

Nigrosin solution, Distilled water, 24 hr old bacterial culture, glass slides, needle, dropper, light microscope, stage and ocular micrometer.

Method

> ❖ Overnight grown culture was smeared on a clean grease free slide.
> ❖ The smear was air dried and heat fixed.
> ❖ It was then flooded with nigrosin and kept for 1 min.
> ❖ The slide was carefully washed with running water, air dried and examined under microscope with the stage and ocular micrometer.

  ➢ **Gram staining**

Materials

Gram's iodine solution, Gram's Crystal violet solution, Safranine solution, 95% ethanol, 24 hr old bacterial culture , glass slides, needle, dropper ,light microscope.

Method

- ❖ A smear was prepared with the bacterial strains on clean grease free slides.
- ❖ The smear was dried and heat fixed.
- ❖ The slide was then flooded with crystal violet and kept for 1 min.
- ❖ Excess stain was washed off with distilled water.
- ❖ Gram's iodine solution was flooded on the slide and kept for 45 seconds and washed off with ethanol, followed by distilled water.
- ❖ Slide was then flooded with safranine solution and allowed to stand for 1 min, then washed off with running water to remove excess stain.
- ❖ Prepared slide was air dried and visualised under the microscope.

➢ Endospore staining

Materials

Malachite green, distilled water, Safranine solution, 48 hr old bacterial culture, glass, dropper, slides, needle, light microscope

Method

- ❖ Bacterial smears were prepared on clean grease free slides and were air dried and heat fixed.
- ❖ Malachite green was slowly added over the slides while keeping them on boiling water for 10 min. Care was taken such that the smears do not dry up at any point and always remain moist.
- ❖ The slides were washed off with running water to remove excess stain.
- ❖ Safranine was flooded on the slides and kept for 1 min and then again washed with running water
- ❖ Prepared slides were air dried and observed under the microscope.

➢ Motility test

Materials

Medium composition (g/L): Nutrient broth medium (peptone: 10 g/L, beef extract 10 g/L, sodium chloride 5g/L, PH 7.3±0.1)

Method

❖ 5 ml sterile nutrient broth was inoculated with the strains and incubated at 37°C for 48hr.

❖ Loopfull of the prepared cultures were placed on a clean grease-free slide and observed under the microscope.

- **Biochemical characterisation of the strains**

  ➢ **Catalase Production Test**

Materials

Glass slide, H_2O_2, bacterial cultures.

Method

❖ Small inoculum of the bacteria was taken on clean glass slide.

❖ Drop of H_2O_2 was added for the observation of the test.

  ➢ **Amylase Production Test**

Materials

Petri plates, nutrient broth, agar agar, starch, bacterial cultures, iodine solution.

Method

❖ Plate of nutrient agar along with 0.4% starch was prepared.

❖ The plates were spotted with the cultures and incubated for 48hrs at 37°C

❖ Plates were then flooded with iodine solution

  ➢ **Lipase Production Test**

Materials

 Nutrient Agar plates with added 1% Tween 80, bacterial cultures

Method:

❖ Nutrient Agar plate containing 1% Tween was prepared.

❖ Plate was spotted with cultures.

❖ Plates were incubated for 96hrs at 37°C.

➢ **Protease Production Test**

Materials

1% Casein containing nutrient agar plate, 10% HCL, bacterial cultures.

Method

❖ Nutrient agar plate containing 1% Casein was prepared.

❖ The plate was spotted with bacterial culture.

❖ Plate was incubated for 72 hrs at 37°C.

❖ Plate was flooded with 10% HCl.

➢ **Indole Production Test**

Materials

Tryptophan broth medium, Kovac's reagent, bacterial culture.

Method

❖ 5ml cultures were grown in one tryptophan broth for 48 hrs at 37°C. An uninoculated tube was kept as control.

❖ 0.5ml Kovac's reagent was added to each of the tubes.

➢ **Nitrate Reductase Test:**

Materials

Nitrate broth [KNO3- 1g/l, Beef Extract- 3g/l, Peptone, pH- 7.0], Nitrate reagent, and bacterial culture.

Method

❖ Nitrate broth was prepared in two test tubes.

❖ One was inoculated with 100 μL of bacterial culture and the other one was kept as control.

❖ These were incubated at 37°C for 48hrs.

❖ 1ml of nitrate reagent was added to both the tubes.

➢ **Citrate Utilization Test:**

Materials

Simmon's citrate medium, bacterial cultures.

Method

- ❖ Simmon's citrate plate was prepared.
- ❖ The plate was spotted with bacterial cultures.
- ❖ Plates were incubated for 48hrs at 37°C.

➢ Gelatinase Production Test:

Materials

Nutrient broth with 12% gelatin, ice, bacterial culture.

Method

- ❖ Nutrient broth tubes containing 12% gelatin were prepared.
- ❖ Tubes were inoculated with 100µl of bacterial culture and another uninoculated tube was kept as control.
- ❖ They were incubated at 37°C for 72 hr

RESULT AND DISCUSSION

A total of forty bacterial samples have been isolated from the different effluent sources. Seven samples were isolated from the soil samples. The natural water sources yielded as many as twenty-nine different bacterial strains. Significantly larger number of bacteria has been isolated from these water sources. Eleven bacterial samples were isolated from aquatic plants *Eichhornia crassipes* and *Lemna trisulca*. Four strains of bacteria could be isolated from the wastewater of urban sewage canal. Figures 2.4, 2.5, 2.6 and 2.7 depict the isolation of bacterial strains from the above-stated sources.
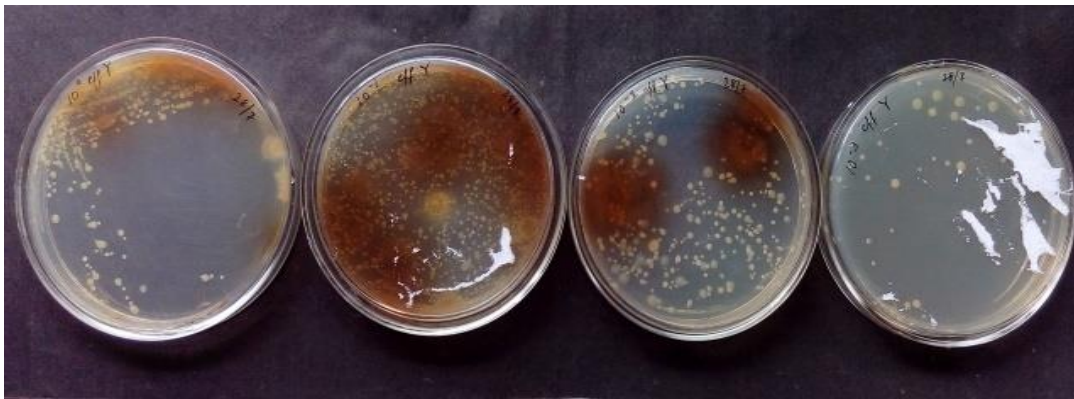
Figure 2.4 Isolation of bacterial strains from different effluent samples

Figure 2.5 Isolation of endophytic bacterial strains from aquatic weeds
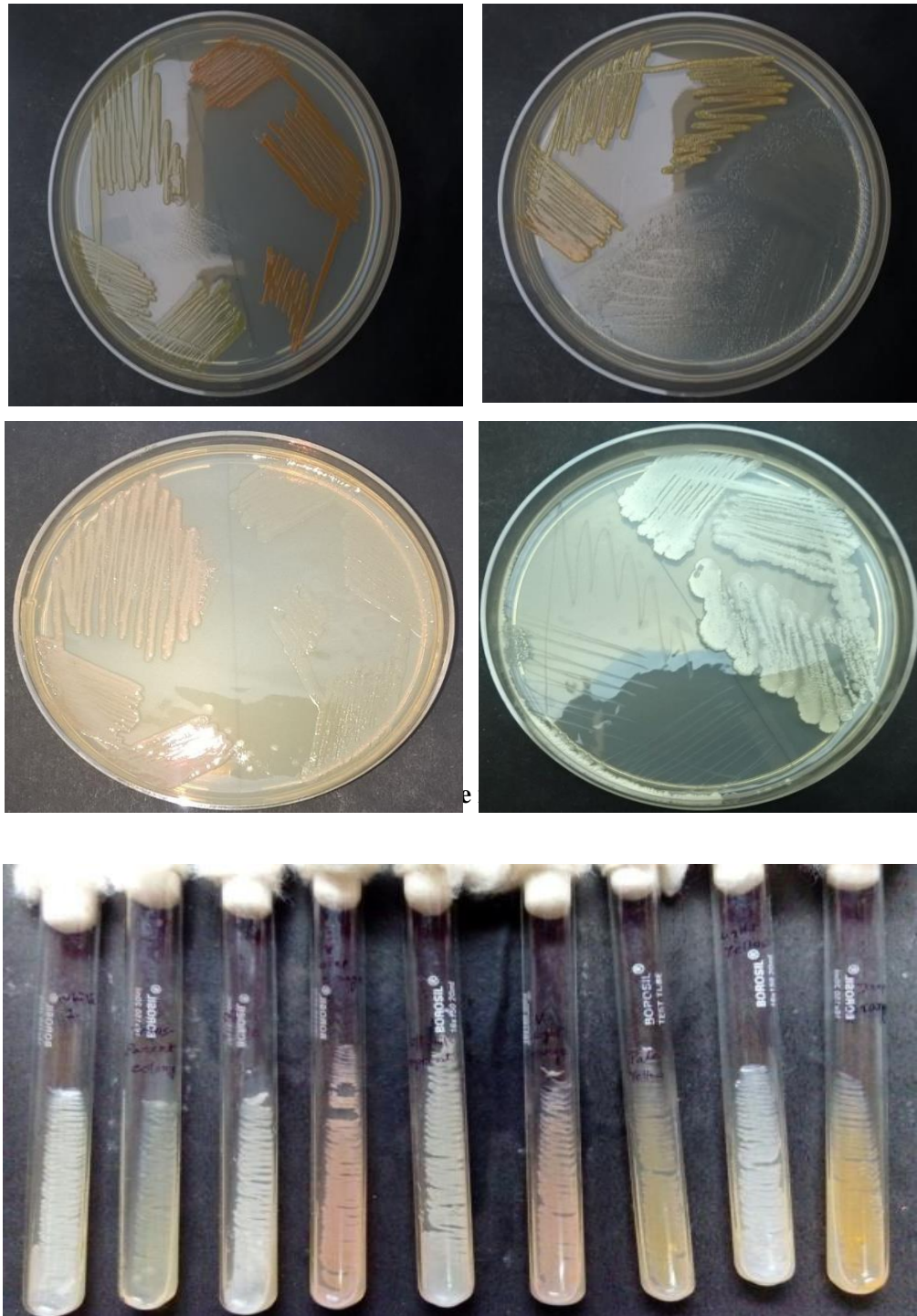
Figure 2.7 Pure cultures of some of the isolated bacterial strains in slants

Selection of the Bacterial Strains

A total of forty bacterial samples have been isolated from the different effluent sources. Twenty-two strains showed decolourisation of one or the other dye on the solid medium.

Table 2.6 shows the detailed list. Figure 2.8 represents a qualitative dye-decolorisation experiment.

Figure 2.8 Qualitative Dye-degradation study

Table 2.6 Qualitative dye degradation studies by bacteria from different effluents

Sl. No.	Strain name	Source	Dye degradation					
			Remazol Brilliant Blue	Congo Red	Cibacron Yellow	Methyl Blue	Crystal Violet	Malachite Green
1	P1	Effluent P	-	+	-	-	-	-
2	P2	Effluent P	-	-	-	-	-	-
3	P3	Effluent P	-	-	-	-	-	-
4	P4	Effluent P	-	-	-	-	-	-
5	P5	Effluent P	-	-	-	-	+	-
6	P6	Effluent P	-	-	-	+	-	+
7	P7	Effluent P	-	-	-	-	-	-
8	P8	Effluent P	-	-	+	-	-	-
9	P9	Effluent P	-	-	-	-	-	+
10	P10	Effluent P	-	-	+	-	-	-
11	P11	Effluent P	-	-	-	-	-	-
12	P12	Effluent P	-	-	-	-	-	+
13	P13	Effluent P	-	-	-	-	-	-
14	P14	Effluent P	+	-	-	-	+	-

15	P15	Effluent P	-	-	-	-	-	-
16	P16	Effluent P	-	-	+	-	-	-
17	P17	Effluent P	-	-	-	-	-	-
18	P18	Effluent P	+	-	-	-	-	-
19	P19	Effluent P	-	-	-	-	-	-
20	P20	Effluent P	-	-	-	+	-	-
21	P21	Effluent P	+	-	-	-	-	-
22	P22	Effluent P	-	-	+	-	-	-
23	P23	Effluent P	-	-	-	-	+	-
24	P24	Effluent P	+	-	-	-	-	-
25	P25	Effluent P	-	-	-	-	-	-
26	P26	Effluent P	-	+	-	+	-	-
27	P27	Effluent P	+	-	+	-	-	-
28	P28	Effluent P	+	-	—	-	-	-
29	A1	Effluent A	-	-	-	-	-	-
30	B2	Effluent B	-	-	-	-	-	-
31	C1	Effluent C	-	-	+	-	-	-
32	D1	Effluent D	-	-	-	-	+	-
33	W1	Effluent W	-	-	-	-	-	-
34	I1	Effluent I	-	-	-	+	-	-
35	X1	Effluent X	-	—	-	-	-	-
36	Z1	Effluent Z	-	-	-	-	-	-
37	F1	Effluent F	-	-	-	-	-	-
38	F2	Effluent F	-	+	-	-	-	+
39	G1	Effluent G	-	-	+	-	-	+
40	G2	Effluent G	-	-	+	-	-	-

Seven samples have been isolated from two different soil samples. Four out of seven showed decolorisation on solid medium (Table 2.7).

Table 2.7 Qualitative dye degradation studies by bacteria from soil samples

Sl. No.	Strain name	Source	Dye degradation					
			Remazol Brilliant Blue	Congo Red	Cibacron Yellow	Methyl Blue	Crystal Violet	Malachite Green
1	S1	Soil 1	-	-	+	+	-	-
2	S2	Soil 1	-	-	-	-	+	-
3	S3	Soil 1	-	-	-	-	-	-
4	S4	Soil 1	-	-	-	-	-	-
5	S5	Soil 2	-	+	-	-	-	-
6	S6	Soil 2	-	-	-	-	-	-
7	S7	Soil 2	-	-	-	-	+	+

Table 2.8 Qualitative dye degradation studies by bacteria from natural water sources

Sl. No.	Strain name	Source	Dye degradation					
			Remazol Brilliant Blue	Congo Red	Cibacron Yellow	Methyl Blue	Crystal Violet	Malachite Green
1	Y1	Natural water source 1	-	-	-	+	-	-
2	Y2	Natural water source 1	-	-	-	-	-	-
3	Y3	Natural water source 1	-	-	-	-	-	-
4	Y4	Natural water source 1	-	-	-	-	-	-
5	Y5	Natural water source 1	+	+	-	-	-	-
6	Y6	Natural water source 1	+	-	-	-	-	-
7	Y7	Natural water source 1	-	-	-	-	-	-
8	Y8	Natural water source 1	-	-	-	-	-	-
9	Y9	Natural water source 1	-	-	-	-	-	-
10	Y10	Natural water source 1	-	-	-	-	-	-

11	Y11	Natural water source 1	-	-	-	-	+	-
12	Y12	Natural water source 1	-	-	-	-	-	-
13	Y13	Natural water source 1	-	-	+	-	-	-
14	Y14	Natural water source 1	-	-	-	+	-	-
15	Y15	Natural water source 2	-	-	-	-	-	-
16	Y16	Natural water source 2	-	+	-	-	-	-
17	Y17	Natural water source 2	-	-	-	-	-	-
18	Y18	Natural water source 2	-	-	-	-	+	-
19	Y19	Natural water source 2	+	-	-	-	-	-
20	Y20	Natural water source 2	-	-	-	-	-	-
21	Y21	Natural water source 2	-	-	-	-	-	-
22	Y22	Natural water source 2	-	-	-	-	-	-
23	Y23	Natural water source 3	-	-	+	-	-	+
24	Y24	Natural water source 3	-	-	-	-	-	-
25	Y25	Natural water source 3	-	-	-	-	-	-
26	Y26	Natural water source 3	-	-	-	+	-	-
27	Y27	Natural water source 3	-	-	-	-	-	-
28	Y28	Natural water source 3	-	+	-	-	-	-
29	Y29	Natural water source 3	-	-	-	-	-	-

The natural water sources yielded as many as twenty-nine different bacterial strains. A significantly larger number of bacteria has been isolated from these water sources (Table 2.8).

Table 2.9. Qualitative dye degradation studies by bacteria from aquatic plant samples

Sl. No.	Strain name	Source	Dye degradation					
			Remazol Brilliant Blue	Congo Red	Cibacron Yellow	Methyl Blue	Crystal Violet	Malachite Green
1	H1	Plant 1	-	-	-	-	-	-
2	H2	Plant 1	-	-	-	-	-	-
3	H3	Plant 1	-	-	-	-	-	-
4	H4	Plant 1	-	-	-	+	-	-

5	H5	Plant 1	-	-	-	-	-	-
6	H6	Plant 1	-	-	-	-	-	-
7	H7	Plant 1	-	-	-	-	-	-
8	Du1	Plant 2	-	-	-	-	-	-
9	Du2	Plant 2	-	-	-	-	-	-
10	Du3	Plant 2	-	-	-	-	-	-
11	Du4	Plant 2	+	-	-	-	-	-

Eleven bacterial samples were isolated from aquatic plants *Eichhornia crassipes* and *Lemna trisulca* (Table 2.9).

Table 2.10 Qualitative dye degradation studies by bacteria from urban sewage canal

Sl. No.	Strain name	Source	Dye degradation					
			Remazol Brilliant Blue	Congo Red	Cibacron Yellow	Methyl Blue	Crystal Violet	Malachite Green
1	Us1	Urban Sewage Canal	-	-	+	-	-	+
2	Us2	Urban Sewage Canal	-	-	-	-	+	+
3	Us3	Urban Sewage Canal	-	-	-	-	-	-
4	Us4	Urban Sewage Canal	-	+	-	-	-	-

Four strains of bacteria could be isolated from the wastewater of urban sewage canal (Table 2.10).

Hence out of the ninety one bacterial strains isolated from all the effluent samples, natural water sources, soil samples, aquatic plants and the urban canal; forty five gave preliminary positive result for decolorisation of the chosen dyes.

Qualitative decolorisation

To get a clearer picture, decolorisation was monitored in liquid medium. The results thus obtained are tabulated below. Percentage decolorisation was calculated using formula previously mentioned in Equation 2.1.

Table 2.11. Quantitative dye degradation by the selected bacterial strains

Sl. No.	Strain	RBB		CR		CY		MB		CV		MG	
		Day 3	Day 7	Day 3	Day 7	Day 3	Day 7	Day 3	Day 7	Day 3	Day 7	Day 3	Day 7
1	P1	-	-	22.17	31.29	-	-	-	-	-	-	-	-
2	P5	-	-	-	-	-	-	-	-	17.8	25.01	-	-
3	P6	-	-	-	-	-	-	27.12	35.18	-	-	47.56	86.20
4	P8	-	-	-	-	26.31	32.17	-	-	-	-	-	-
5	P9	-	-	-	-	-	-	-	-	-	-	99.0	99.03
6	P10	-	-	-	-	32.74	41.22	-	-	-	-	-	-
7	P12	-	-	-	-	-	-	-	-	-	-	69.15	91.07
8	P14	24.06	52.69	-	-	-	-	-	-	23.61	22.17	-	-
9	P16	-	-	-	-	27.33	35.17	-	-	-	-	-	-
10	P18	24.3	44.12	-	-	-	-	-	-	-	-	-	-
11	P20	-	-	-	-	-	-	31.12	33.74	-	-	-	-
12	P21	34.85	64.73	-	-	-	-	-	-	-	-	-	-
13	P22	-	-	-	-	11.21	17.46	-	-	-	-	-	-
14	P23	-	-	-	-	-	-	-	-	27.21	31.48	-	-
15	P24	29.87	75.47	-	-	-	-	-	-	-	-	-	-
16	P26	-	-	11.93	16.73	-	-	16.21	19.33	-	-	-	-
17	P27	29.3	42.15	-	-	18.22	25.1	-	-	-	-	-	-
18	P28	35.2	46.22	-	-	-	-	-	-	-	-	-	-
19	D1	-	-	-	-	-	-	-	-	23.56	37.14	-	-
20	I1	-	-	-	-	-	-	33.68	45.12	-	-	-	-
21	F2	-	-	17.52	26.43	-	-	-	-	-	-	35.41	41.1
22	G1	-	-	-	-	11.2	12.11	-	-	-	-	33.61	41.23
23	G2	-	-	-	-	25.33	37.36	-	-	-	-	-	-
24	C1	-	-	-	-	10.56	21.44	-	-	-	-	-	-
25	S1	-	-	-	-	26.19	35.22	31.66	43.76	-	-	-	-
26	S2	-	-	-	-	-	-	-	-	17.26	28.19	-	-
27	S5	-	-	31.53	38.25	-	-	-	-	-	-	-	-
28	S7	-	-	-	-	-	-	-	-	32.61	32.56	11.24	13.27
29	Y1	-	-	-	-	-	-	9.11	14.36	-	-	-	-
30	Y5	23.41	36.22	19.1	19.0	-	-	-	-	-	-	-	-
31	Y6	35.1	49.1	-	-	-	-	-	-	-	-	-	-
32	Y11	-	-	-	-	-	-	-	-	24.51	31.21	-	
33	Y13	-	-	-	-	35.61	41.77	-	-	-	-	-	-
34	Y14	-	-	-	-	-	-	31.22	36.97	-	-	-	-
35	Y16	-	-	23.55	31.26	-	-	-	-	-	-	-	-
36	Y18	-	-	-	-	-	-	-	-	23.66	35.17	-	-
37	Y19	34.0	45.23	-	-	-	-	-	-	-	-	-	-
38	Y23	-	-	-	-	11.06	14.23	-	-	-	-	32.81	37.98
39	Y26	-	-	-	-	-	-	11.23	23.65	-	-	-	-
40	Y28	-	-	26.17	34.71	-	-	-	-	-	-	-	-
41	H4	-	-	-	-	-	-	16.21	23.55	-	-	-	-
42	Du4	18.01	24.61	-	-	-	-	-	-	-	-	-	-
43	Us1	-	-	-	-	21.16	33.92	-	-	-	-	22.44	42.9
44	Us2	-	-	-	-	-	-	-	-	23.11	37.24	30.39	32.2
45	Us4	-	-	17.16	22.79	-	-	-	-	-	-	-	-

From Table 2.11, it was observed that all the bacterial strains having dye-decolorising ability could decolorise at least 20% (except S7) on the 3rd day and at least 35% on the 7th day of the study. It is also observed that the two dyes Remazol Brilliant Blue (RBBR) and Malachite Green (MG) had been decolorised to the largest extent ($\leq$50%) amongst all the dyes that were subjected to the decolorisation study by the bacterial strains. Strains P14, P21 and P24 showed decolorisation of RBBR dye and strains P6, P9 and P12 showed decolorisation of MG dye more than 50%. From the quantitative assay these six strains were selected for further work (Figure 2.9).
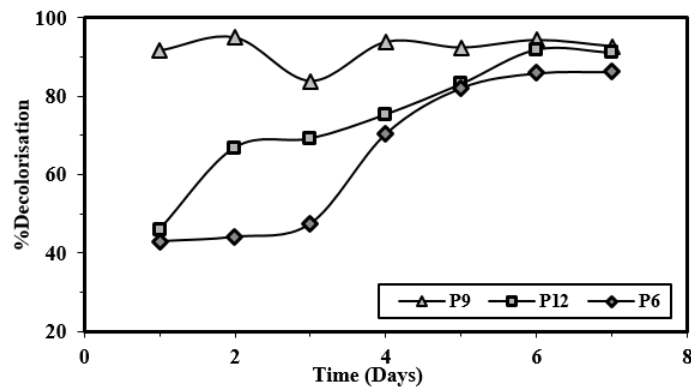
A
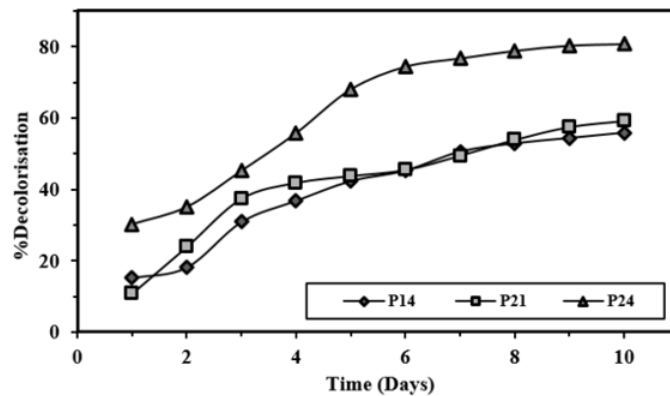
B

Figure 2.9 Malachite Green (A) and Remazol Brilliant Blue R (B) decolorisation patterns of bacteria that could perform more than 50% decolorisation of the dyes

Two strains (P9 and P24) which could show dye maximum decolorisation were chosen to further proceed with.

Identification of the Selected Strains

Strains P9 and P24 were subsequently identified through biochemical and 16S rDNA sequencing studies.

Colony Morphology

Colonies grown on nutrient agar plates (Himedia) for 48h showed the following features (Table 2.12):

Table 2.12 Colony morphology of the selected strains

Characters	P9	P24
Shape	circular	circular
Size	2–4 mm in diameter	2–4 mm in diameter
Colour	yellowish	cream
Texture	non-glossy	Non-glossy
Margin	smooth	smooth

Bacterial morphology

Microscopic study of the bacterium are tabulated in Table 2.13.

Table 2.13 Bacterial morphology of the strains

Characters	P9	P24
Shape	Slightly curved rod	Rod
Size	Diameter: 0.2–0.4 µm Length:1.5–2.0 µm	Diameter: 0.5 µm Length: 1-2µm
Gram nature	-ve	Positive
Endospore	-ve	Positive
Motility	-ve	Non-motile

Biochemical properties

Biochemical properties of the selected strains are given in Table 2.14 and Figure 2.10 represents some of the biochemical tests.

Table 2.14 Biochemical properties of the selected strains

Name of the tests	P9	P24
Catalase production test	+ve	+ve
Amylase production test	-ve	+ve

Lipase production test	-ve	-ve
Protease production test	+ve	+ve
Citrate utilisation test	-ve	-ve
Nitrate reductase test	-ve	+ve
Gelatinase production test	+ve	+ve
Indole production test	+ve	-ve
Lactose fermentation test	-ve	-ve
Maltose fermentation test	-ve	-ve
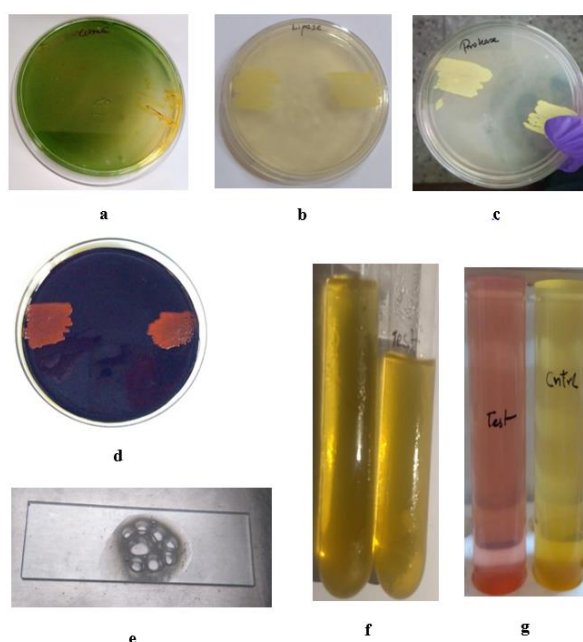
Figure 2.10: Biochemical characterization of the bacterial strains using Citrate (a) Lipase (b), Protease (c), Amylase (d), Catalase (e), Gelatinase (f), and Indole (g) production test

The strain 9 was identified as *Stenotrophomonas koreensis* by routine microbiological tests and 16S rRNA profiling (accession no. MK578830 received on submitting the nucleotide sequence to GenBank). The phylogenetic tree (Figure 2.11A) obtained by neighbor-joining method shows the evolutionary relationships of this species with its homologous strains found in the GenBank database. The species is closely related to *Stenotrophomonas acidiminiphila, S. maltophila* and *S. ginsengisoli*. Morphological studies indicated that the bacterium is rod-shaped (approximately 1-2 μm in length), non-motile, Gram-negative, and does not produce endospores. The colonies are round, with a

smooth surface and margin, non-glossy, and pale yellow. Biochemical investigations revealed that the strain is positive for catalase, protease, and oxidase activities.
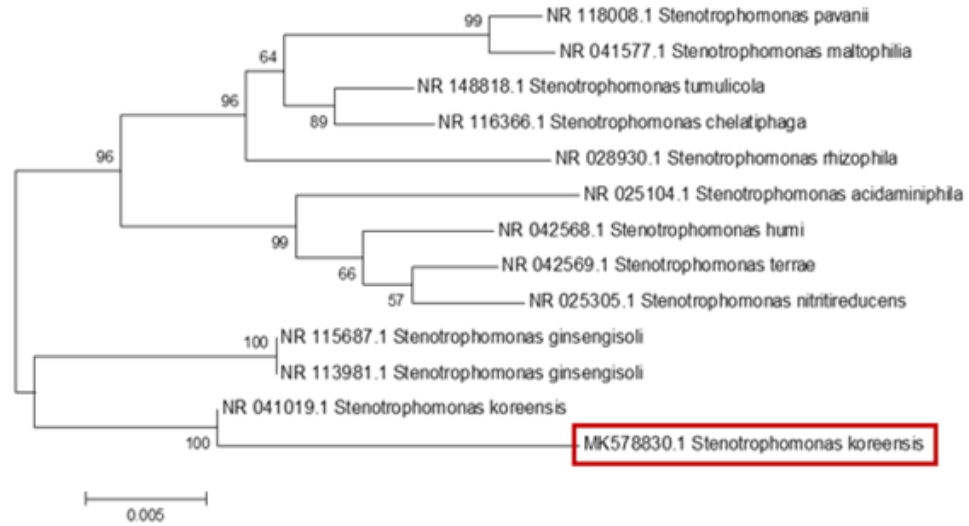
A
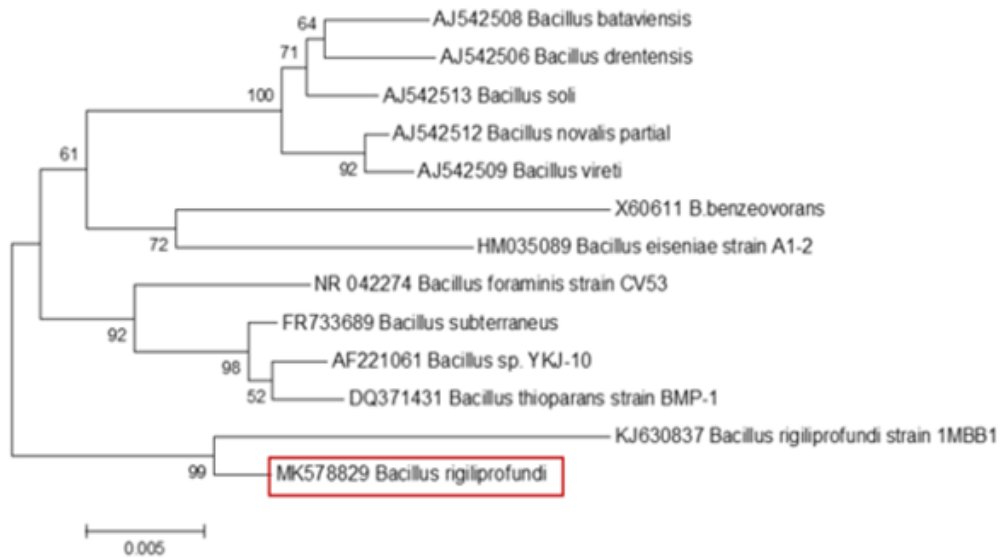
B

Figure 2.11 Phylogenetic tree of *Stenotrophomonas koreensis* (A) and *Bacillus rigiliprofundi* (B)

The strain P24 was identified morphologically, biochemically, and through 16S rDNA profiling. The morphological and biochemical characteristics are presented in Table 1. The strain was Gram-positive, endospore-forming, and rod-shaped (approximately 1-2µm in length and 0.5 µm in width). The colonies are pale cream, circular with a smooth surface and margin. The strain is positive for catalase and oxidase activities. The strain was identified as *Bacillus rigiliprofundi* by 16S rDNA profile analysis. The nucleotide sequence was submitted to GenBank (accession no. MK578829). The neighbor-joining method was employed to construct a phylogenetic tree that shows this species' evolutionary relationships with other homologous strains (Figure 2.11B). The strain was found to be closely related to *Bacillus novalis*, *B.vireti*, *B.subterraneus* and *B.thioparans*.

CONCLUSION

A total of ninety one strains of bacteria were isolated from several different sources like effluents from tanneries, textile industries, jute mills and dairies; from water samples from a pond, an urban canal, a river and an estuary; from soil samples, and from two common aquatic weeds. All these bacterial strains were checked for their ability to decolorise Remazol Brilliant Blue R, Congo Red, Cibacron Yellow, Methyl Blue, Crystal violet and Malachite Green which are heavily used as colorants in textile and leather industries and are highly toxic. Qualitative assays on solid medium was done to choose dye decolorisers preliminarily, followed by quantitative assays in liquid medium to estimate their degradation potential in terms of percentage decolorisation. Based on the initial results the strains *Stenotrophomonas koreensis* and *Bacillus rigiliprofundi* were selected for decolorising malachite green and Remazol brilliant blue dyes respectively as they decolorised these dyes more than 50% within 3-9 days' time for further study and optimisation.

REFERENCES

Ada, K., Ergene, A., Tan, S. and Yalçın, E., Adsorption of Remazol Brilliant Blue R using ZnO fine powder: Equilibrium, kinetic and thermodynamic modeling studies. J. Hazard. Mater. , 2009, vol. 165, pp.637-644.

Alaya, V., Kodi, R.K., Ninganna, E., Gowda, B. and Shivanna, M.B., 2021. Decolorization of Malachite green dye by Stenotrophomonas maltophilia a compost bacterium. *Bulletin of the National Research Centre*, *45*(1), pp.1-13.

Ardila-Leal, L.D., Poutou-Piñales, R.A., Pedroza-Rodríguez, A.M. and Quevedo-Hidalgo, B.E., 2021. A Brief History of Colour, the Environmental Impact of Synthetic Dyes and Removal by Using Laccases. *Molecules*, *26*(13), p.3813.

Biswas, S., Basak, P. and Jasu, A., 2019. Exploring different sources for Malachite Green decolorizing bacteria. *JOURNAL OF THE INDIAN CHEMICAL SOCIETY*, *96*(4), pp.425-428.

Brunel, D. and Dumur, F., 2020. Recent advances in organic dyes and fluorophores comprising a 1, 2, 3-triazole moiety. *New Journal of Chemistry*, *44*(9), pp.3546-3561.

Eichlerová, I., Homolka, L., Lisá, L. and Nerud, F., Orange G and Remazol Brilliant Blue R decolorization by white rot fungi *Dichomitus squalens, Ischnoderma resinosum* and *Pleurotus calyptratus.* Chemosphere, 2005, vol. 60, pp.398-404.

Felsenstein J. Confidence limits on phylogenies: An approach using the bootstrap. Evolution, 1985, vol. 39, pp: 783-791.

Hussain, S., Quinn, L., Li, J., Casey, E. and Murphy, C.D., 2017. Simultaneous removal of malachite green and hexavalent chromium by Cunninghamella elegans biofilm in a semi-continuous system. *International Biodeterioration & Biodegradation*, *125*, pp.142-149.

Mechichi, T., Mhiri, N. and Sayadi, S., Remazol Brilliant Blue R decolourization by the laccase from *Trametes trogii.* Chemosphere, 2006, 64, pp.998-1005.

Mohammed, H., 2021. Synthesis, Identification, and Biological Study for Some Complexes of Azo Dye Having Theophylline. *The Scientific World Journal*, *2021*.

Parshetti, G., Kalme, S., Saratale, G. and Govindwar, S., 2006. Biodegradation of Malachite Green by Kocuria rosea MTCC 1532. *Acta Chimica Slovenica*, *53*(4).

Saitou N. and Nei M. The neighbor-joining method: A new method for reconstructing phylogenetic trees. Mol Biol Evol , 1987. vol. 4, pp.406-425.

Saratale, R.G., Saratale, G.D., Kalyani, D.C., Chang, J.S. and Govindwar, S.P., Enhanced decolorization and biodecolorisation of textile azo dye Scarlet R by using developed microbial consortium-GR*., Bioresour. Technol., 2009, vol. 100, pp.2493-2500.

Sinha, R. and Jindal, R., 2020. Elucidation of malachite green induced behavioural, biochemical, and histo-architectural defects in Cyprinus carpio, as piscine model. *Environmental and Sustainability Indicators*, *8*, p.100055.

Tamura K., Nei M., and Kumar S. Prospects for inferring very large phylogenies by using the neighbor-joining method. Proc Natl Acad Sci (USA). 2004. vol. 101: pp. 11030-11035.

Tamura K., Stecher G., Peterson D., Filipski A., and Kumar S. (2013). MEGA6: Molecular Evolutionary Genetics Analysis version 6.0. Mol Biol Evol. vol. 30: pp. 2725-2729

Vignesh, A., Manigundan, K., Santhoshkumar, J., Shanmugasundaram, T., Gopikrishnan, V., Radhakrishnan, M., Joseph, J., Ayyasamy, P.M., Kumar, G.D., Meganathan, R. and Balagurunathan, R., 2020. Microbial degradation, spectral analysis and toxicological assessment of malachite green by Streptomyces chrestomyceticus S20. *Bioprocess and biosystems engineering*, *43*(8), pp.1457-1468.

Yang, C.W., Chang, Y.T., Hsieh, C.Y. and Chang, B.V., 2021. Effects of Malachite Green on the Microbiomes of Milkfish Culture Ponds. *Water*, *13*(4), p.411.

Chapter 3
Studies on Malachite Green Degradation by the Strain *Stenotrophomonas koreensis*

INTRODUCTION

Ryan et al. (2009) exhaustively discussed the versatility of the genus *Stenotrophomonas*. *Stenotrophomonas* sp has been reported to have several biotechnological applications. It enhances plant growth and development. Up to 180% increase in growth of crops like wheat, tomato, lettuce, sweet pepper, melon, celery, and carrots in the saline soils of Uzbekistan [Berg et al. 2010], production of the plant hormone Indole Acetic Acid (IAA) [Suckstorff et al. 2003], fixation of Nitrogen [Liba et al. 2006], and oxidation of elemental Sulphur [Banerjee et al. 2002] by this genus has been reported. These bacteria can metabolize many organic compounds, eventually protecting plants from phytotoxic effects [Ryan et al., 2009]. Among all the species of the genus *Stenotrophomonas*, *S. maltophila* is probably the best-studied one. Although *S. maltophila* is an opportunistic multi-drug-resistant pathogen [Brooke 2012, Looney et al. 2009, Sánchez 2015], this species exhibits a range of degradative properties. It can degrade polypropylene glycols [Tachibana 2003] and decolorize triphenylmethane dyes like malachite green and crystal violet [Alaya et al. 2021]. In the presence of copper, *S. maltophila* produces laccase and can decolorize dyes like methyl blue, toluidine blue, methyl green, methyl orange, congo red etc. [Galai 2009, 2012] The strain *Stenotrophomonas koreensis* has not been studied sufficiently and remained almost untapped for its potential applications. Only one application has been documented to date: *S. koreensis* can produce biosurfactants capable of abating heavy metals like Cadmium and Lead [Patil et al. 2012]. To the best of our knowledge, before this study, *Stenotrophmonas koreensis* had not been reported as far as dye degradation is concerned.

MATERIALS AND METHODS

Dyes, Chemicals and Media

Malachite green oxalate, Methyl orange, Safranin, Methyl Red, Direct Yellow 27, Acid Orange 6, Cotton Blue, Basic Blue 3, and Naphthol Green B, polyvinyl alcohol (PVA), and sodium alginate were obtained from Sigma Aldrich. Dextrose, fructose, D-ribose, peptone, tryptone, urea, thiourea, sodium azide, calcium nitrate, calcium chloride, sodium nitrite, and beef extract were purchased from Himedia. Molasses were obtained locally. Nutrient broth (Peptone 10 g/L; Beef extract 10 g/L; Sodium chloride 5 g/L; pH adjusted to 7) from Himedia Laboratories was used to isolate the bacterial strains.

Decolorization experiments

A loopful of *Stenotrophomonas koreensis* was inoculated in 100mL nutrient broth in a 250 ml flask and maintained at 37°C overnight for 18h in shaking condition. 5ml of the prepared bacterial culture was inoculated into 100ml malachite green oxalate powder dissolved in distilled water (100mg/L) and incubated at 37 °C. At particular intervals, 4ml aliquots were taken out, centrifuged at 10000rpm for 8min and the optical density of the supernatant was measured at 614 nm in an Agilent Cary 60 UV-Vis spectrophotometer. All experiments were performed in triplicate. An uninoculated solution of malachite green (100mg/L) was kept as control. The decolorization percentages were calculated according to the formula maintained previously in Chapter 2 as Equation 1. The same equation is again given below, (Equation 1):

$$\textbf{Percentage decolorisation} = \frac{\textbf{Initial absorbance} - \textbf{Final absorbance}}{\textbf{Initial absorbance}} \textbf{ X 100}$$

Equation 2.1

Analysis of the decolorized product and confirmation of degradation of the dye

To analyze the decolorization and confirm degradation, UV-Vis, TLC, HPLC and FTIR were performed with the control dye and its degraded product. A scan (200-800nm) of the dye before and after decolorization was carried out in a UV-Vis (Agilent, Cary 60) spectrophotometer to view the changes in the spectra. The decolorized product was centrifuged at 10000 rpm for 5 min to separate the cell mass. The supernatant was lyophilized to dryness, and the residue thus obtained was dissolved in a small volume of HPLC grade methanol and used for further analysis by TLC, HPLC, and FTIR. For TLC, two solvent systems were used: (a) Propanol and (b) Butanol: Acetic acid: Water (4:1:2). The plates were visualized in an iodine chamber. FTIR of the dye and the product obtained after decolorization was performed using Bruker, USA (alpha model) spectrophotometer in the wavenumber range $450cm^{-1}$ to $4500cm^{-1}$. HPLC analysis was carried out (Waters model 2690) with C18 column. Methanol was used as the mobile phase with a flow rate of 1ml/min.

Effect of various Carbon and Nitrogen sources on decolorization

It is often seen that supplying nutrients accelerates the process of biodegradation of dyes. In an attempt to analyze the effect of Carbon (10g/L) and Nitrogen (1g/L) supplements on the decolorization medium, four different carbon sources (dextrose, fructose, D-ribose, and molasses) and nine different nitrogen sources (organic: peptone, tryptone, urea, thiourea, soymeal extract, beef extract and inorganic: sodium azide, calcium nitrate, sodium nitrite) were explored. The control consisted of an uninoculated malachite green solution (100mg/L) in distilled water, unsupplemented by any other organic or inorganic component.

Response Surface Methodology for optimization of physical parameters for decolorization

The Response Surface Methodology (RSM) based on central composite design (CCD) is frequently used for experimental design, modeling, and optimization. Three independent physical factors: pH, temperature, and inoculum concentration, were taken into account

for efficient decolorization of malachite green. RSM was employed to determine the optimal decolorization conditions using Minitab 19.0. Twenty experimental runs were performed. Each variable was studied at five levels. The experimental sequences were completely randomized in order to reduce errors. A model equation was generated and validated by experimental data. A quadratic polynomial equation described the relationship between the dependent and independent variables:

$$\mathbf{Y = \beta_0 + \sum_{i=1}^{n} \beta_i X_i + \sum_{i=1}^{n} \beta_{ii} X_i^2 + \sum_{i<j} \beta_{ij} X_i X_j}$$

Equation 3.1

Y is the predicted target function, i.e., the dye decolorization, β_0 is the model constant, β_i is the linear coefficient, β_{ii} is the quadratic coefficient, β_{ij} is the interaction effect coefficient, X_i and X_j are the dimensionless coded values and n is the number of independent variables. Linear regression was plotted (predicted vs. actual), and the model's prediction accuracy was cross-verified by Leave-One-Out-Cross-Verification (LOOCV) method in MATLAB R2021a.

Decolorization of other dyes by the bacteria

Decolorization of eight different dyes (50mg/L): Methyl orange, Safranin, Methyl Red, Direct Yellow 27, Acid Orange 6, Cotton Blue, Basic Blue 3, and Naphthol Green B, were used for the study of decolorization by this strain to explore if the strain was able to decolorize dyes other than malachite green.

Immobilization of the strain

Preparation of the biobeads

1g each of polyvinyl alcohol (PVA) and sodium alginate were mixed in 70 ml boiling water. The solution was autoclaved at 121^0C for 15 minutes and cooled. Variable volumes (1-9 ml) of bacterial culture were added to the sterile solution. A cold, sterile

solution of 5% calcium chloride was also prepared. The mixture of PVA, sodium alginate, and bacterial culture was extruded drop-wise onto the 5% calcium chloride solution to form beads. The beads thus obtained were re-suspended into fresh cold, sterile calcium chloride solution under gentle agitation for hardening. Loosely adhered cells and excess calcium chloride was washed away with sterile distilled water.

Decolorization experiments with the immobilized bacteria

The beads were tested for their ability to decolorize malachite green (100mg/L). Beads obtained by immobilizing the variable volumes (1-9ml) of bacterial cultures were incubated for 10 h with dye solution at 37 °C with occasional mixing. Percentages of decolorization were recorded at specific intervals. After completion of 10hr period, beads were removed and washed thoroughly but carefully in sterile distilled water. These washed beads were again used for the second batch of decolorization experiments.

Decolorization of Malachite Green by *S. koreensis* in the presence of heavy metals

The potential of *S. koreensis* to decolorize malachite green in the presence of heavy metals was analyzed. The decolorization percentages were recorded after adding heavy metals in the form of soluble salts: sodium arsenite, lead acetate, potassium dichromate, and cadmium acetate in various concentrations, and an uninoculated control was kept where no heavy metal salt was added.

Determination of enzyme activity

The activity of different enzymes responsible for malachite green decolorization was studied for *S. koreensis*. Enzyme analyzes were performed using methods described by Jadhav and Govindwar, 2006 and L.-N.Du et al., 2011. Bacterial cultures grown overnight were centrifuged at 10000rpm for 8 min. Cell biomass was washed thrice, suspended in 5 ml phosphate buffer, sonicated (sonicator output 60 amp, three strokes of 30 s each keeping 2 min interval at 4ºC) . The resultant cell-lysate was the source of crude enzyme for the enzyme analysis. Laccase activity was estimated by taking 10% ABTS (2,2′-Azino-bis 3-ethylbenzothiazoline-6-sulfonic acid) diammonium salt in 0.1 M

acetate buffer (pH 4.9) and measuring ABTS oxidation at 420 nm using molar extinction coefficient 29300 $M^{-1}cm^{-1}$. Reaction mixture contained 100 μL cell-lysate and the total volume was maintained at 3 ml. Tyrosinase activity was determined by adding 100 μL cell lysate in 100 mM phosphate buffer (pH 7.4) containing 0.01% catechol, total reaction volume being 3 ml. The catechol quinone thus produced was measured at 410 nm with molar extinction coefficient 1623 $M^{-1}cm^{-1}$. Lignin peroxidase activity was measured by observing the production of propionaldehyde at 300 nm using molar extinction coefficient 20 $M^{-1}cm^{-1}$. This was done by adding 100 μL cell-lysate in a total reaction mixture of 2.4 ml containing 100 mM n-propanol, 250 mM tartaric acid and 10 mM H_2O_2. MG reductase activity was estimated by monitoring the reduction of malachite green at 620 nm using the extinction coefficient 1.47×10^5 $M^{-1}cm^{-1}$. Reaction mixture (4 mL) consisted of 20mgL^{-1} malachite green, 50 μM NADH and 100 μL cell-lysate in 50 mM potassium phosphate buffer (pH 7.4). NADH-DCIP Reductase activity was measured by monitoring the reduction of DCIP at 590 nm using the extinction coefficient 90 $mM^{-1}cm^{-1}$. The reaction mixture (4 mL) contained 50μM NADH, 50 μM DCIP and 100 μL cell-lysate in   50mM phosphate buffer (pH 7.4).

Degradation Kinetics

The kinetics of degradation of malachite green by *S. koreensis* under optimal decolorization conditions was studied by the procedure mentioned in Du et al. (2012). After the strain was inoculated into the dye solution, aliquots (4ml) were collected at specific time intervals and centrifuged at 10000 rpm for 8 min. The absorbance of the supernatant was measured at 614 nm. The following equations can describe the kinetics of degradation of dyes by microorganisms according to Das et al, 2010:

$$C_t = C_0 - k_0 t$$

Equation 3.2

$$C_t = C_0 e^{-kt}$$

Equation 3.3

$$\frac{1}{C_t} = \frac{1}{C_0} + k_2 t$$

<div align="right">**Equation 3.4**</div>

where

C_t = concentration of the dye in mg/L at time t

C_0= initial concentration of the dye in mg/L

t= time of incubation in minutes

k_0= zero order rate constant

k_1=first order rate constant

k_2=second order rate constant

The results obtained were plotted in C_t vs. t, ln Ct vs. t, and 1/Ct vs. t graphs and then analyzed.

Toxicity studies

The ecotoxicological assessment of the biodegradation product of the toxic dye malachite green by *S. koreensis* was performed with a wide range of aquatic and terrestrial organisms, representing the key levels of the ecosystem following Gioia et al. (2018); Amin et al. (2020) and Khan et al. (2020), while adhering to the OECD guidelines. To calculate an endpoint for quantitatively expressing the toxicity of the dye and the degradation product, a range of treatment solutions were prepared by two-fold serial dilutions as mentioned in Gioia et al. (2018). Hence, undiluted, 50% diluted, 25% diluted, 12.5% diluted, and 6.25% diluted initial dye concentration used in all previous experiments (translating to 100, 50, 25, 12.5 and 6.5 mg/L malachite green respectively) along with their corresponding degradation products were tested.

Aquatic toxicity studies

Aquatic toxicity was measured using four indicative organisms of the four levels of the aquatic ecosystem: the primary producer, algae *Anabaena flos-aque*, (algae growth inhibition test), aquatic plant *Lemna minor* (growth inhibition test), primary consumer crustacean *Daphnia magna* (acute immobilisation) and secondary consumer zebra-fish *Danio rerio* (acute toxicity).

Algae growth inhibition test

Algae growth inhibition test was conducted for a period of 96h maintaining the OCED 201 (2011) guidelines for toxicity testing. The unicellular blue-green algae *Anabaena flos-aque* was used for this study. The cyanobacterial pure cultures were subcultured in BG11 medium [$NaNO_3$ 1.5g, K_2HPO_4 0.04g, $MgSO_4.7H_2O$ 0.075g, $CaCl_2.2H_2O$ 0.036g, Citric acid 0.006g, Ferric ammonium citrate 0.006g, EDTA (disodium salt) 0.001g, Na_2CO_3 0.02g, Trace metal mix A5 1.0mL, distilled water 1L (pH 7.1 post-sterilization); Trace metal mix A5: H_3BO_3 2.86g, $MnCl_2.4H_2O$ 1.81g, $ZnSO_4.7H2O$ 0.222g, $NaMoO_4.2H_2O$ 0.39g, $CuSO_4.5H_2O$ 0.079g, $Co(NO_3).6H_2O$ 49.4 mg, distilled water 1L] and maintained under with 16h light and 8h dark photoperiod at 25±2°C. Aliquots of algal culture were inoculated into BG 11 medium with malachite green and corresponding degradation product separately. The initial biomass density was maintained at 0.1 mg/mL for all the experiments. *A. flos-aque* cultures including a dye-less control and the degradation product were also set up similarly. These were incubated at 28 °C under 16h illumination in continuous shaking condition for 96h. Care was taken such that no other organic or inorganic contaminants could intervene the system. After 96h, 5mL algal aliquots were filtered through Whatman GF/F 25mm filter paper and dried at 60 °C for 8h. The average specific growth rate is calculated as the log of the biomass increase over a specific period of time and is calculated by the formula (3.5) [OECD 201 (2011)]:

$$\mu_{i-j} = (\ln X_j - \ln X_i)/ (t_j - t_i)$$

where:

$\mu_{i\text{-}j}$ *is the average specific growth rate from time i to j;*

X_i *is the biomass at time i;*

X_j *is the biomass at time j;*

t_i *is the time (in days) of the ith biomass measurement after beginning the exposure;*

t_j *is the time (in days) of the jth biomass measurement after beginning the exposure*

The percentage inhibition of growth rate was calculated from the following Equation (Equation 3.6) [OECD 2011]:

$$\%I_r = \frac{\mu_c - \mu_r}{\mu_c} \times 100$$

where:

$\%I_r$ is the percentage inhibition in average specific growth rate;

μ_c is the average specific growth rate in the control group;

μ_r is the average specific growth rate for the treatment group

Lemna acute toxicity assay

The second level of aquatic toxicity bioassay was performed using the fresh-water macrophyte *Lemna minor*, through experiments designed according to the OECD 221 (2006) guidelines for toxicity testing. The aquatic plants were collected during the month of June from the Jadavpur University ponds and were thoroughly cleaned and then cultured in Hoagland's medium for eight weeks. The healthy plants were screened out and used for further work and maintained under laboratory conditions for another 7 days. Then, 3 colonies, each consisting of 4 fronds were aseptically transferred into 250 ml borosilicate glass beakers containing 100 ml distilled water amended by the dye (6.25-100 mg/L), the corresponding degradation products and a dye-less control. Each of the test solutions, along with the control were kept in triplicate at 25 ºC and 16h photoperiod. After an exposure of 96 h, the plant biomass for each treatment were recorded as a measure of toxicity. For estimation of the fresh weight, excess water was carefully blotted out from the samples from each set and transferred to pre-weighed tubes. Now tubes were re-weighed and the fresh weights were obtained by subtracting the weight of the empty tubes from the total weight. The specific growth rate and % growth inhibition were estimated from Equations 3.5 and Equation 3.6 respectively. The total chlorophyll content was also measured for all the treatment groups. For the estimation of chlorophyll content, the plants were washed several times in order to remove any traces of dye, and method described in Arnon, (1949) was followed. Total chlorophyll was extracted in 80% acetone (2 ml) in a pre-cooled mortar-pestle and the extract was centrifuged at 3000 rpm for 15 min. The supernatant was used for the spectrophotometric assay using Agilent Cary 60 UV-Vis spectrophotometer.

Daphnia magna acute immobilisation assay

Daphnia magna is a microcrustacean, representing the lowest level of aquatic zoological organism. For the third level of aquatic toxicity testing, these were used in accordance with the OECD 202 guidelines [OECD, 2004]. Adult daphnids were procured from Neet Aquarium, Tamil Nadu and were cultured in 2 L glass beakers having 1.6 L hard water (160 mg/L CaCaO3) each having 20 adult daphnids. The set-ups were maintained in the incubator at 20ºC with a 16h photoperiod. The daphnids were transferred to fresh water each week and the neonates obtained from the third broods were used for further studies.

For the acute immobilization tests, five neonates were carefully transferred in 100ml glass beakers containing 80 ml test solutions (6.25-100 mg/L malachite green and the corresponding degradation products) using sterile glass pipettes and the beakers were kept covered with watch glasses. No food was provided during this phase and immobilization or death was recorded after 24 and 48h.

Danio rerio acute toxicity assay

Acute toxicity test was performed using zebra fish (*Danio rerio*) to estimate the effect of malachite green (6.25-100 mg/L) and the corresponding degradation product following the OECD 203 (2019) guidelines with some modifications. Each set consisting of ten zebrafish of average length 2.0±1.0cm and average weight 0.45±0.05g were exposed to malachite green, the degradation product and a dye-less control. Experiments were conducted in glass aquaria holding 10L water with a photoperiod of 16h and water temperature 25 °C. Fish mortality and abnormal behaviour or appearance were recorded at regular intervals. Histopathological analysis of tissue sections were also performed.

Toxicity assays with land organisms

Toxicity studies on beneficial soil microorganisms

Strains *Bacillus subtilis* (ATCC 21332) and *Bacillus pumilus* (ATCC 7061) which are commonly found in soil, were used to assess the impact of the dye (100 mg/L) and its degradation product. To estimate the impact of the dye and the degradation product on the growth of these bacteria in liquid medium, 1ml logarithmically growing cultures having optical density 1 at 600nm was inoculated in 100 ml nutrient broth. Growth was analysed by incubating the bacteria in the dye, the degradation product and a dye-less control and the cell density was checked periodically till stationary phase was reached. The antibacterial effect of Malachite Green as well as the degradation product on these bacteria were evaluated. Disc diffusion method was employed to assess the impact of MG and the degradation products, while sterile distilled water was taken as control. Diameters of zones of inhibitions were measured after an overnight (18h) incubation at 37°C.

Eisenia fetida acute toxicity assay (contact test)

Acute toxicity assessment (contact test) was performed using earthworm (*Eisenia fetida*), according to the OECD 207 (1984) guidelines. The *E. fetida* were acquired from Aastha Earthworms, West Bengal. Sterile 30ml borosilicate glass culture vials were lined with same size of filter papers (suitably cut to fit within the vials) soaked in test solutions. In each vial, one healthy adult earthworm was carefully placed. The test was conducted for 48hr. Five vials (carrying one earthworm each) were maintained for each of the test solutions, the corresponding degradation product and sterile distilled water as control. No food was provided during the tenure of the study. Mortality rates were recorded every 24h intervals.

Phytotoxicity

Toxicity of the Malachite Green and the degradation product was evaluated using two economically important crop plants: wheat and pulses. Seed germination index, and root and shoot lengths were taken into account. Tests were performed by methods as described in Biswas et al. (2016). *Triticum aestivum* and *Lens culinaris* were obtained locally. Ten seeds of each of the crops were placed in separate petriplates lined with filter papers soaked in equal volumes of test solutions (Malachite Green, the degradation product and a dye-less control). Germination was continuously monitored on a day to day basis. The lengths of plumules of the germinated seeds were measured and the number of seeds germinated was counted each day until further germinations stopped. Seeds which showed emergence of radical piercing through the seed coat were considered to be germinated. Data for germination and were recorded on the 3rd, 9th and 16th days.

Genotoxicity

Allium cepa bulbs of uniform size and weight (3-3.5g approximately) were obtained locally and the outer loose flaky scales were removed carefully with the help of a pair of forceps. The fresh root primordia that emerged as a result of the denudation step were immersed in the test solutions (6.25-100 mg/L Malachite Green, the corresponding degradation products and a dye-less control). These set-ups were maintained at a

temperature of 25 °C for 72h with a 16h photoperiod. Terminal 1cm portions of the actively growing root tips were excised and rinsed with distilled water and fixed in Carnoy's solution1 (1:3 Glacial acetic acid: ethanol). The fixed root tips were hydrolysed in 1N HCl and then stained with 2% aceto-orcein. Slides were prepared with a drop of acetic acid (45%) followed by squashing. The squashed root tips were then observed under Leica DM 750 microscope and photographed with Leica DFC295 camera.

Cytotoxicity

Two cell lines (keratinocyte HaCaT and cancer cell line HepG2) were used for this study. MTT assay and DAPI imaging of the cells using various concentrations of Malachite Green (100, 50, 25, 12.5 and 6.25 mg/L) and the corresponding degradation products were performed. HaCaT cells were cultured at 37 °C in Dulbecco's Modified Eagle Medium (DMEM) media having 10% Foetal Bovine Serum (FBS) with 1% antimycotic-antibiotic solutions and were maintained at 5% CO_2 and 95% humidity. HepG2 cells were cultured in Minimum Essential Medium (MEM) media containing 1X antibiotic and 10% FBS at 37 °C and were maintained at 95% humidity and 5% CO_2. Both the cell lines were seeded in 96 well plates at a density of 1 x 10^4 cells per well. The cells were incubated for 24 hours and they were treated with varying concentrations of the dye and the degradation product in order to evaluate the toxicity following standard MTT cell proliferation assay. Furthermore, the effects of the test solutions over the cellular viability was assessed using DAPI fluorescent staining following the manufacturer's protocol and visualized by fluorescence microscope (Olympus IX71).

Blood/serum toxicity and histopathology

The undiluted dye (100 mg/L) and the degradation product were tested for the blood/serum toxicity and histopatholoy using mice (*Mus musculus*). All the experiments were performed following the institute animal ethical approval. All the animals were individually maintained with proper ventilation and 12 h light and dark cycles and provided with sterilized food pellets and water ad libitum. For the purpose of evaluation of acute systemic toxicity of the malachite green and the degradation product, mice were fed with 2 g/ Kg of body weight for 30 days of duration. After completion of the study

period, the mice were anesthetized using Diazepam (IP, 10 mg/kg body weight) and Xylazine (IP, 10 mg/kg body weight) subsequently. Followed by anesthesia, about 1 ml of blood was collected using facial vein puncture for serological analysis. The control and test animals were euthanised and organs like kidney, lungs, liver, spleen and heart were aseptically collected for histopathological analysis. All the organ samples were fixed using 10% Neutral Buffered Formalin and subsequently maintained in the room temperature. The fixed tissue samples were subjected to hematoxylin and eosin (H&E) staining followed by paraffin-embedding and sectioning respectively.

All studies performed with animals were conducted on approval of the Institute Animal Ethical Committee of the Indian Institute of Technology, Kharagpur.

Statistical Analysis

All data were analysed by one-way ANOVA with Tukey-Kramer multiple comparison test.

RESULT AND DISCUSSION

Decolorization of Malachite Green by *Stenotrophomonas koreensis*

Malachite green oxalate solution (100 mg/L) in distilled water was subjected to 5mL culture of *S. koreensis* and decolorization was observed intermittently. Nearly 90% decolorization was recorded at 2h. Decolorization gradually increased to 98% at the end of 4h (Figure 3.1). No additional supplement had been added in the decolorization medium. This is the first report of *S. koreensis* concerning the degradation of malachite green.
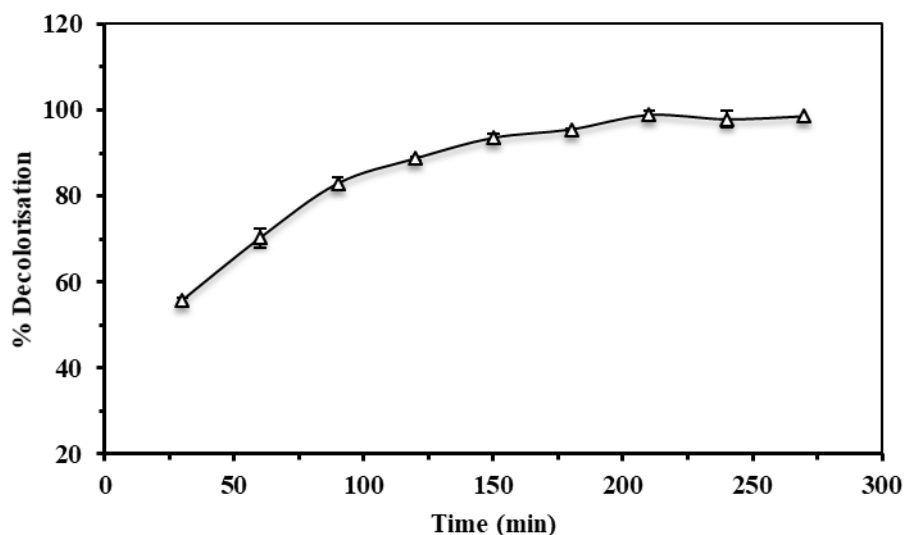
Figure 3.1 Malachite green decolorisation profile of *Stenotrophomonas koreensis*

To date, very few studies have reported such high rates of decolorization (98% decolorization in 4h) of malachite green from aqueous solution in the absence of a nutrient-rich medium. Only recently, Song et al. (2020) reported that *Pseudomonas veronii* could utilize malachite green as the sole carbon source. *P. veronii* degraded 93.5% malachite green (50 mg/L) in seven days from an aqueous solution [Song et al. 2020]. High malachite green decolorization has been reported by Lv G.Y. et al. (2013), where the strain *Deinococcus radiodurans R1* achieves 97% decolorization of malachite green within 0.5 h, initial dye concentration being 200 mg/L in tryptone yeast medium.

Laccase enzyme isolated from the strain *Trichoderma asperellum* also showed excellent malachite green decolorization (97.18%) within 98.58 min [Shanmugam et al. 2017]. However, this exceptional result may be attributed to the purified enzyme where obviously, additional steps of purification had to be performed. The only other strain that shows a comparable efficiency level was reported by Du et al. (2012), where *Micrococcus sp. strain BD 15* has been shown to decolorize malachite green (100mg/L) up to 97% within 1 hr.

Confirmation of Biodegradation of the dye

TLC results indicated complete degradation of the dye and formation of new compounds. In the propanol solvent system, Malachite Green showed an Rf value of 0.7380, whereas the degraded product showed two spots with Rf values 0.571 and 0.714 (data not shown). In the butanol: acetic acid: water (4:1:2) solvent system, three spots appeared with Rf values 0.488, 0.627, and 0.744, while the control spot had an Rf value of 0.651 (data not shown).

For decolorization of dyes, HPLC is considered to be a valuable technique to differentiate between degradation and biosorption. The disappearance of particular peaks and the simultaneous appearance of resultant peaks indicate degradation of dye components and the production of new compounds. Three prominent peaks were observed at retention times 4.415, 4.721, and 5.170 minutes on performing HPLC of the degradation product, while the control dye gave a peak at 4.550 minutes (Figure 3.2).
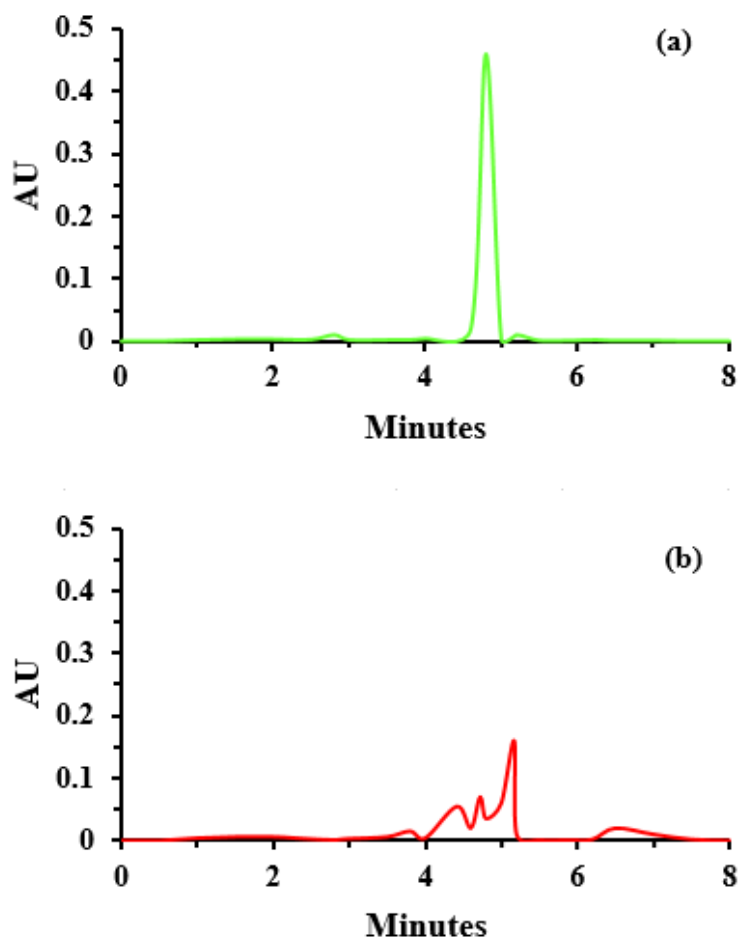
Figure 3.2 HPLC chromatogram of malachite green before (a) and after (b) degradation

In the UV-Vis spectrophotometric analysis, a characteristic λ_{max} of malachite green was observed at 614 nm in the UV-Vis spectrum (Figure 3.3), which is absent in degraded product indicating the disruption of the structure of malachite green due to degradation. A peak around 250 nm in the malachite green indicates the characteristic peak of the benzene ring. In the degraded product, the intensity of this peak increases considerably, indicating the formation of more benzene rings accompanied by extended conjugation in structure due to degradation. A peak around 205 nm in the degradation product indicates the characteristic peak of the solvent water and the merged peak around 230 nm may be due to the formation of conjugated products of degradation.
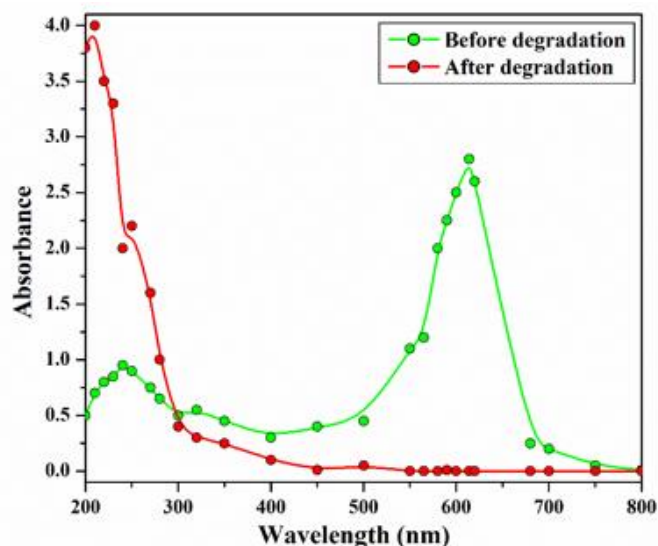
Figure 3.3 UV-Vis spectra of malachite green before and after degradation

In FTIR spectrum (Figure 3.4) in 1400-1600cm^{-1} aryl amine, C=N and NH2 stretching of primary and secondary amine are present in control malachite green. With degradation, the breaking of bonds decreases peak intensity, indicating a considerable decrease in these groups (aryl amine C=N and NH2). The formation of more COOH and C=O groups and increase in amines resulted in the enhancement of peak intensity over 2500-3000 cm^{-1} in the degraded product. Two to three bands around 1600 cm^{-1} due to C=C of benzene ring present in the malachite green have diminished after degradation, indicating benzene ring opening. Characteristic meta/para-substituted benzene ring peak around 650-900 cm^{-1} was present in the control dye. However, in the degraded product, the intensity of these peaks decreased considerably, which may be due to the opening of the benzene ring by degradation resulting in disruption of para and meta substituted position. Around 3200-3400 cm^{-1} the N-H stretching and shifting towards 3600 cm^{-1} after degradation indicates the formation of –OH group present either in alcoholic or phenolic form. Again peak intensity in the range 3200-3400 cm^{-1} for –OH of -COOH has increased significantly, indicating the formation of a lot of acidic -COOH groups. The hump around 3200-3600 cm^{-1} indicate the presence of hydrogen-bonded –OH groups in the degraded product, whereas in undegraded malachite green, this hump is absent, and the sharp peak is present in considerably less intensity between 3500-3600 cm^{-1} (may be due to oxalic acid of malachite green oxalate). Prominent aromatic –CH stretching around 2980 cm^{-1} in the control dye is not present in the degraded product.
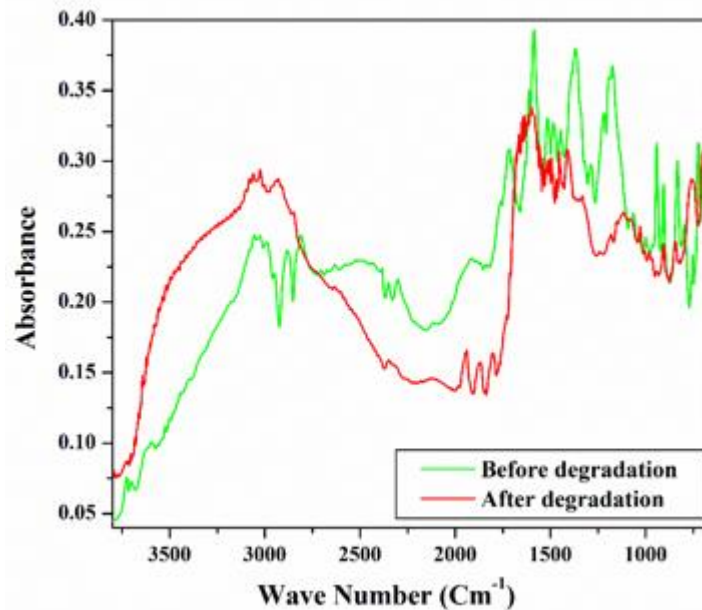
Figure 3.4 FTIR spectra of malachite green before and after degradation

From all the above analyzes, it was clear that decolorization of malachite green took place due to biodegradation of dye by *S. koreensis*.

Impact of Nitrogen and Carbon supplements on decolorization

Often, the supply of additional carbon or nitrogen sources causes stimulation of the dye degradation process [Sihag et al. 2014]. The impact of organic and inorganic nitrogen supplements (1g/L) on the decolorization process was also explored. Six organic sources (soymeal extract, beef extract, peptone, tryptone, urea, and thiourea) and three inorganic sources (sodium azide, sodium nitrite, and calcium nitrate) of Nitrogen were used (Figure 3.5a and 3.5b). The organic complex supplements outperformed the inorganic supplements. The addition of soymeal extract resulted in 95% decolorization within 1h and 98% within 2.5h. Peptone enhanced the decolorization to 98.6% within 2.5hr. Urea also had a strong positive impact on decolorization (97.91% in 2.5hr). The effect of carbon sources (10g/L) like dextrose, fructose, ribose, and molasses were studied. Figure 3.5c shows the comparative results. Dextrose and fructose boosted decolorization to 90% in 1h and 94% in 2.5h due to the bacteria's absorption and metabolization of the readily available carbon sources [Carolin et al. 2021].
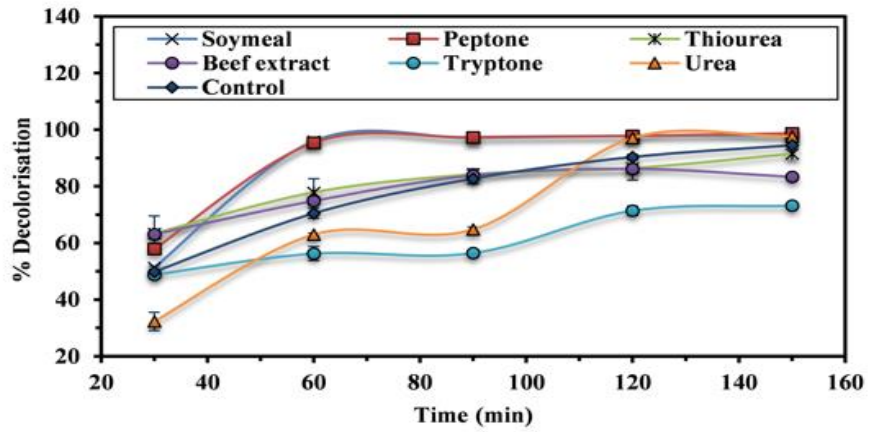
a
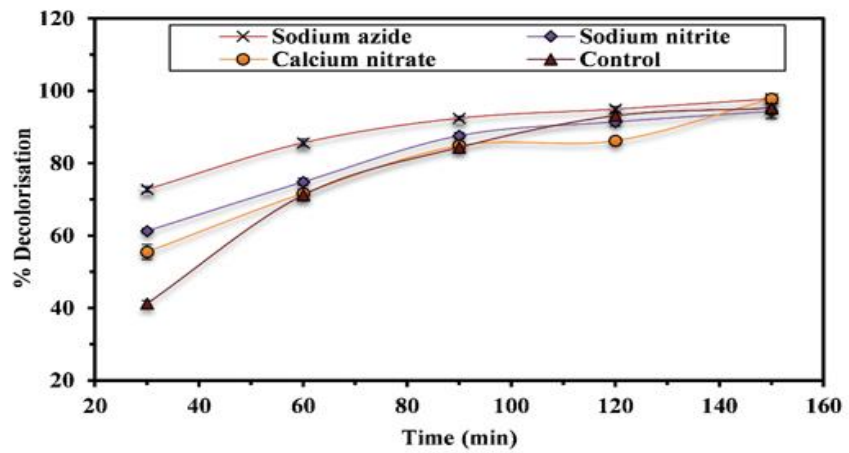
b
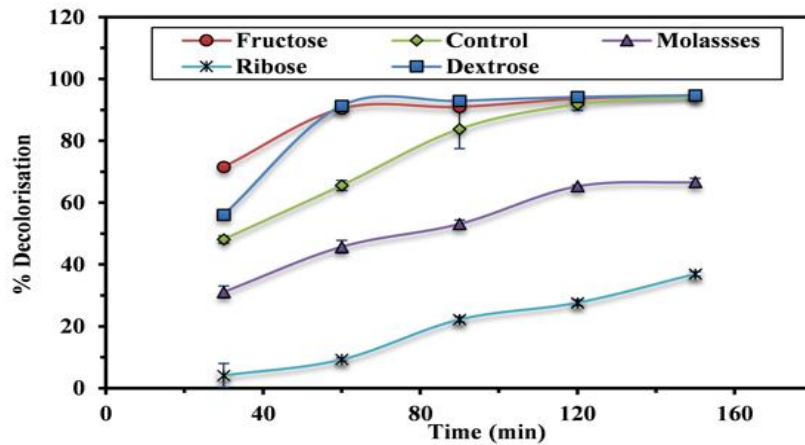
c

Figure 3.5 Optimisation of malachite green degradation by *S. koreensis* using different organic (a) and inorganic nitrogen (b) and carbon (c) sources

Physicochemical conditions affect the rate and efficiency of dye degradation to a considerable extent. Vignesh et al. (2020) reported about 60% decolorization of malachite green by *Streptomyces chrestomyceticus* in 96h, but on supplementation of 1% glucose and pH7, the decolorization increased to 99%. In this study, the supplements of carbon sources like fructose amplified the decolorization of malachite green by *S. koreensis*. Fructose enhances bacterial decolorization of methyl orange by *Aeromonas* sp. strain DH-6 (Du et al., 2015). For methyl orange decolorization by *Micrococcus yunnanensis*, glucose was found to be the optimal carbon source [Carolin et al. 2021], but on the other hand, glucose was also reported to inhibit malachite green decolorization by *Kocuria rosea* [Parshetti et al. 2006]. We observed that the addition of ribose and molasses inhibited the process of decolorization by *S. koreensis*. However, Parshetti et al. (2006) reported 100% decolorization of malachite green by *Kocuria rosea* in the presence of 0.5% molasses. So it can be presumed that the effects of carbon supplements on the process of decolorization greatly vary with the bacterial strains and the dyes involved.

Degradation of malachite green by *S. koreensis* was enhanced by applying supplementary nitrogen sources, especially soymeal extract and peptone. Modi et al. (2010) reported similar results where peptone strongly enhanced azo dye decolorization. Peptone was reported to be the best nitrogen source for producing malachite green degrading enzymes like laccase and manganese reductase in white-rot fungi [Levin et al. 2010]. Anthraquinone dye degrading laccase production by *Pleurotus ostreatus* was enhanced in the presence of urea [Jang et al. 2005]. Hence, it can be concluded that the presence of organic nitrogen supplements in the decolorization media positively influences the production and functioning of enzymes responsible for the degradation of malachite green and thus hastens decolorization.

Estimation of a response surface for maximal decolorization

Central Composite Design (CCD) was applied to optimize the three variable factors: pH, temperature, and inoculum size. The highest decolorization was 98.78%, at pH 6, temperature 45ºC, and inoculum 6.36ml. The response obtained thereby were expressed

as a function of the independent variables (Table 3.1). A regression model was created in Minitab 19.0.

The model equation for the decolorization was expressed as:

Percentage Degradation = -32.7 + 8.65 pH + 3.658 Temperature + 1.59 Inoculum - 0.796 pH*pH- 0.04460 Temperature*Temperature - 0.384 Inoculum*Inoculum+ 0.0336 pH*Temperature + 0.573 pH*Inoculum + 0.0294 Temperature*Inoculum

Equation 3.7

Table 3.1. Details of RSM Analysis

Details of Response Surface Methodology (Central Composite Design)					
Independent Variables	**Levels**			**Star point α=1.68**	
	Low (-1)	**Central (0)**	**High (+1)**	**-α**	**+ α**
pH	1.6	6	10.5	1.5	13.57
Temperature (⁰C)	20	46.27	70	2.95	87.04
Inoculum size (mL)	1	3	5	0.36	6.36
Details of Optimization					
Run No.	*pH*	*Temperature (⁰C)*	*Inoculum size (mL)*	*% Decolorization*	
1.	6.0	45.0	3.00	89.51	
2.	10.5	20.0	1.00	40.55	
3.	6.0	45.0	3.00	89.51	
4.	1.5	70.0	5.00	32.47	

5.	6.0	45.0	3.00	89.51
6.	6.0	45.0	0.36	76.17
7.	10.5	20.0	5.00	64.11
8.	13.6	45.0	3.00	61.54
9.	10.5	70.0	1.00	41.86
10.	10.5	70.0	5.00	71.30
11.	1.5	70.0	1.00	23.66
12.	6.0	45.0	3.00	89.51
13.	6.0	45.0	3.00	89.51
14.	1.5	20.0	1.00	37.47
15.	6.0	3.0	3.00	13.45
16.	6.0	45.0	3.00	89.51
17.	6.0	45.0	6.36	98.78
18.	6.0	87.0	3.00	7.88
19.	1.5	20.0	5.00	40.40
20.	1.6	45.0	3.00	63.85

The prediction accuracy was cross-validated by the Leave-One-Out-Cross-Verification (LOOCV) method using MATLAB R2021a. Cross-validation is a technique used to

analyze test errors. Here, the data is divided into two parts: a training set and a validation set. In LOOCV, each observation serves as the validation set, while the remaining (n-1) observations (n is the total number of observations) serve as the training set. The model is fitted, and the data is used to forecast an observation value. The process is repeated n times. This technique aids in the reduction of bias. In this study, the model's fitness was substantiated by the cross-validated correlation coefficient (94.05%) between the actual and predicted decolorization and indicated that the model was significantly close to the actual experimental results (Figure 3.6). Hence the model could be applied for correct predictions.
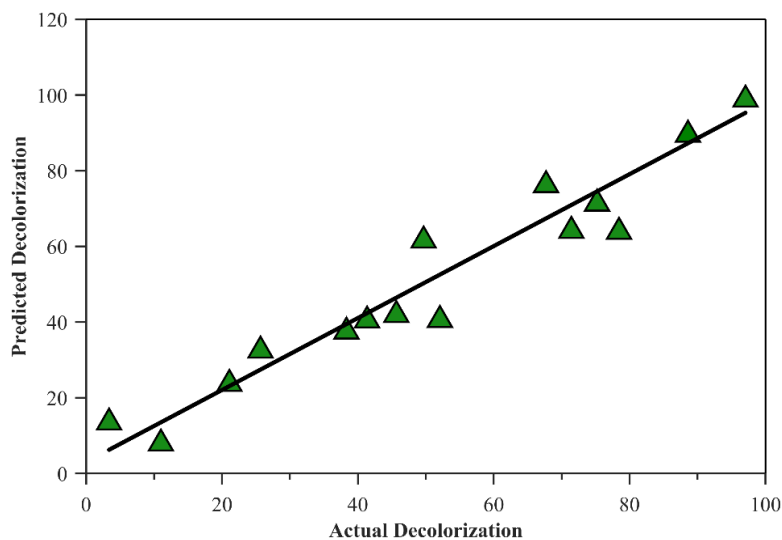
Figure 3.6 Regression plot of decolorization: prediction by the model vs. actual decolorization

ANOVA results indicated that the model was highly significant, as suggested by the F value (21.4) and a very low p value (Table 3.2). The p values of the linear terms were <0.01indicating pH, temperature, and inoculum size had a significant influence on decolorization.

Table 3.2 ANOVA for RSM model

Parameters	Value
p value	<0.0001
F value	21.4
R^2	0.9507

Effect of interactions of the process variables

The contour plots generated using Minitab 19.0 (Figure 3.7a, 3.7b, 3.7c) indicates the collective effects exerted by combinations of the process variables. A pH in the range of 6 to 8 and a temperature of 40 °C to 50 °C gives the highest decolorization (Figure 3.7a). An increase in the inoculum size correspondingly improves decolorization (Figure 3.7b). The maximum removal efficiency was obtained at 45 ℃ and 6.36mL inoculum. Below 30 ℃ and beyond 60 ℃, decolorization is significantly reduced. When inoculum and temperature are varied simultaneously, the temperature, rather than the inoculum size, profoundly influences the decolorization percentage (Figure 3.7c). Although more inoculum leads to greater decolorization, if the optimum temperature is not provided, the decolorization would be of low grade. pH 6-8 is optimal for the decolorization process. pH plays a role as vital as the temperature in malachite green degradation. Highly acidic pH like 4 or highly alkaline pH like 10 is inhibitory to the decolorization process. Rather than the conventional "one-factor-at-a-time" optimization approach, the RSM model provides an idea of the combined effect of the variable parameters. Using RSM also gives an additional advantage of identifying a "range" rather than a particular value for an optimized response, decolorization.

Experimental confirmation of RSM

Another three experimental runs validated the model under the optimal conditions obtained from CCD (pH 6, temperature 45^0C, and inoculum size 6.36ml). The decolorization percentage obtained experimentally under the given optimal conditions was 97%. Hence, the experimentally derived aligned with the decolorization predicted by the model (98.78%).
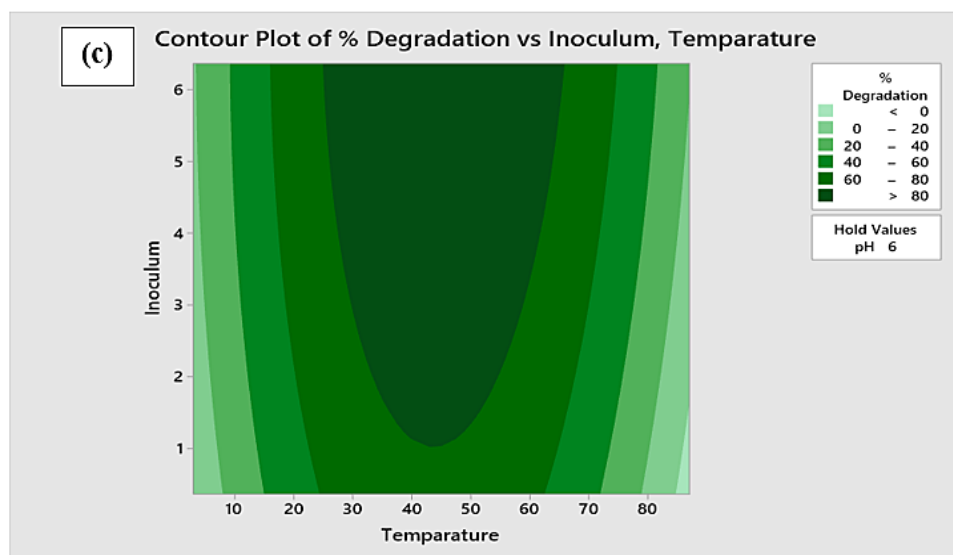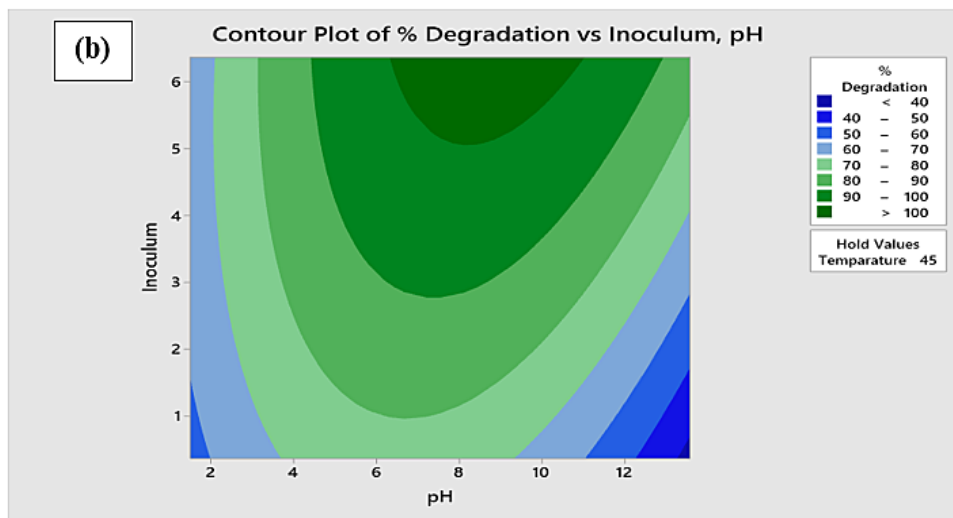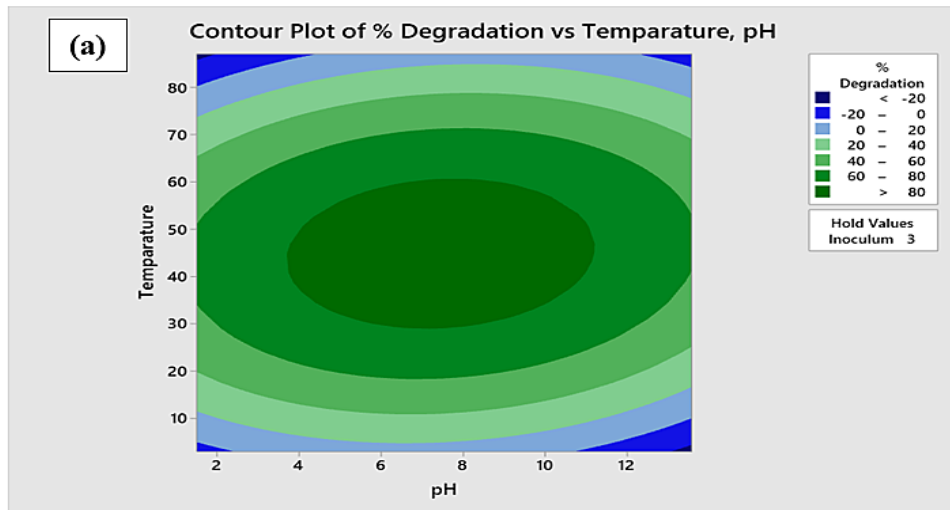
Figure 3.7 RSM contour plot: effect of (a) temperature and pH, (b) inoculum size and pH and (c) inoculum size and temperature on decolorization

In our study, *S. koreensis* was able to show maximum degradation of malachite green at a considerably higher range of temperature (40ºC -50 ºC). Although dye biodegradation is known to occur most commonly at temperatures up to 35 ºC, biodegradation at higher temperatures has also been documented. Purified enzyme Triphenylmethane Reductase (TMR), responsible for decolorizing triphenylmethane dyes like malachite green and crystal violet, was isolated from *Citrobacter* sp. and worked optimally at temperature 60ºC [Hou et al. 2004]. Surface-expressed TMR on E. coli exhibited high activity and stability at 50 ºC [Gao et al. 2014]. Azoreductases present in two strains of *Pseudomonas aeruginosa* were reported to work optimally at 40ºC [Elfarash et al. 2017]. The range of suitable pH for decolorization of malachite green by *S. koreensis* was 6 to 8. The decolorization of malachite green has been reported to occur over a wide range of pH: ranging from alkaline to acidic. *Pseudomonas veronii* can decolorize malachite green maximally at a nearly neutral pH (7.1) [Song et al. 2020]. The optimum pH for malachite green degradation by *Photobacterium leiognathi* is 8 [Sutar et al. 2019]. Slightly acidic pH was optimal for the degradation of malachite green by *Achromobacter xylosoxidans* [Qiao et al. 2011].

Potential of *S. koreensis* on the decolorization of other dyes

Several dyes, including some azo and triphenylmethane dyes, were treated with *S. koreensis*. Various decolorization patterns were observed (Figure 3.8). The most promising result was recorded in the azo dye Methyl Orange, which was decolorized up to 96% at the end of 10 days. More than 80% decolorization was also recorded for Methyl red. However, this trend was not followed by the other azo dyes like Acid orange 6 or Direct Yellow. Safranin and Direct Yellow showed the least decolorization. Overall, *S. koreensis* could efficiently decolorize a triphenylmethane dye (malachite green) and an azo dye (methyl orange) simultaneously offers a promising alternative for bioremediation of textile or tannery effluents which very often contain multiple dyes.
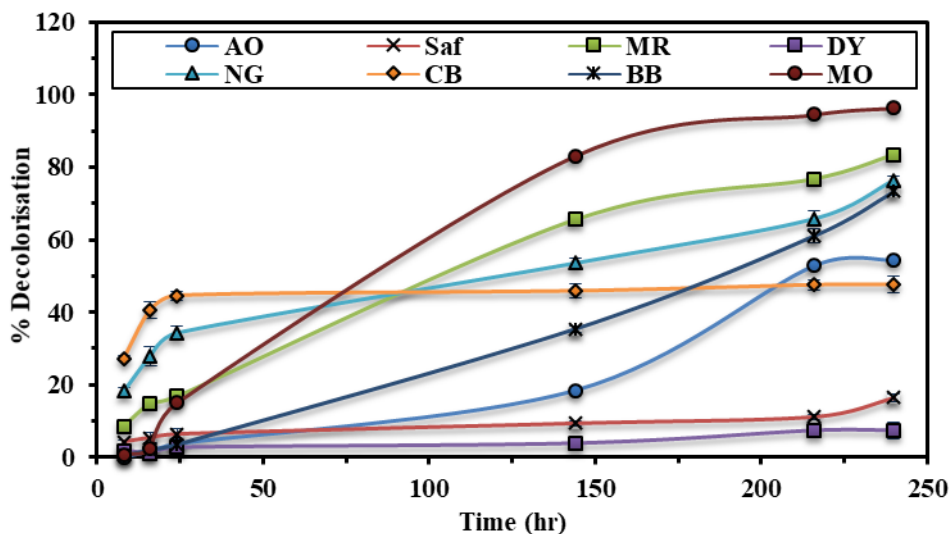
Figure 3.8 Decolorization of some industrial dyes (Methyl orange: MO, Safranin: Saf, Methyl Red: MR, Direct Yellow 27: DY, Acid Orange 6: AO, Cotton Blue: CB, Basic Blue 3: BB, Naphthol Green B: NG) apart from malachite green by *S. koreensis*

Chemically and structurally diverse synthetic dyes are frequently present in the industrial wastewater from tanneries and textiles. As a result, a consortium of microbes is required to decolorize the effluents, with each strain decolorizing a different dye. Reports of a single strain capable of decolorizing multiple classes of dyes with very different structural and chemical characteristics are rare. *S. koreensis* can decolorize triphenylmethane dye malachite green as well as azo dyes like methyl orange and methyl red. Another example of a bacterium capable of decolorizing an azo dye as well as a triphenylmethane dye is *Kocuria rosea MTCC 1532*. It was able to decolorize both methyl orange and malachite green [Parshetti et al., 2006].

Immobilization of *S. koreensis*

Bacteria are often immobilized into beads for easier handling. Variable volumes of *S. koreensis* cultures were immobilized into PVA-sodium alginate beads (Figure 3.9). When 9ml *S. koreensis* culture was immobilized into beads and employed to decolorize malachite green (100mg/L), it showed 95.49% decolorization in 10 h (Figure 3.10).

However, the efficiency of decolorization was much lower than the culture in its basic form. If 9ml culture is immobilized into beads and used, the same decolorization percentage (95%) could be obtained in 3 h. However, immobilization provides other advantages over liquid culture. Apart from handling convenience, these beads can be recovered and reused easily after two to three washes of sterile distilled water. Although decolorization was much slower in the second batch, more than 68% of dye could be decolorized in 96 h. Blank beads (without bacterial culture) were also employed to decolorize malachite green but showed no decolorization. The prepared beads remain viable for up to three weeks if stored at 4 °C.

(a)   (b)
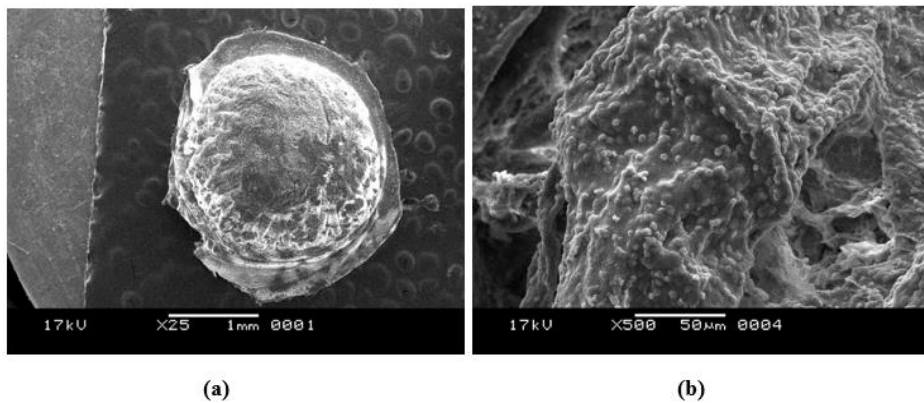
Figure 3.9 SEM micrographs of *S. koreensis* loaded biobead: (a) bead and (b) its internal structure
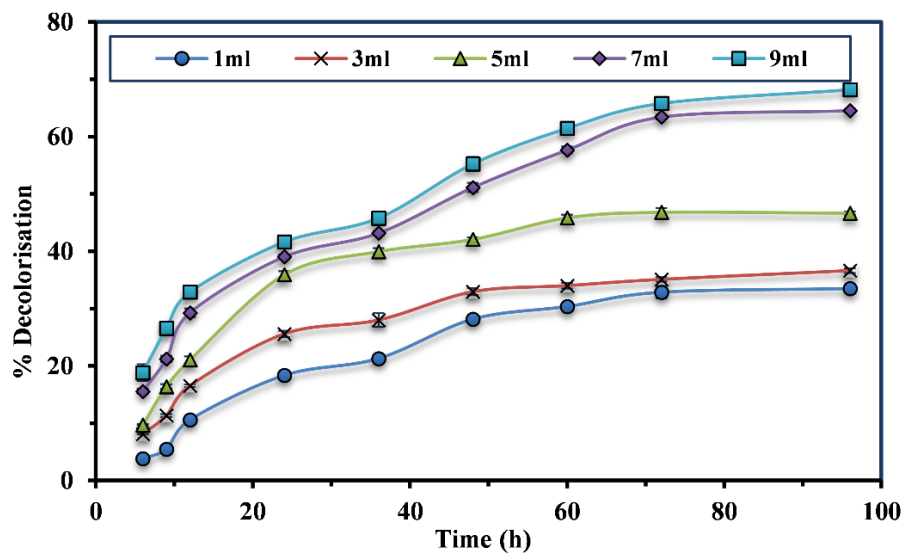
Figure 3.10 Decolorization of malachite green using immobilized *S. koreensis* with varying amount of bacterial culture

Many authors have studied the decolorization of dyes by microorganisms immobilized in beads. About 81.7% Yellow GR dye was degraded by *Bacillus subtilis* immobilized in sodium alginate beads (Narayanan et al., 2015). Electrospun cellulose acetate nanofibrous web (CA-NFW) was used by San et al. (2014) to immobilize bacterial strains and degrade 95% methylene blue within 24h. *Aspergillus oryzae* was used as a natural immobilization agent to immobilize *Pseudomonas sp.* DY1, which showed up to 93% malachite green decolorization [Yang et al. 2011]. Phugare et al. (2010) described Plaster of Paris as a cheap, readily available material to immobilize yeast cells and decolorize malachite green.

Effect of heavy metals on decolorization of malachite green

A time-dependent decolorization study was conducted in the presence of the heavy metals: chromium, cadmium, lead, and arsenic, which are nearly almost invariably present in tannery and textile effluents (Figure 3.11). In all the cases, heavy metals negatively impacted decolorization compared to the control (no heavy metal). As a general trend, high doses of heavy metals in the media cause retardation in bacterial growth. An increase in heavy metal concentration correspondingly resulted in a decrease in decolorization percentages. Patil et al., 2012 reported *S. koreensis* to remove lead and cadmium from the medium by producing bio-surfactants. However, only 10% decolorization was recorded in the presence of 0.1 g/L cadmium. *S. koreensis* decolorized more than 80% malachite green in 3h in the presence of 0.01g/L lead in the medium. Decolorization was reduced to less than 30% in the presence of 0.1g/L chromium. The effect of arsenic was relatively milder: even at a concentration of 0.25 g/L arsenic, 87% decolorization could be achieved within 3h.
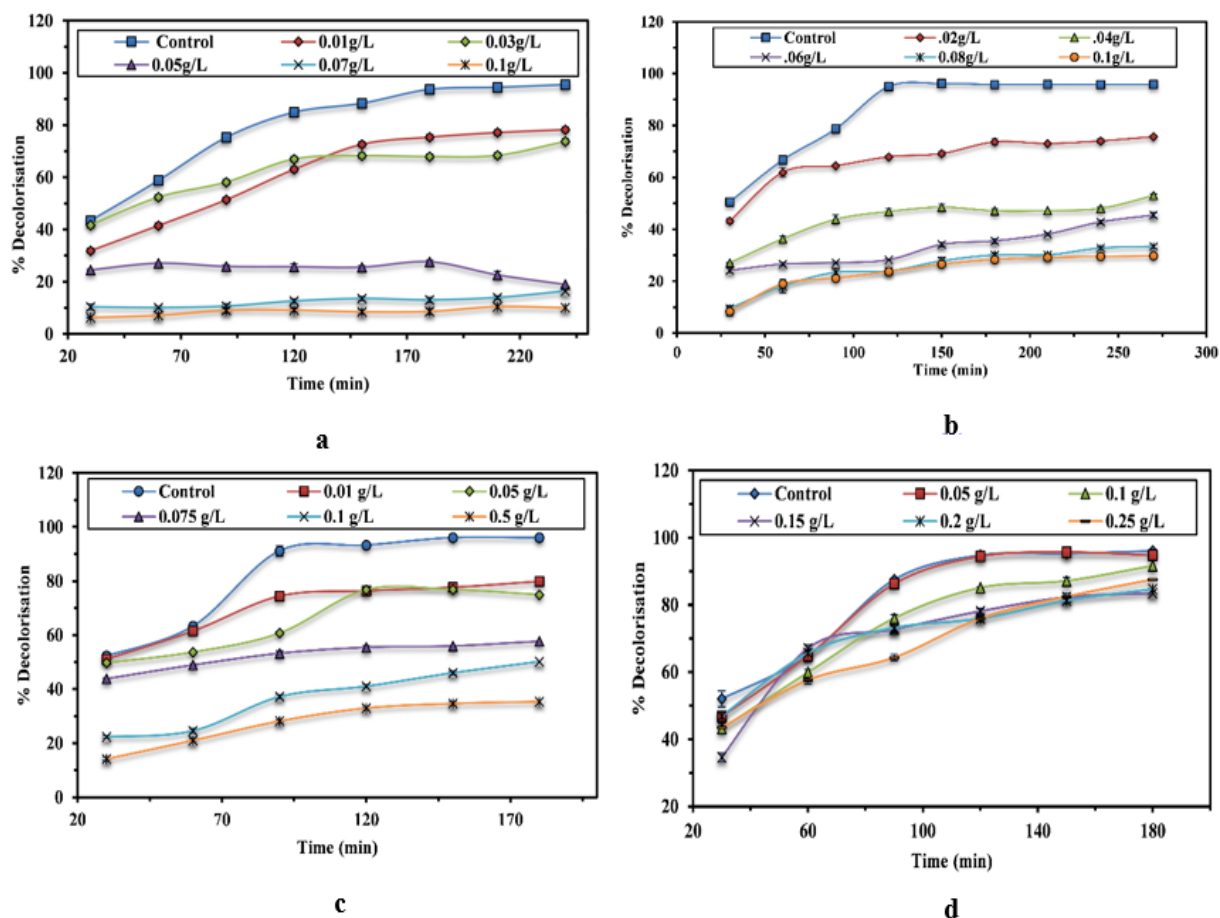
Figure 3.11 Effect of heavy metals (a) cadmium, (b) chromium, (c) lead and (d) arsenic on the degradation efficiency of malachite green by *S. koreensis*

Congo red degradation by *Pseudomonas sp.* was reported to remain significantly unaffected by the presence of the heavy metal chromium due to its highly potent chromium reductase enzyme [Gopinath et al. 2011]. Zinc, copper, and lead inhibited the decolorization of dye Poly R-478 in *Lentinula edodes* [Hatvani & Mécs 2003]. Lorenzo et al. (2006) reported a striking observation: some heavy metal ions like Ag^+, Mn^{2+}, Cd^{2+}, and Zn^{2+} exhibited a slight stimulatory effect on laccase production from *Trametes versicolor,* which resulted in the enhanced decolorization efficiency for indigo carmine dye. *Pseudomonas aeruginosa* strain HF5 was able to decolorize more than 90% Reactive Red 120 even in the presence of 100 mg/L lead [Hafeez et al. 2018]. *Psychrobacter alimentarius* KS23 and *Klebsiella oxytoca* N7 decolorized 83% Reactive Black 5 in the presence of 100mg/L Chromium [Khalid et al. 2015]. *S. maltophila* is resistant to heavy metals and can grow in their presence [Alonso et al. 2000, Pages et al. 2008]. However, whether the presence of heavy metals affects its decolorizing ability has not been studied. Patil et al. (2012) reported *S. koreensis* resistant to heavy metals like

Cadmium and Lead. In the present study, it was observed that *S. koreensis* could decolorize malachite green in the presence of heavy metals to varying degrees, depending upon their concentrations.

Enzyme Analysis

Bacteria produce dye degrading enzymes in two forms: constitutive and inducible. The constitutive enzymes are present at all times, even in the absence of dyes, while inducible enzymes are secreted only in the presence of the dyes [Sari and Simarani, 2019]. Table 3.3 represents the data obtained on the analysis of the malachite green degrading enzymes of *S. koreensis*. The laccase and lignin peroxidase concentration was higher in the control cells than those obtained after decolorizing malachite green. The activities of tyrosinase, MG reductase, and NADH-DCIP reductase increased significantly in cells that decolorized malachite green, suggesting that the dye induced the activity of these three enzymes when present in the medium. Thus from the experimental results, it can be concluded that tyrosinase, MG reductase, and NADH-DCIP reductase contribute significantly to the decolorization of malachite green by *S. koreensis*.

Table 3.3 Activities of different malachite green (MG) degrading enzymes in *S. koreensis*

Enzymes	Control cells	Cells harvested after decolorization of MG
Laccase[a]	0.0042±0.0002	0.0024±0.0011***
Tyrosinase[a]	0.0843±.0017	0.0856±0.038**
Lignin Peroxidase[a]	0.074±0.0022	0.062±0.0015
MG Reductase[b]	0.0218±0.0016	0.0318±0.0005*
NADH-DCIP Reductase[c]	0.0696±0.0137	0.1466±0.0153 **

Values are means of three sets of experiments ± SE. Significantly different from control cells at *$p<0.05$;**$p<0.01$;***$p<0.001$ by two-tailed p-values comparison.

[a] μmol/ mim/mL,

[b] μg MG reduced /min/mg cells,

[c] μg DCIP reduced /min/mg cells

Bacteria produce several enzymes which can degrade dyes. Azo-reductase, laccase, lignin peroxidase, aminopyrine N-demethylase, manganese peroxidase, malachite green reductase, triphenylmethane reductase etc. are some of the widely studied dye-degrading enzymes. Both purified enzymes [Shanmugam et al. 2017; Yang

et al., 2016] and bacterial cultures have been used to degrade dyes. Significant increases in the activities of MG reductase and NADH-DCIP reductase were reported for the degradation of malachite green, indicating the involvement of these inducible enzymes in *Saccharomyces cerevisiae* [Jadhav and Govindwar, 2006]. Mn-peroxidase, NADH-DCIP, and MG reductase were responsible for the biodegradation of malachite green by *Pseudomonas* sp [Du et al., 2011]. Tyrosinase, laccase, Lignin Peroxidase, NADH-DCIP reductase, and MG reductase facilitated malachite green degradation by *Aeromonas* sp. [Du et al., 2018]. Liu et al. (2020) cloned the genes Lac (laccase), MnP (manganese peroxidase), and LiP (lignin peroxidase) from *Aspergillus* sp. TS-A into the fungus *Pichia pastoris*. The recombinant genes were expressed in *P. pastoris* and showed efficient degradation of the azo dye Congo Red. Moreover, it was observed that the combined effect of all the three enzymes was more robust than the individual enzyme. Hence, similarly, the genes responsible for malachite green degradation in *S. koreensis* can be expressed in other species and exploited for heavy metal resistant malachite green degradation.

Kinetics of degradation

It is necessary to perform kinetic investigations to understand the conditions and mechanisms for pollutant degradation [Zhan et al., 2020]. The kinetics of degradation was analyzed under the optimal decolorization conditions. Figure 3.12 (a), (b), and (c) shows the plots for the kinetics study. It can be observed from the kinetic plots that the R^2 value for the ln C_t vs. t plot is the highest, i.e., 0.978 (compared to the other models, where R^2 values are 0.84 and 0.82 for the zero order and second-order kinetics, respectively), indicating the reaction is best fitted to the equation $\mathbf{C_t = C_0 e^{-kt}}$. Therefore the decolorization of malachite green by *S. koreensis* can be described by a first-order model, and the first-order rate constant k_1 is 0.04min⁻¹. The first-order rate constant represents the amount of malachite green biodegraded or eliminated from the solution in a given period. In this study, the first-order rate constant is 0.04 per min, which means that ~0.04% of the amount of dye remaining in the solution is biodegraded each minute [Hinderliter & Saghir, 2014]. The rate constant is calculated from the slope of the ln C_t vs. t plot, as shown in Figure 3.12b.
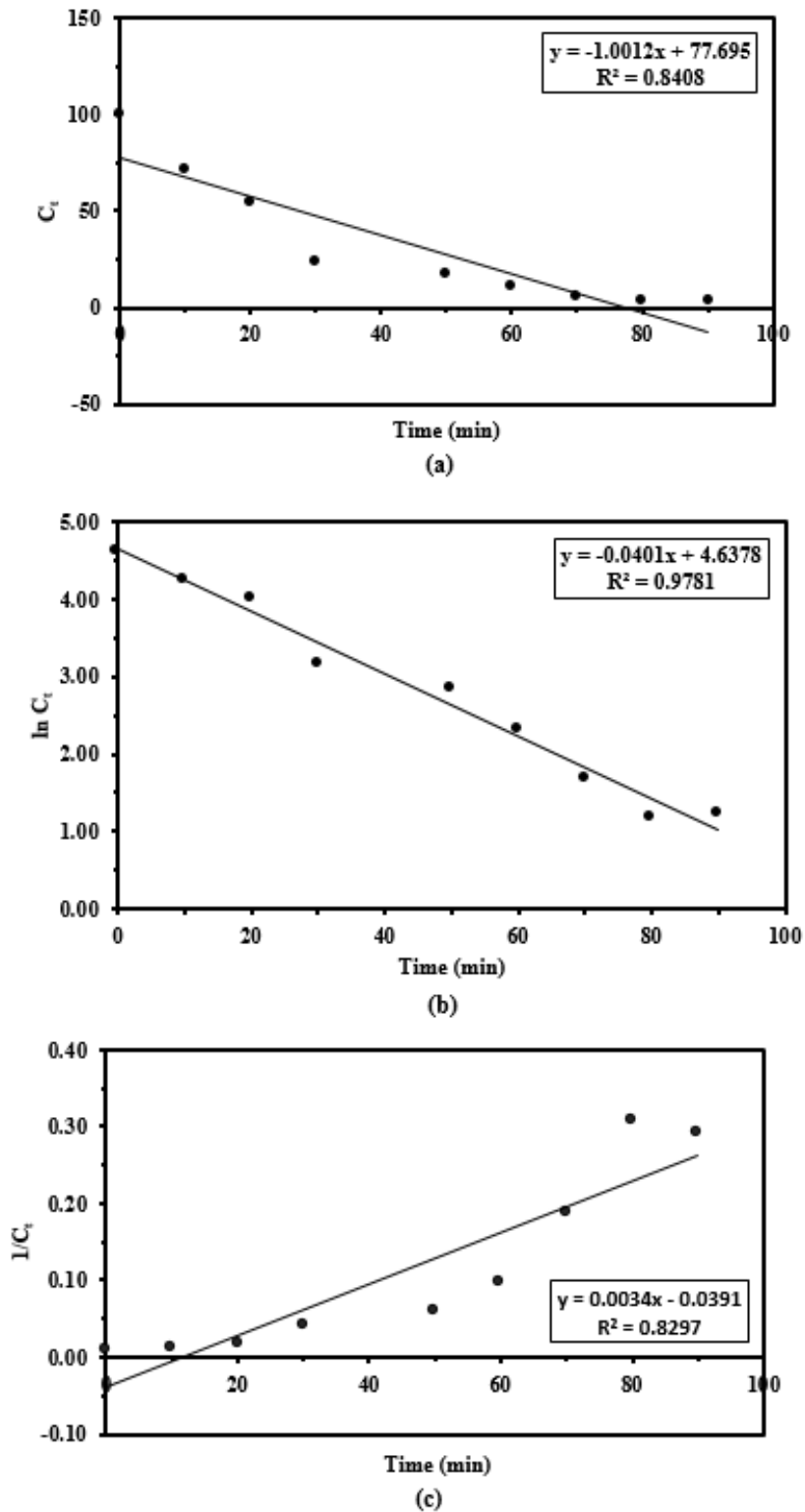
Figure 3.12 Kinetic model of decolorization of malachite green by *S. koreensis*: Ct vs t (a), 1/Ct vs t (b) and lnCt vs t (c)

The kinetics of biodegradation gives crucial information about the efficiency of the process and the viability of scaling it up [Wanyonyi et al., 2017]. Biodegradation of dyes following the first-order reaction kinetics has been reported by many authors previously. Biodegradation of acid dye Azo Red 18 followed the first-order kinetics [Koupaie et al., 2012]. *Ochrobactrum* sp followed the first-order kinetics during the degradation of malachite green [Vijayalakshmidevi and Muthukumar, 2014]. Etezad and Sadeghi-Kiakhani (2021) reported that the biodegradation of malachite green by soil bacteria followed the first-order reaction kinetics. Enzymatic degradation of Reactive Orange 13 by *Alcaligenes faecalis* followed first-order kinetics [Shah et al., 2012]. Wanyonyi et al. (2017) reported a similar observation where enzymes from *Bacillus cereus* degraded malachite green following first-order kinetics.

Toxicity of malachite green before and after treatment

The ecotoxicological evaluation of malachite green biodegradation by *S. koreensis* was performed with a wide range of aquatic and terrestrial organisms, representing the key levels of the ecosystem. To calculate an endpoint for quantitatively expressing the toxicity of the dye and the degradation product, a range of treatment solutions were prepared by two-fold serial dilutions as mentioned in Gioia et al. 2018. Hence, the undiluted, ½ diluted, ¼ diluted, 1/8 diluted and 1/16 diluted dye (translating to 100, 50, 25, 12.5 and 6.5 mg/L malachite green) and the corresponding degradation products were tested.

Aquatic toxicity

Algae acute toxicity assay

A gradual decrease of the average specific growth rate could be observed with the increase in dye concentration giving clear indication of toxicity to the algae (Figure 3.13). The undiluted degradation product showed 26% inhibition, while dye concentrations higher than 50 mg/L lead to complete inhibition of growth (Figure 3.14). The percentage inhibition of growth was also calculated from the specific growth rate. For 6.25 mg/L malachite green and its degradation product, the percentage inhibition of growth were 44.31% and 4.26% respectively, indicating a significantly lesser toxicity

(p<0.05) of the degradation product than the original dye. Algae forms the basic level of all aquatic ecosystems. The impacts of the toxic element that inhibits the growth of these primary producers will inevitably reach the ecosystem's upper layers. Only a very limited amount of research has been performed to determine the toxic effects of textile dyes on microalgae compared to other toxicants like heavy metals [Gita et al., 2019]. The effect of Indigo dye containing effluent on *Scenedesmus quadricauda* was studied by Chia and Musa (2014). They observed a systematic decrease of cell number with the increase in effluent concentration. The specific growth rate of yeast continually decreased with increasing concentrations of Reactive Blue 172 and Direct Red 28 [Solis et al., 2012]. Gita et al. (2019) studied the effect of Optilan yellow, Drimarene blue and Lanasyn brown on *Chlorella vugaris*. They observed 100% growth inhibition for 30ppm dye concentrations for all the three dyes [Gita et al., 2019]. All of the above-mentioned literature supported the observations of the present study. Although there are a few articles on the toxicity of dyes on algae, this is the first report on the toxicity assessment of the degradation product of malachite green on any microalgae. Since there is a paucity of data on the toxic effects of malachite green and its degradation product on microalgae, this article will aid future investigations.
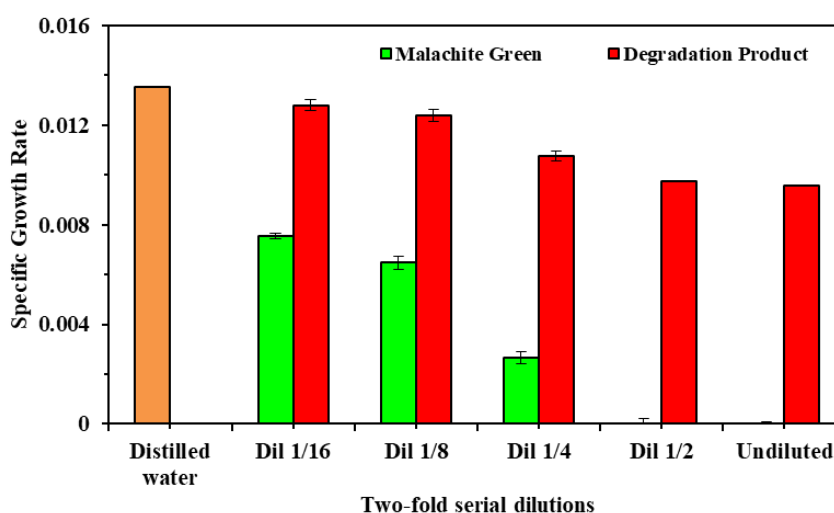
Figure 3.13 Change in the specific growth rate of *Anabaena flos-aque* in presence of different concentration of malachite green and the degradation product
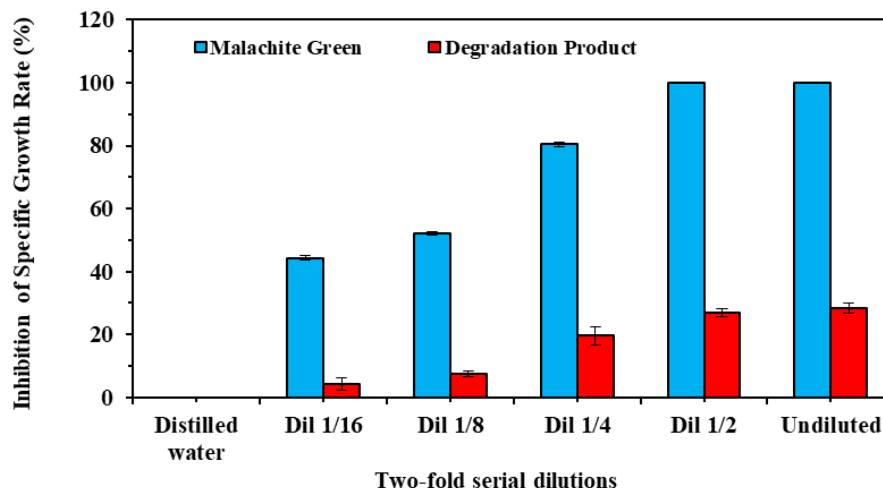
Figure 3.14 Inhibition of specific growth rate of *Anabaena flos-aque* under the influence of malachite green and the degradation product

Lemna **acute toxicity assay**

The floating macrophyte *Lemna minor* is a common biological indicator used for toxicity estimation. The specific growth rates of the plants steadily decreased with the increase in the dye concentration till 50 mg/L (Figure 3.15 and Figure 3.16). The highest specific growth rate was recorded for the control group. The specific growth rates of the plants grown in all the concentrations of the degradation product were significantly higher ($p < 0.01$) than the corresponding concentrations of the dye. More than 73% inhibition of growth was recorded for the undiluted malachite green. A similar trend could be noted in case of the chlorophyll content of the *L. minor*. The lowest total chlorophyll (0.3 mg/g fresh weight) was recorded for in the plants grown in the highest concentration of the dye (Figure 3.17). Almost colourless fronds appeared in the *Lemna* grown in 100 mg/L malachite green (Figure 3.18). Lesser chlorophyll contents correspond to lower photosynthetic capability and results in a lower biomass. Chlorophyll content of plants grown in the degradation product, although less than that of the control, was significantly higher ($p < 0.01$) than that of the plants grown in the higher dye concentrations.

Lemna minor is a bio-indicator plant that colonies in freshwater bodies and is commonly employed for the evaluations of environmental and toxicological concerns. Adomas et al (2020) studied the effect of the textile dyes Gentian Violet on the growth parameters of *L. minor*. They reported that Gentian violet changed the putrescine (Put) production

pathway, raised tyramine content, inhibited S-adenosyl methionine decarboxylase activity, and inhibited ornithine decarboxylase (ODC) activity. Micropollutants like caffeine, benzophenone, bisphenol, etc., exerted inhibitory effects on the growth and chlorophyll production of *Lemna minor* [Fekete-Kertész et al., 2015]. Presence of even very nominal amount of dye in the growth media can cause distortions of the leaf and root anatomy. For example, 0.01μg/L Congo Red causes severe shriveling of upper and lower epidermis. At 0.04μg/L Congo Red, reduction of mesophyll tissues and dissolution of aerenchyma occurs in *L. minor* and leaves start falling at the bottom of the aquarium [Al-Zurfi et al., 2020].
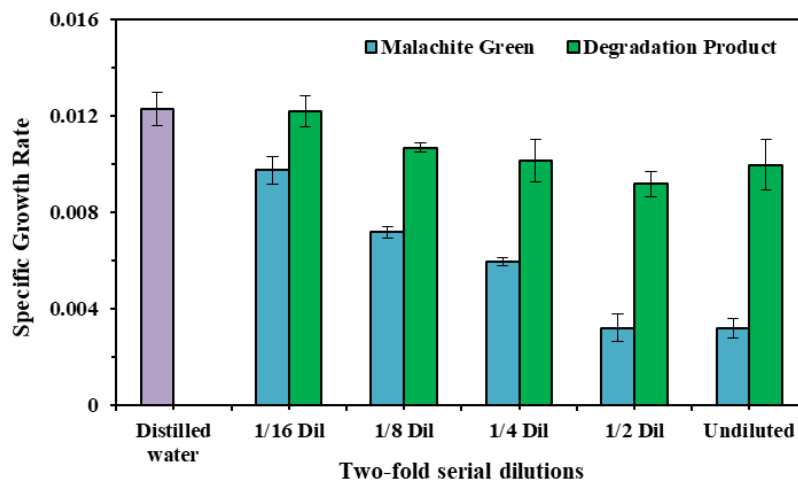
Figure 3.15 Effect of malachite green and the degradation product on the specific growth rate of *Lemna minor*
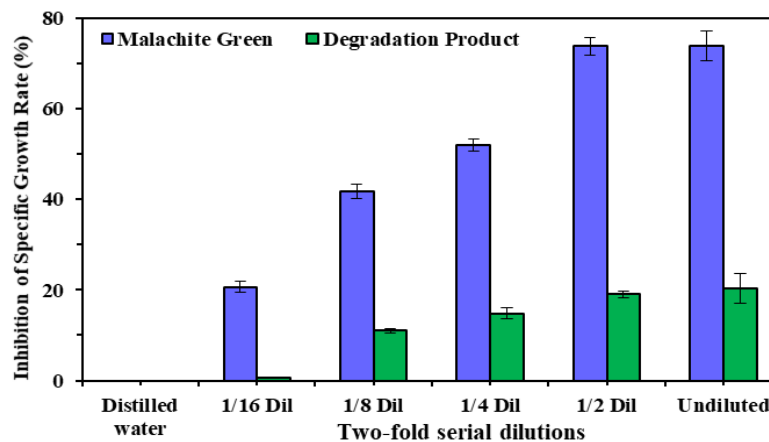
Figure 3.16 Inhibition of the specific growth rate of *Lemna minor* under the influence of malachite green and the degradation product
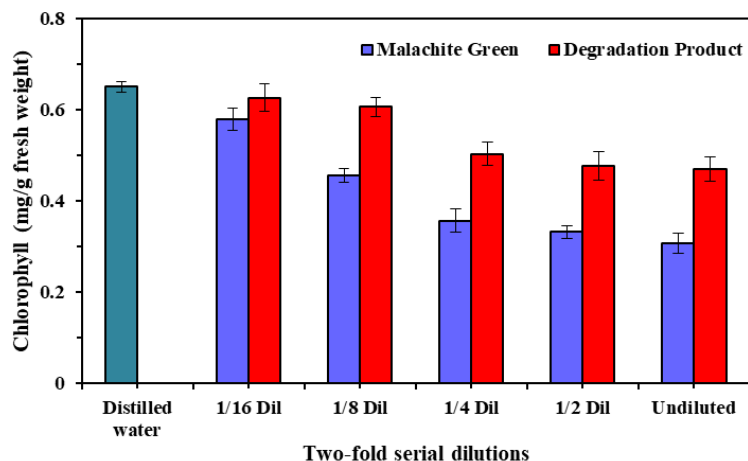
Figure 3.17 Chlorophyll content of *Lemna minor* in presence of malachite green and the degradation product
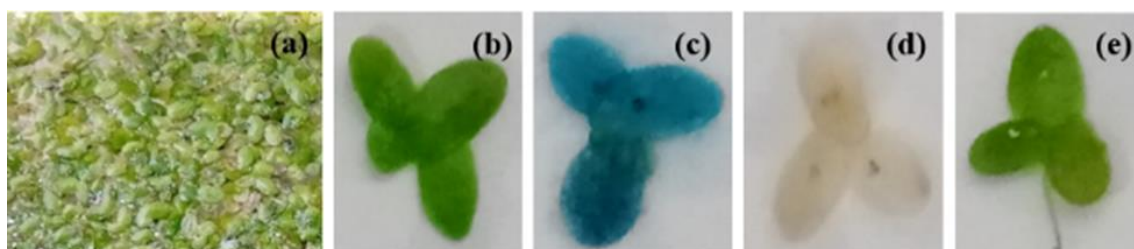
Figure 3.18 Control *Lemna minor* (a) and (b); *L. minor* fronds exposed to diluted (1/4th dilution) malachite green (c); Colourless frond of *L. minor* generated on exposure of the aquatic plant to undiluted malachite green(d); and undiluted degraded product causes almost no alteration (e)

Daphnia magna **immobilisation assay**

The dye and the degradation product were tested for potential ecotoxicity on the representative zooplakton *Daphnia magna*. No deaths were observed in the lowest dye concentration (6.25 mg/L) in the first 24 h. While all of the daphnids died within 2h of exposure in the highest dye concentration (100 mg/L), more than 86% viability was recorded for the daphnids treated with the undiluted degradation product. Significantly higher viability (p <0.01)) was observed in the *Daphnia* neonates for those exposed to the degradation product than those exposed to the dye, as represented in Figure 3.19. A microscopic image of *D. magna* with internalized malachite green is depicted in Figure 3.20. *Daphnia magna*, the aquatic microcrustacean can survive in a variety of water-bodies ranging from fresh water ponds to acidic lakes [Ebert, 2005]. The toxicity of

textile dyes and their degradation products have been tested on *D. magna* by some authors. Gioia et al. (2008) decolorised the two toxic azo dyes Acid Red 88 and Acid Black 172 by immobilised laccase enzyme of *Trametes villosa*. In the *D. magna* acute toxicity test, the dye Acid Red 88 showed lesser toxicity than the degradation product. Approximately 100% and 60% death of the neonates were recorded for the undiluted degradation products and the dye (100mg/L) respectively. The non-genotoxic dye Direct Blue 218 has a 48h LC50 of 3.6mg/L for *D. magna* [Bae and Freeman, 2007]. Lumbaque et al. (2015) observed that the degradation product of the azo dye Reactive Black 5 was slightly more toxic than the original dye due to the production of aromatic amines during the degradation process. For azo dyes, in most of the cases, the degradation products were more toxic than the original dyes, due to the production of copious amounts of aromatic amines. The 48h EC50 value for *Daphnia magna* ranged from 0.29-0.77 mg/L for azo dye Reactive Black 5 [Material Safety Data Sheet of Malachite Green Oxalate salt, Sigma-Aldrich, 2014; Kanhere et al., 2014]. However, in case of triphenylmethane dyes like malachite green, the observations are different. Plachtová et al., (2018) reported that except for algae and cyanobacteria, the superparamagnetic iron oxide nanoparticles had no harmful effect on *Lemna minor* or *D. magna* up to a concentration of 1 g/L. This result is consistent with the observations of the present study where the product of malachite green degradation by *S. koreensis* is significantly less toxic than the original dye ($p < 0.05$).
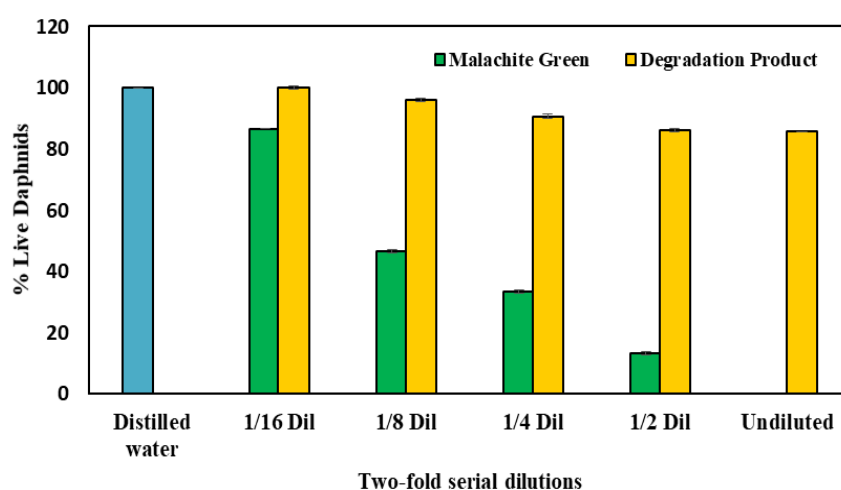
Figure 3.19 Effect of malachite green and the degradation product on *Daphnia magna*: Percentage of live Daphnids in different concentration of Dye and its degraded product.

Figure 3.20 Microscopic view of malachite green taken up by *Daphnia magna*

***Danio rerio* acute toxicity assay**

Zebrafish (*Danio rerio*) treated with malachite green showed loss of equilibrium, production of excessive mucus, and convulsion. The fish treated with the undiluted dye showed hemorrhagic lines anterior to the anal fin and 100% fish mortality was recorded within 38min. For the lowest dose of malachite green (6.25 mg/L), all the fish died within 3h (Table 3.4). The experiment was carried out for 7 days with the corresponding dosages of the degradation product, although no death or abnormal behavior was recorded for degraded product.

Liver of zebrafish is a model for studying liver diseases in humans. Bile improves lipid-soluble nutrient absorption while also facilitating the excretion of cholesterol and toxic metabolites, especially bilirubin [Romano et al., 2020]. Prominent dilations of the bile ducts were observed in the fish exposed to the dye and it progressively increased with the increase in concentration of the dye while the ones treated with the degradation product showed no significant morphological changes (Figure 3.21). Dilation of the bile ducts in case of alcoholic liver disease in zebrafish had been previously reported by Lin et al. (2015). Dilated bile duct may be a manifestation of cholestasis which is a disease that disrupts bile flow, resulting in bile fluid accumulation in the liver. Significant morbidity and mortality may be caused by cholestasis due to pruritus, malnutrition, portal hypertension, biliary cirrhosis etc. [Pham and Yin, 2019]. The actual blocking of bile flow at the level of extrahepatic biliary ducts is a major mechanism of cholestasis and retained bile leads to hepatotoxicity [Shah and John, 2019]. Failure to transport these bile salts results in their accumulation in the liver. The bile salts' powerful detergent-like effect causes membrane injury and degradation of membrane function which is reflected by the histopathological examinations of *Danio* liver tissues (Figure 3.22).

Histopathology of zebrafish exposed to the treatments (1/8th dilution and above) gave clear indication that liver tissues showed significant damage for the dye-treated fish while the ones treated with the degradation product remained almost unaffected, apart from slight dilations of sinusoids. The polygonal shape of the hepatocytes was clearly disrupted, along with irregular or broken cell borders indicated cell damage in case of the dye-treated fish. The hepatocytes of dye-treated fish showed abundant pyknotic nuclei indicating their moribund condition on H&E stained sections, compared to the control and degradation product treated ones. Lin et al., 2015 investigated hepatocytes with condensed cytoplasm in *Danio rerio* and reached the conclusion that they contained glycogen or mucosubstances like glycoproteins, glycolipids or mucins. Severely dilated sinusoids were also observed in the liver of the dye-treated zebrafish. Dilation of sinusoids is caused by enlargement of hepatic capillaries and usually leads to blockage in the hepatic venous outflow [Branchatelli et al., 2018].

Table 3.4 Percentage mortality of *Danio rerio* on exposure to malachite green (MG) and its degradation product (DP)

Two-fold serial dilutions	Percentage fish mortality							
	40 min		80 min		160 min		320 min	
	MG	DP	MG	DP	MG	DP	MG	DP
1/16 Dil	0	0	30	0	80	0	100	0
1/8 Dil	20	0	40	0	100	0	100	0
1/4 Dil	50	0	70	0	100	0	100	0
1/2 Dil	80	0	100	0	100	0	100	0
Undiluted	100	0	100	0	100	0	100	0

Figure 3.21 Gross appearance of the common bile duct (arrow) in *Danio rerio*. (a) Normal appearance of the common bile duct in the control (non-treated) fish, (b) Bile duct of the fish exposed to undiluted degradation product, and (c) Severely dilated bile duct of the fish treated with undiluted Malachite green
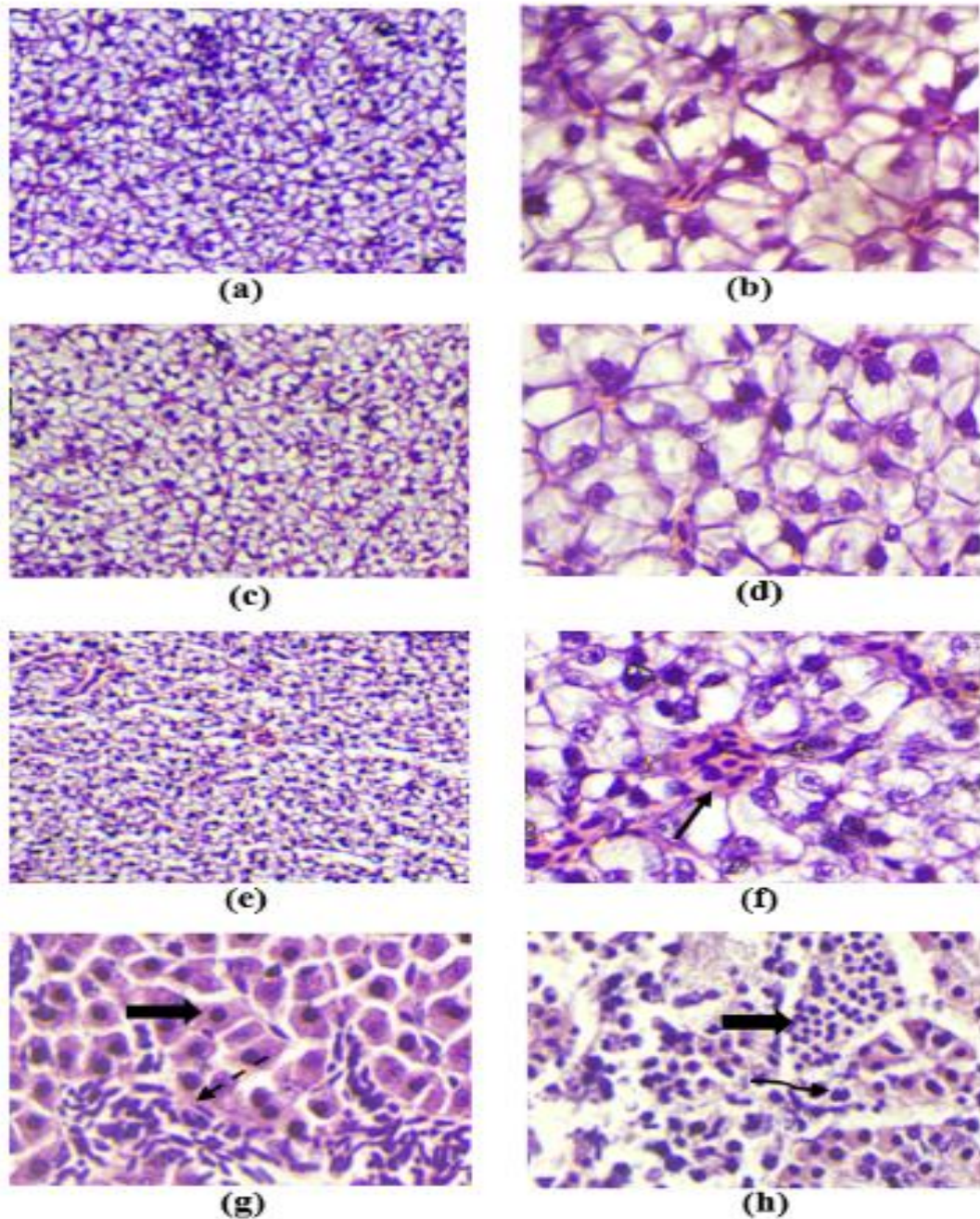
Figure 3.22 Liver section of control *Danio rerio* showing normal polygonal hepatocytes and sinusoids, H & E stain x100 (a), x400(b). Micrograph of liver section of *Danio* treated with the degradation product. Almost no alteration of tissue structure is seen, apart from a slightly dilated sinusoids. H & E stain x100(c), x400(d). Micrograph of liver sections from *Danio* treated with 100 mg/L malachite green x100 (e), x400 (f, g, h). Severely dilated sinusoids (f, arrow), increased macrophages and loss and shrinkage of the polygonal cells into angular masses (g, broken arrow), Pyknotic nuclei (g, h broad arrow), deformed and dilated bile duct (h, bent arrow)

Malachite green has been already reported to exert detrimental toxicity on liver [Donya et al., 2012]. But our study revealed that the product obtained after the biological degradation of malachite green by this bacterium renders it remarkably safe. Thus, it can be stated that degradation of the dye by the bacteria leads to mitigation of the toxic effects that the untreated dye exerts on aquatic life.

Toxicity to beneficial soil bacteria

Microbial toxicity assay

Several bacteria that inhabit the soil adds to the soil fertility by processes like nutrient mineralization, promotion of plant growth hormones or playing roles as plant pest repellents. We chose two such strains *Bacillus subtilis* and *Bacillus pumilus* to see if the dye and its degradation product exert any toxic effect on them (Figure 3.23 and 3.24). This was important because, the dyes that come out through the effluents not only pollute the rivers, water-bodies and oceans alone, but also contaminate adjoining land areas. The growth curves of the two bacterial strains were observed after exposing them to the undiluted dye (100 mg/L) and its degradation product. In case of the undiluted dye-exposure, a prominent extension of the lag phase was observed. The lag phase is known to prepare the bacteria for the upcoming phases of the growth cycle. An extended lag phase therefore indicates that the bacteria required more time to prepare itself for reproduction which, in turn, is a clear sign of toxicity. On the other hand, the bacteria grown in presence of the undiluted degradation product followed a very similar timescale as of the control. The removal of toxicity in the degradation product could thereby be claimed.
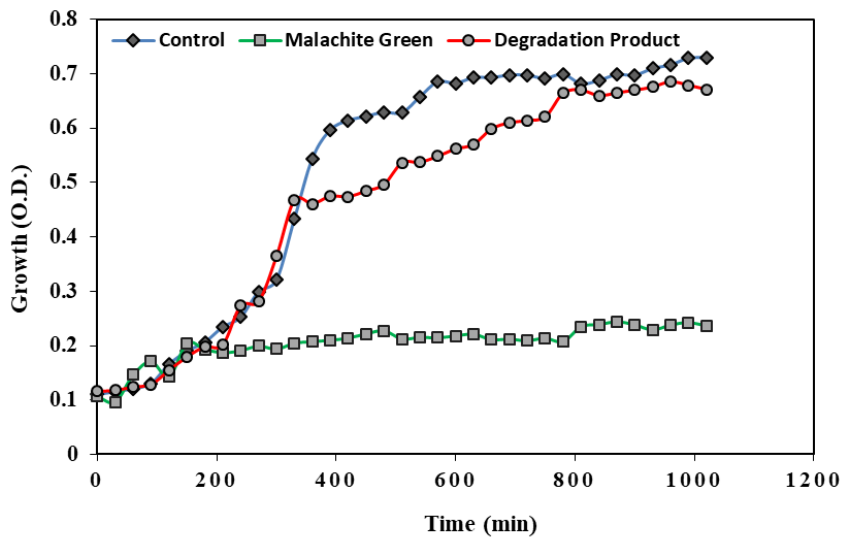
Figure 3.23 Growth curve of *Bacillus subtilis* after exposure to dye and degradation product
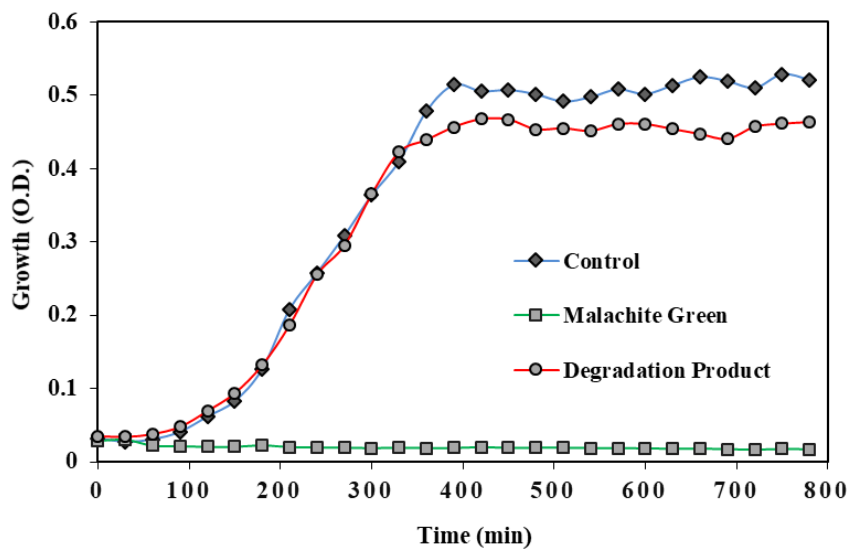
Figure 3.24 Growth curve of *Bacillus pumilus* after exposure to dye and degradation product

For a closer look and to assess the exact amount of decrease in toxicity, a conventional agar-cup assay was performed. No inhibition zone was observed in case of the degradation product, while clear halo of 53 mm and 62 mm was recorded for the malachite green for *B. subtilis* and *B. pumilus* respectively (Figure 3.25 and Table 3.5). Microbial toxicity studies have been used by many authors for testing the ecotoxicity of dyes and their degradation products. *Staphylococcus aureus* was subjected to malachite

green and product of its degradation by *Bacillus vietnamensis*. Compared to the malachite green (50 mg/L), the degradation product showed no inhibition zone at all, indicating its lesser toxicity to *S. aureus* [Kabeer et al., 2019]. Malachite green (100 mg/L) was more toxic than its degradation products on *Escherichia coli* [Chen et al., 2009]. Chaturvedi and Verma (2015) employed the bacterium *Ochrobactrum pseudogrignonense* to degrade malachite green. Agar cup assays with *S. aureus* indicated that the degradation products were significantly safer than the undegraded malachite green. *Enterobacter asburiae* degraded malachite green and its degradation products were non-toxic to *Micrococcus luteus*, *Klebsiella pneumonie* and *Aspergillus sp* [Mukherjee and Das, 2013]. Gopinathan et al. (2014) observed that malachite green extended the lag phase of non-target soil bacteria and fungi like *Bacillus subtilis, Azotobacter* sp. *Saccharomyces cerevisiea* etc. The observations of the present study were consistent with these reports.

Table 3.5 Agar cup assay of *B. subtilis* and *B. pumilus* with dye and degradation product

Bacterial strains	Control	Malachite Green	Degradation product
	Diameter of inhibition zone (cm)		
Bacillus subtilis	No inhibition	0.53±0.015	No inhibition
Bacillus pumilus	No inhibition	0.62±0.025	No inhibition

Values are expressed as Mean±SD of three replicates

a   b
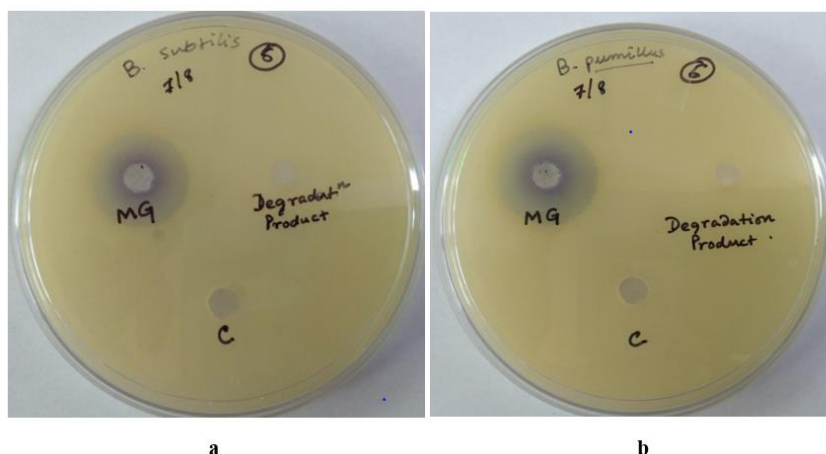
Figure 3.25 Agar cup assay of malachite green and the degradation product with (a) *Bacillus subtilis* and (b) *Bacillus pumilus*

Eisenia fetida acute toxicity assay

Just like the beneficial soil bacteria, earthworm *Eisenia fetida* also contributes to soil fertility. They are also known as "natural tillers of the earth" and form an integral part of vermicomposting. These organisms are important from the aspect of organic farming which is now regarded as one of the most ecologically sustainable techniques for increasing soil fertility, rather than the use of chemical fertilisers. Earthworms respire through their skin and the chemicals to which they are exposed are directly absorbed inside their body through the skin. A contact toxicity test was performed by exposing the earthworms to dye and the degradation product. In 48h, only a slight decrease in viability was observed (93.4%) when compared to the control (100% viability). *E. fetida* exposed to the undiluted malachite green showed severe damage leading to their decomposition, while the ones exposed to the undiluted degradation product showed no significant alteration in their appearance (Figure 3.26 and 3.27). Significantly reduced toxicity in terms of the organism's viability was exhibited by the degradation product compared to dye concentrations ¼ th dilution onwards ($p < 0.01$).

Several authors have reported bloody lesions, depigmentation and detachment of posterior part of the body under the effect of toxic pesticides in earthworms [Rao and Kavitha, 2004; Reddy and Rao, 2008; Yasmin and Souza, 2010]. Similarly, toxic textile dyes can be lethally ecotoxic towards *E. fetida*. For example, the textile dye Acid Red causes DNA damage and death in coelomates including *E. fetida* [Sathya et al., 2009]. Gopinathan et al. (2014) studied the effect of malachite green on some non-target soil organisms including *E. fetida*. The estimated 48h LC_{50} was 2.6 mg cm^{-2}. The azo dye Red BS and Methyl Red were tested on *Pheretima posthuma*. The LD_{50} of Red BS and Methyl Red dye solution was 120.22 and 218.77 mgL^{-1}, respectively. Initially sluggish movements were observed, followed by reduction in pigmentation, development of multiple lesions and death. When the degradation product was evaluated in *P. posthuma*, the toxicity was much lower: no deaths were reported after 48 hours of application of degradation product of the 100mg/L Red BS [Gupte et al., 2013]. Observations of the present study are consistent with the above reports.
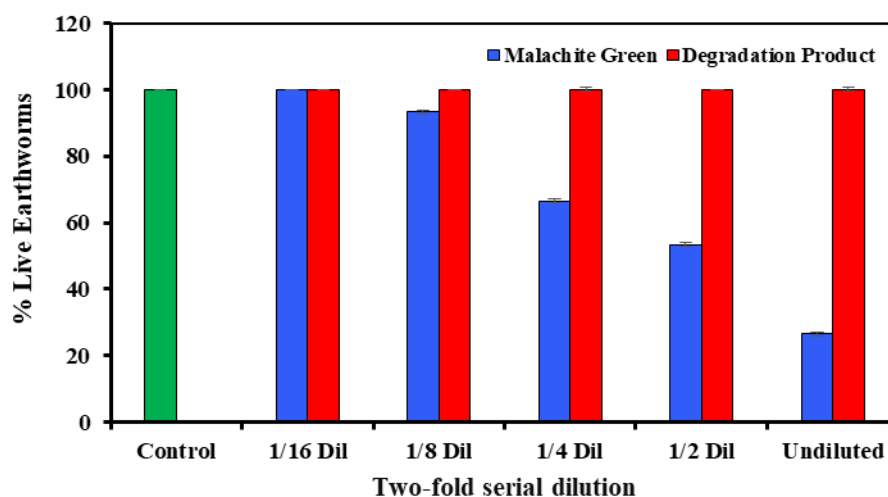
Figure 3.26 Effect of malachite green and the degradation product on *Eisenia fetida*
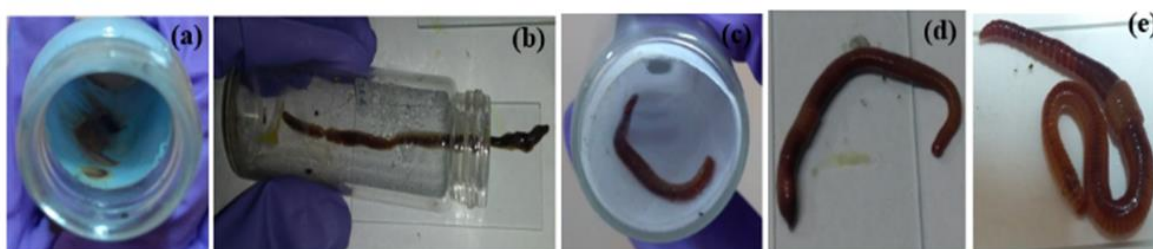
Figure 3.27 Results of ecotoxicological studies with *Eisenia fetida* : (a) and (b) Completely damaged *E. fetida* carcass on exposure to undiluted malachite green; (c) and (d) *E. fetida* on treatment with the degraded product; (e) Control *E. fetida*

Phytotoxicity

Wheat and pulses are the major cereal crops and forms the staple diet of the Indian subcontinent. Germination of seeds is a fairly common approach to determine phytotoxicity of the chemicals to the crops. Out of the two crops, *Triticum aestivum* seemed to be more affected by the toxicity of the dye, where germination was completely inhibited on exposure to the undiluted dye (100 mg/L), while the corresponding degradation product lead to 58.3% germination. In case of *Lens culinaris*, more than 85% germination was recorded for the 1/16th dilution of the degradation product, which is nearly comparable to water (89.35%). Significantly higher germination rates were recorded for both the crops grown in the degradation product than those grown in the dye (Figure 3.28). Phytotoxicity is the inhibitory effect exerted by a toxic element on plant germination and overall growth. If utilized for irrigation in agricultural fields, untreated industrial effluents contaminated with dyes and other hazardous chemicals may be detrimental. When water is scarce, however, sufficiently treated and recycled wastewater can be utilized instead. In this scenario, phytotoxicity testing is critical. Several plant

species have been used for the assessment of phytotoxicity. Lucerne seeds grown in malachite degradation products showed germination rates similar to water [Du et al., 2011]. *Nicotiana tabacum* and *Lactuca sativa* seeds showed similar results [Yang et al., 2015]. Amin et al. (2020) studied both aquatic and terrestrial phytotoxicity of Direct Red-81and its degradation product. The dye inhibited *Lemna minor* growth, while its degradation product was significantly less toxic. Phytotoxicity tests with *Vigna radiata*, *Raphanus sativus,* and *Abelmoschus esculentus* showed similar results where the untreated dye was more toxic than the degradation product. The degradation of Congo Red by recombinant enzymes expressed by *Pichia pastoris* yielded degradation products that were less toxic than the original dye [Liu et al., 2020]. In our study, phytotoxicity experiments indicated that biodegradation of malachite green by *S. koreensis* generated significantly safer and less toxic compounds.
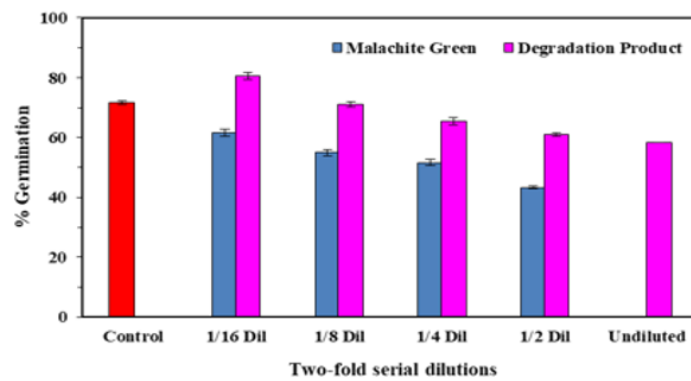
a
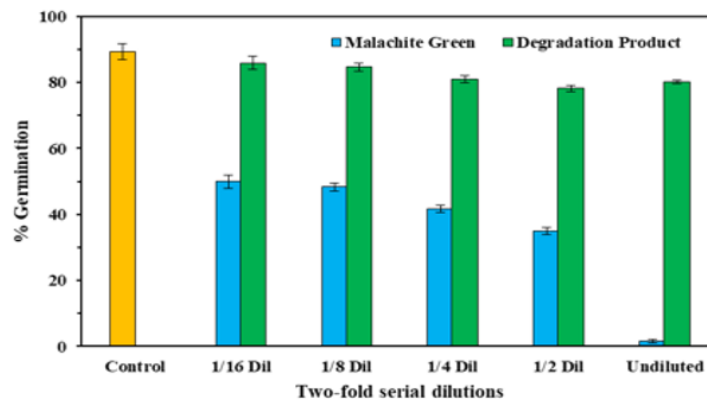
b

Figure 3.28 Effect of malachite green and the degradation product on the germination of (a) *Triticum aestivum and* (b) *Lens culinaris*

Serum toxicity in mice

It was observed that the serum albumin values of the dye-treated (100 mg/L) animals increased when compared with the degradation product. Serum albumin has been reported to have a positive correlation with hypothyroidism [Koga et al., 2009]. Increased serum levels may be attributed to its impaired metabolism as a result of the malachite green treatment. The albumin and cholesterol values of the animals exposed to the undiluted degradation product were observed to be significantly lower than the dye treated animals. Similarly, the increase in the serum cholesterol levels may be due to the effect of thyroid hormone on the cholesterol synthesis and metabolism. The presence of elevated amount of both HDL and LDL cholesterol in blood serum could be due to the effect of hypothyroidism that ultimately resulted in the increased values of cholesterol. Most of the circulating enzymes, transporters of mammalian system can be regulated by the macromolecular concentration of metabolites. It was reported by Sinha et al., (2018) that the incidence of hypothyroidism might be associated with Non-Alcoholic Fatty Liver Disease (NAFLD). The increased values of total protein and uric acid of the malachite green treated animals were comparable with the effects of NAFLD. These might be due to the stress experienced by the endoplasmic reticulum of liver cells that may have led to oxidative stress and insulin resistance to the dye treated animals. The onset of these effects might have induced hyperuricemia and higher total protein concentration in serum of the dye treated animals when compared with the control. It is well known that malachite green could directly impart toxic effect to the liver [National Toxicology Program, 2005]. Here, in this current study, malachite green treatment seems to have exerted toxicity to the animals similar to NAFLD. The degradation product treated animals' serum values for total protein; uric acid was significantly low when compared with dye treated animals. It can be inferred from these observations that malachite green degradation by the *S. koreensis* showed reduced toxicity levels in animals when compared with the toxicity levels exerted by the original dye. However, the values of triglyceride have not shown any increase in the dye treated animals. This might be due to the short course of the dye treatment to the animals. Figure 3.29 depicts the serum toxicity analysis.
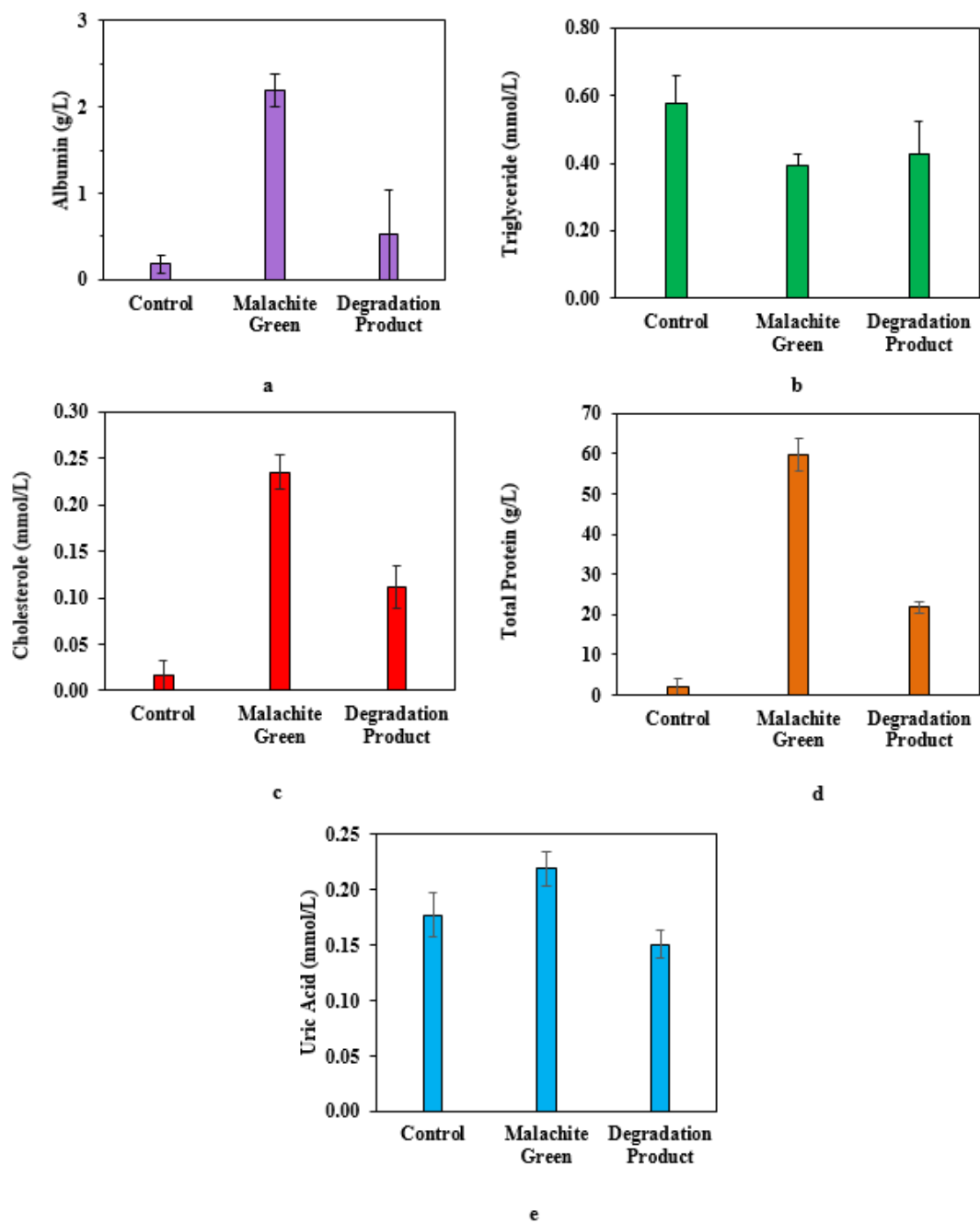
Figure 3.29 Serum analysis of *Mus musculus* after exposure to dye and degradation product (a) albumin, (b) triglyceride, (c) cholesterol, (d) total protein and (e) uric acid

Genotoxicity

The genotoxic effect of malachite green and its degradation product were analyzed by taking into account the MI (mitotic index) and the frequency of chromosomal aberrations in onion root tip cells. *Allium cepa* was used as a model plant because it has many advantages as a research material, such as ease of handling, sensitivity, quick analysis, low cost, and the ability to be used in correlation with other models that use mammalian cells [Chaparro et al., 2010]. The MI is defined as the number of cells undergoing mitosis divided by the total number of cells where all stages of mitosis are included in the count. Higher or lower MI with respect to the control can be indicative of an alteration of mitosis mechanisms [Leme and Marin-Morales, 2009].The MI was scored for each concentration of malachite green and the degradation product by analyzing approximately 5,000 cells. The control showed the MI 8.18%. There is a clear reduction of MI corresponding with the increase of the dye concentration. The minimum MI was obtained 4.37% for the undiluted malachite green, whereas for the undiluted degraded product, the MI was 5.28%. This observation suggests that the toxicity of the dye was definitely reduced from its original form. Besides scoring MI, evaluation of chromosomal abnormalities in dividing cells were studied for estimating toxicity of the dye and the degradation product. All the results indicated that the degradation product was less toxic than the dye, but more toxic than the control (water). Study of chromosomal aberrations provide important information and may be considered an efficient method to investigate the genotoxic potential of the various textile dyes and effluent [Kalyani et al., 2012]. The chromosomal aberrations are shown in Figure 3.30. Several types of chromosomal aberrations were observed such as c-mitosis, laggards, anaphase bridges, sticky chromosomes and telophase bridges. Increasing the concentration of the dye led to an increase in the rate of aberration as in Table 3.6. Among all the chromosomal abnormalities, C-metaphase, chromosome-bridge and sticky chromosomes were observed more frequently. Stickiness in the chromosome may arise due to DNA depolymerisation, nucleoprotein dissolution, breakage and exchange in basic folding fibre units of chromatids, and stripping of protein covering of the DNA in chromosomes [VC and Stephen, 1980]. Fiskesjö (1985) stated that a sticky chromosome has an irreversible toxic effect that may lead to cell cycle cessation. The chromosome bridges indicate the clastogenic activity of the toxic agent [Leme and Marin-Morales, 2009]. The laggard chromosomes are formed due to the degradation or depolymerization of the chromosomal DNA [Liu et al., 2004]. Genotoxicity studies fulfil the essential

purpose to determine the toxic potential of a compound from the environmental point of view. In our study, although the biodegraded malachite green also showed a reduction in MI and some chromosomal aberrations, but they were in a significantly lower rate than that of the original dye. In *A.cepa* root-tip cells, those treated with the degradation product had 50% lesser chromosomal aberrations than those treated with the untreated dye.

Table 3.6 Genotoxicity analysis of malachite green and the degradation product using *A. cepa*

Analysis	Control	Malachite Green			Degradation product		
		Two-fold serial dilutions			Two-fold serial dilutions		
		1/16 Dil	1/8 Dil	Undiluted	1/16 Dil	1/8 Dil	Undiluted
Mitotic Index (MI)	8.18±0.11	6.42± 0.07	5.25±0.02	4.37±0.05	6.92±0.06	5.73±0.06	5.28±0.02
Percentage of aberration	0.00	15.82±0.36	24.49±0.85	57.75±0.72	11.27±0.18	16.56±0.7	23.51±0.35
C-metaphase	0.00	17.33±0.88	22.67±0.88	29.67±1.2	12.00±0.58	16.33±0.3	21.00±1.15
Anaphase bridge	0.00	5.67±0.33	13.33±0.88	20.33±0.88	3.67±0.33	7.67±0.33	12.33±0.33
Sticky Chromosome	0.00	0.33±0.33	6.67±0.33	10.67±0.88	0.00	2.67±0.58	7.67 ±0.88
Laggard	0.00	1.67±0.67	3.33±0.88	5.67±1.45	0.00	1.33±0.58	4.00±0.92
Telophase bridge	0.00	3.98±0.14	9.36±0.38	14.34±0.44	1.68±0.33	3.33±0.33	8.1±0.36
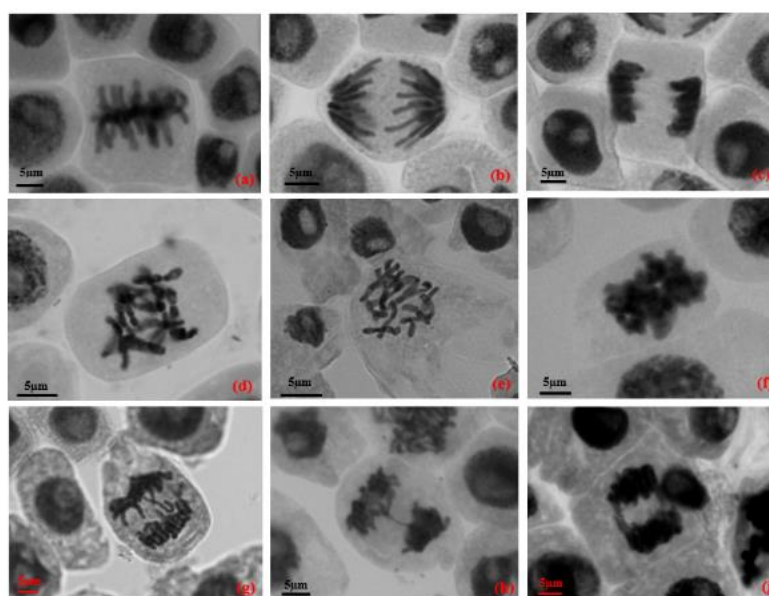
Figure 3.30 Normal chromosomes (a) Metaphase, (b) Anaphase, (c) Telophase; and chromosomes with aberrations (d) & (e) C- metaphase, (f) Sticky chromosome, (g) Laggard, (h) Chromosome bridge in Anaphase, (i) Telopahse bridge observed during genotoxicity study of the dye and the degradation product

Cytotoxicity assays with human cell lines

To test the toxicity of the dye and the degradation product, on human cell lines, growth of HaCat and HepG2 were used. Viability of both the cell lines were significantly higher for the degradation product treated cells than those exposed to all dilutions of the dye, which was evident through the MTT results ($p < 0.01$). That the bacterial treatment of the dye has reduced its toxicity to a considerable extent is clearly reflected in the results (Figure 3.31).
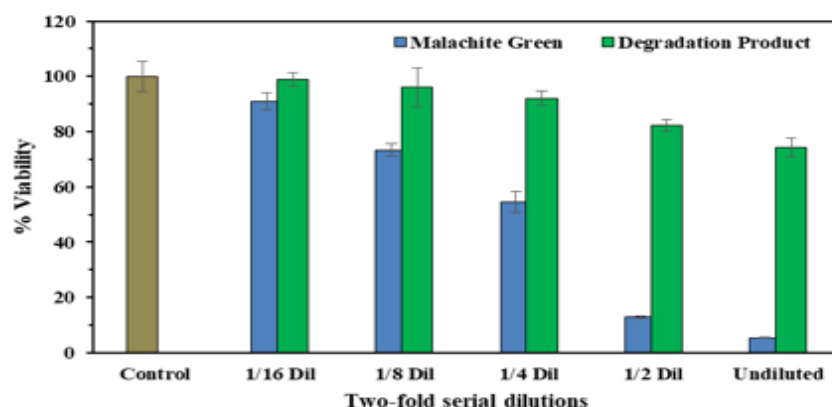
a
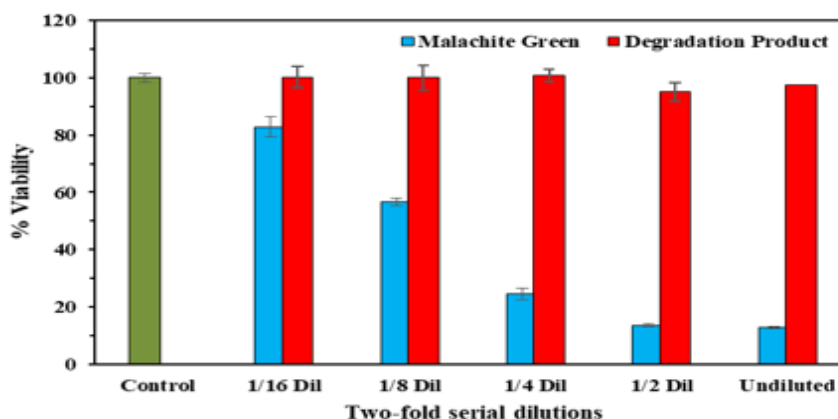
b

Figure 3.31 Effect of malachite green and the degradation product on HepG2 (a) and HaCat (b) cell lines

From the DAPI staining it can be clearly inferred that the degradation product was less toxic to both the cell lines when compared to the dye (100 mg/L). Increase in dye

concentration lead to increased cell death. Nuclear fragmentation is prominently visible in much higher densities in the cells exposed to the dye than those exposed to the undiluted degradation product obtained after the bacterial treatment (Figure 3.32).
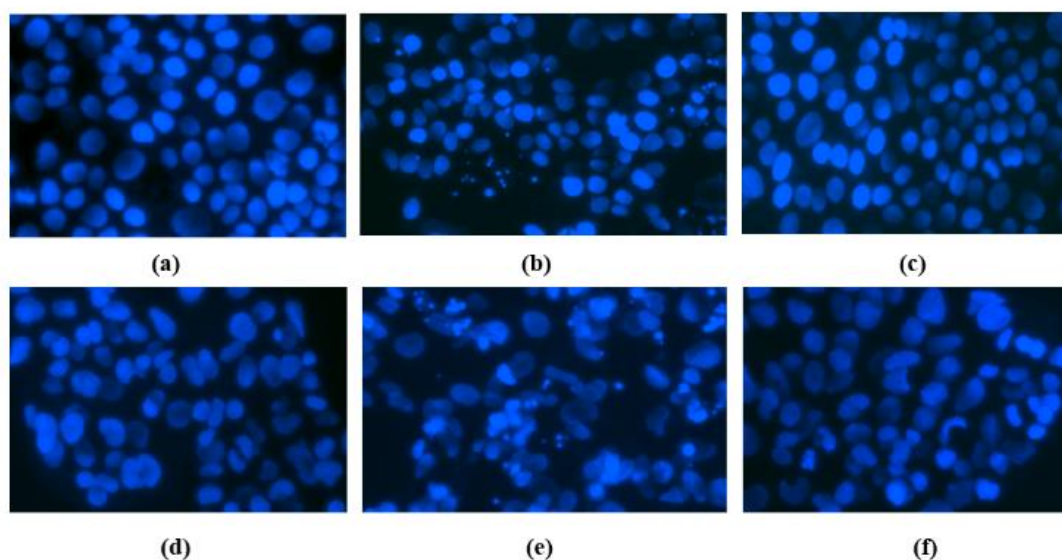
Figure 3.32 DAPI imaging of HaCaT (a) control, (b) dye-treated, (c) degradation product treated cells and HepG2 (d) control, (e) dye-treated, (f) degradation product treated cells

Histopathology with mice

The liver tissue of the animals fed with Malachite green the dye showed the presence of degenerated hepatocyte cells when compared with the ones treated with the degradation product group and the control group (Figure 3.33). The hepatocytes of the animals fed with malachite green were strewn in the hepatic parenchyma with deeply stained nucleus. Degeneration of hepatocyte of the dye-fed animals was observed in various spots. The hepatic cells of malachite green group animals did not show any prominent nucleus which might be due to the ductal hyperplasia induced by the Malachite green dye. Hepatic blood vessels of the MG treated animals were observed to be dilated when compared with the dye and control group. No toxicological symptoms were observed in the histopathological sections of kidney and spleen of the animals. The medullary and cortical region of the kidney of all group of animals were prominent without any evidence of morphological disorientation. The reticular frame work of the spleen cells treated with the dye, its degradation product or the control group animals did not show any change in their orientation.
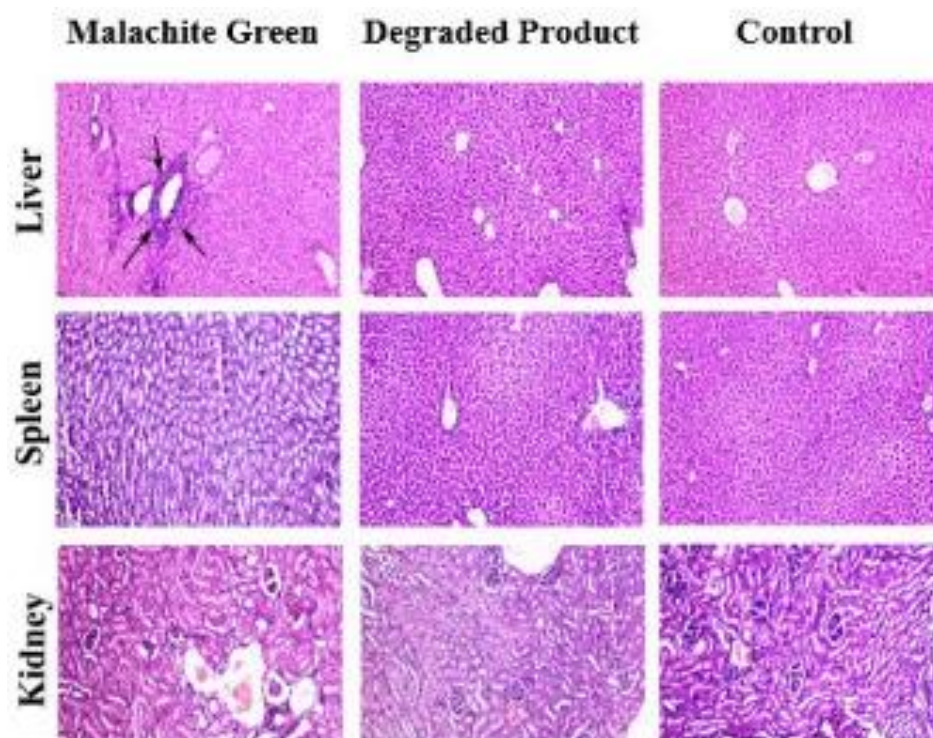
Figure 3.33 Histopathology of kidney, spleen and liver tissues of *Mus musculus* fed with malachite green, its degradation product

Ecotoxicity of dyes and their corresponding degradation products have been previously studied by many authors but were restricted to only a few species for each work [Amin et al. 2020; Gupte et al., 2013; Khan et al, 2020]. The novelty of the in the present work lies in fact that the entire range of representative organisms from the land and aquatic ecosystem were taken into account. The use of a battery of bioassays with organisms from several taxonomic groups allows for a more accurate assessment of the environmental impact of a chemical molecule or mixture introduced into a given ecosystem [Gioia et al., 2018]. Biological experiments using a variety of processes and organisms have been used to assess the toxicity of dyes and the products generated from various decolorization treatments [Bafana et al., 2011]. Ecotoxicity results might be difficult to compare to other reported data since they are dependent on various aspects, such as the chemical nature of the dyes, the approach used in the bioassay, the biological model, the research question and the expression of outcomes [Gioia et al., 2018].

In essence, we tested the product obtained after the biodegradation of malachite green by *Stenotrophomonas koreensis* to compare its toxicity with the untreated dye. We started off at the base of the aquatic ecosystem, the green photosynthetic algae *Anabaena flos-aque* and the aquatic macrophyte *Lemna minor* (growth inhibition test). We worked with

Daphnia magna, the zooplankton (acute immobilisation) and then the aquatic vertebrate *Danio rerio* (fish acute toxicity). We also tested the representative organisms from the land ecosystem. The soil bacteria *Bacillus subtilis* and *Bacillus pumilus* were used to perform the microbial toxicity. The two economically important crop plants *Triticum aestivum* and *Lens culinaris* were used to evaluate phytotoxicity. Genotoxicity was studied using the root tip cells of *Allium cepa*. Acute toxicity assay was performed in earthworms (*Eisenia fetida*). We worked with the higher mammal *Mus musculus* for the serum toxicity analysis. Finally, human cell lines HaCat and HepG2 were also studied for evaluating the cytotoxicity of the degradation product in comparison with the dye.

CONCLUSION

The strain *Stenotrophomonas koreensis* showed outstanding decolorization of the toxic industrial dye malachite green. Decolorization was caused by the degradation of the dye, which was confirmed by UV-Vis, FTIR spectrophotometry, TLC and HPLC results. The strain demonstrated excellent decolorization of malachite green even in plain water as a solvent, and the decolorization efficiency could be further increased on optimization of some physical parameters or by the addition of cheap, readily available supplements. This study undoubtedly reports one of the most effective dye decolorizations, biological or otherwise, documented to date. The biodegradation follows first-order reaction kinetics. Tyrosinase, MG reductase, and NADH-DCIP reductase enzymes facilitate the degradation process. *S. koreensis* can also decolorize methyl orange, an azo dye with an entirely different structure and chemical nature from the triphenylmethane malachite green. The strain remains active in the presence of heavy metals like cadmium, chromium, lead, and arsenic, which are commonly prevalent in industrial effluents. *Stenotrophomonas koreensis* may be exceptionally functional for treating tannery or textile effluents which usually contain mixtures of different dyes and heavy metals. The strain could be immobilized into reusable PVA-sodium alginate beads to facilitate easier handling. The degradation products were subjected to toxicological testing (according to the OECD guidelines for testing of chemicals) with a wide variety of organisms belonging to the land and aquatic ecosystems, ranging from the prokaryotic unicellular bacteria to higher animals like mice and even human cell lines. Hence, the ecotoxicological studies confirmed that the bacterially degraded dye product was significantly safer than the untreated dye. Hence, *S. koreensis* can become the ideal tool for bioremediating dye-contaminated effluents and combating industrial dye pollution, although further investigations on the scale-up are required.

REFERENCES

Adomas, B., Sikorski, Ł., Bęś, A. and Warmiński, K., 2020. Exposure of Lemna minor L. to gentian violet or Congo red is associated with changes in the biosynthesis pathway of biogenicamines. Chemosphere, 254, p.126752.

Alaya, V., Kodi, R. K., Ninganna, E., Gowda, B., & Shivanna, M. B. (2021). Decolorization of Malachite green dye by Stenotrophomonas maltophilia a compost bacterium. *Bulletin of theNational Research Centre*, *45*(1), 1-13.

Alonso, A., Sanchez, P., & Martínez, J. L. (2000). Stenotrophomonas maltophilia D457R contains a cluster of genes from gram-positive bacteria involved in antibiotic and heavy metalresistance. *Antimicrobial agents and chemotherapy*, *44*(7), 1778-1782.

AL-ZURFI, S.K.L., ALBDAIRI, N.A. and ALMADANY, S.A., 2020. Phytoremediation of congo red and brilliant green using lemna minor. *Plant Cell Biotechnology and Molecular Biology*, pp.1-10.

Amin, S., Rastogi, R.P., Chaubey, M.G., Jain, K., Divecha, J., Desai, C. and Madamwar, D., 2020. Degradation and toxicity analysis of a reactive textile diazo dye-Direct Red 81 by newlyisolated Bacillus sp. DMS2. Frontiers in microbiology, 11, p.2280.

Amin, S., Rastogi, R.P., Chaubey, M.G., Jain, K., Divecha, J., Desai, C. and Madamwar, D., 2020. Degradation and toxicity analysis of a reactive textile diazo dye-Direct Red 81 by newlyisolated Bacillus sp. DMS2. Frontiers in microbiology, 11, p.2280.

Arnon, D.I., 1949. Copper enzymes in isolated chloroplasts. Polyphenoloxidase in Beta vulgaris. Plant physiology, 24(1), p.1.

Bae, J.S. and Freeman, H.S., 2007. Aquatic toxicity evaluation of new direct dyes to the Daphnia magna. Dyes and Pigments, 73(1), pp.81-85

Bafana, A., Devi, S.S. and Chakrabarti, T., 2011. Azo dyes: past, present and the future. *Environmental Reviews*, *19*(NA), pp.350-371.

Banerjee, M. & Yesmin, L. Sulfur-oxidizing plant growth promoting rhizobacteria for enhanced canola performance. US Patent 07491535 (2002)

Berg, G., Egamberdieva, D., Lugtenberg, B., & Hagemann, M. (2010). Symbiotic plant-microbe interactions: stress protection, plant growth promotion and biocontrol by Stenotrophomonas. In *Symbioses and stress: joint ventures in biology* (1 ed.), Vol. 17, pp. 445-460

Biswas, S., Bhattacharya, A. and Basak, P., 2018. Effect of tannery effluent on germination and early seedling growth of Oryza sativa var. IET-4786. In Utilization and Management of Bioresources (pp. 243-251). Springer, Singapore.

Brancatelli, G., Furlan, A., Calandra, A. and Burgio, M.D., 2018. Hepatic sinusoidal dilatation.Abdominal Radiology, 43(8), pp.2011-2022.

Brooke, J. S. (2012). Stenotrophomonas maltophilia: an emerging global opportunistic pathogen. *Clinical microbiology reviews*, *25*(1), 2-41.

Carolin, C. F., Kumar, P. S., & Joshiba, G. J. (2021). Sustainable approach to decolorize methylorange dye from aqueous solution using novel bacterial strain and its metabolites characterization. Clean Technol Envir., 23(1), 173-181

Chaparro, T.R., Botta, C.M. and Pires, E.C., 2010. Biodegradability and toxicity assessment of bleach plant effluents treated anaerobically. Water Science and Technology, 62(6), pp.1312- 1319.

Chaturvedi, V. and Verma, P., 2015. Biodegradation of malachite green by a novel copper- tolerant Ochrobactrum pseudogrignonense strain GGUPV1 isolated from copper mine waste water. Bioresources and Bioprocessing, 2(1), pp.1-9.

Chen, C.H., Chang, C.F. and Liu, S.M., 2010. Partial degradation mechanisms of malachite green and methyl violet B by Shewanella decolorationis NTOU1 under anaerobic conditions. Journal of Hazardous Materials, 177(1-3), pp.281-289.

Chia, M.A. and Musa, R.I., 2014. Effect of indigo dye effluent on the growth, biomass production and phenotypic plasticity of Scenedesmus quadricauda (Chlorococcales). Anais da Academia Brasileira de Ciências, 86, pp.419-428.

Donya, S.M., Farghaly, A.A., Abo-Zeid, M.A., Aly, H.F., Ali, S.A., Hamed, M.A. and El-Rigal, N.S., 2012. Malachite green induces genotoxic effect and biochemical disturbances in mice. *Eur Rev Med Pharmacol Sci*, *16*(4), pp.469-82.

Du L N, Wang S, Li G, Wang B, Jia X M, Zhao, Y H, Chen Y L (2011). Biodegradation of malachite green by *Pseudomonas sp.* strain DY1 under aerobic condition: characteristics, degradation products, enzyme analysis and phytotoxicity. Ecotoxicology 20:438-446

Du L N, Wang S, Li G, Wang B, Jia X M, Zhao, Y H, Chen Y L (2011). Biodegradation of malachite green by *Pseudomonas sp.* strain DY1 under aerobic condition: characteristics, degradation products, enzyme analysis and phytotoxicity. Ecotoxicology 20:438-446

Du, L. N., Li, G., Zhao, Y. H., Xu, H. K., Wang, Y., Zhou, Y., & Wang, L. (2015). Efficient metabolism of the azo dye methyl orange by Aeromonas sp. strain DH-6: characteristics and partial mechanism. Int Biodeter Biodegr, 105, 66-72.

Du, L. N., Pan, K. K., Li, G., Yang, Y. Y., & Xu, F. C. (2018). Efficient degradation of Malachite Green by Aeromonas sp. strain DH-6. *Applied and Environmental Microbiology*, *3*(2), 1-8.

Du, L. N., Zhao, M., Li, G., Zhao, X. P., & Zhao, Y. H. (2012). Highly efficient decolorization of malachite green by a novel Micrococcus sp. strain BD15. Environ Sci Pollut R., 19(7), 2898-2907.

Du, L. N., Zhao, M., Li, G., Zhao, X. P., & Zhao, Y. H. (2012). Highly efficient decolorization of malachite green by a novel Micrococcus sp. strain BD15. Environ Sci Pollut R., 19(7), 2898-2907.

Ebert, D., 2005. Ecology, epidemiology, and evolution of parasitism in Daphnia. National Library of Medicine.

Elfarash, A., Mawad, A. M., Yousef, N. M., & Shoreit, A. A. (2017). Azoreductase kinetics and gene expression in the synthetic dyes-degrading Pseudomonas. *Egyptian journal of basic and applied sciences*, *4*(4), 315-322.

Etezad, S. M., & Sadeghi-Kiakhani, M. (2021). Decolorization of Malachite Green Dye Solution by Bacterial Biodegradation. *Progress in Color, Colorants and Coatings*, *14*(2), 79-87.

Fekete-Kertész, I., Kunglné-Nagy, Z., Gruiz, K., Magyar, Á., Farkas, É. and Molnár, M., 2015. Assessing toxicity of organic aquatic micropollutants based on the total chlorophyll content of Lemna minor as a sensitive endpoint. Periodica Polytechnica Chemical Engineering, 59(4), pp.262-271.

Fiskesjö, G., 1985. Allium test on river water from Braån and Saxån before and after closure of a chemical factory. Ambio, pp.99-103.

Galai S, Limam F, Marzouki M N (2009) A new *Stenotrophomonas maltophilia* strain producing laccase. Use in decolorization of synthetics dyes. Appl. Biochem. Biotechnol. 158:416-431

Gao, F., Ding, H., Feng, Z., Liu, D., & Zhao, Y. (2014). Functional display of triphenylmethane reductase for dye removal on the surface of Escherichia coli using N-terminal domain of ice nucleation protein. *Bioresource technology*, *169*, 181-187.

Gioia, L., Ovsejevi, K., Manta, C., Míguez, D. and Menéndez, P., 2018. Biodegradation of acid dyes by an immobilized laccase: An ecotoxicological approach. Environmental Science: Water Research & Technology, 4(12), pp.2125-2135.

Gioia, L., Ovsejevi, K., Manta, C., Míguez, D. and Menéndez, P., 2018. Biodegradation of acid dyes by an immobilized laccase: An ecotoxicological approach. Environmental Science: Water Research & Technology, 4(12), pp.2125-2135.

Gita, S., Shukla, S.P., Saharan, N., Prakash, C. and Deshmukhe, G., 2019. Toxic Effects of selected textile dyes on elemental composition, photosynthetic pigments, protein content and growth of a freshwater chlorophycean alga Chlorella vulgaris. Bulletin of environmental contamination and toxicology, 102(6), pp.795-801.

Gopinath, K. P., Kathiravan, M. N., Srinivasan, R., & Sankaranarayanan, S. (2011). Evaluation and elimination of inhibitory effects of salts and heavy metal ions on biodegradation of Congo red by Pseudomonas sp. mutant. Bioresour. Technol., 102(4):3687-3693

Gopinathan, R., Kanhere, J. and Banerjee, J., 2015. Effect of malachite green toxicity on non target soil organisms. Chemosphere, 120, pp.637-644.

Gupte, S., Keharia, H. and Gupte, A., 2013. Toxicity analysis of azo Red BS and Methyl Red dye solutions on earthworm (Pheretima phosthuma), micro-organisms, and plants. Desalination and Water Treatment, 51(22-24), pp.4556-4565.

Gupte, S., Keharia, H. and Gupte, A., 2013. Toxicity analysis of azo Red BS and Methyl Red dye solutions on earthworm (Pheretima phosthuma), micro-organisms, and plants. Desalination and Water Treatment, 51(22-24), pp.4556-4565.

Hafeez, F., Farheen, H., Mahmood, F., Shahzad, T., Shahid, M., Iqbal, M., & Hussain, S. (2018). Isolation and characterization of a lead (Pb) tolerant *Pseudomonas aeruginosa* strain HF5 for decolorization of reactive red-120 and other azo dyes. Ann. Microbiol., 68(12), 943-952.

Hatvani, N., & Mécs, I. (2003). Effects of certain heavy metals on the growth, dye decolorization, and enzyme activity of *Lentinula edodes*. Ecotoxicol Environ Saf, *55*(2), 199-203.

Hinderliter P., & Saghir S.A., (2014). Pharmacokinetics, in Encyclopedia of Toxicology (Third Edition), Academic Press. 849-855

Hou, H., Zhou, J., Wang, J., Du, C., & Yan, B. (2004). Enhancement of laccase production by Pleurotus ostreatus and its use for the decolorization of anthraquinone dye. Process Biochem., 39(11), 1415-1419

Jadhav, J. P., & Govindwar, S. P. (2006). Biotransformation of malachite green by Saccharomyces cerevisiae MTCC 463. *Yeast*, *23*(4), 315-323.

Jadhav, J. P., & Govindwar, S. P. (2006). Biotransformation of malachite green by Saccharomyces cerevisiae MTCC 463. *Yeast*, *23*(4), 315-323.

Jang, M. S., Lee, Y. M., Kim, C. H., Lee, J. H., Kang, D. W., Kim, S. J., & Lee, Y. C. (2005).

Triphenylmethane reductase from Citrobacter sp. strain KCTC 18061P: purification, characterization, gene cloning, and overexpression of a functional protein in Escherichia coli. *Applied and environmental microbiology*, *71*(12), 7955-7960.

Kabeer, F.A., John, N. and Abdulla, M.H., 2019. Biodegradation of malachite green by a newly isolated Bacillus vietnamensis sp. MSB17 from continental slope of the Eastern Arabian Sea: Enzyme analysis, degradation pathway and toxicity studies. Bioremediation Journal, 23(4), pp.334-342.

Kalyani, D.C., Telke, A.A., Surwase, S.N., Jadhav, S.B., Lee, J.K. and Jadhav, J.P., 2012. Effectual decolorization and detoxification of triphenylmethane dye malachite green (MG) by Pseudomonas aeruginosa NCIM 2074 and its enzyme system. Clean Technologies and Environmental Policy, 14(5), pp.989-1001.

Kanhere, J., Gopinathan, R. and Banerjee, J., 2014. Cytotoxicity and genotoxicity of malachite green on non-target aquatic organisms: Chlorella pyrenoidosa and Daphnia magna. Water, Air, & Soil Pollution, 225(9), pp.1-8.

Khalid, A., Arshad, J., Mahmood, S., Aziz, I., & Arshad, M. (2015). Effect of chromium forms on the biodegradation of reactive black-5 azo dye by Psychrobacter and Klebsiella species. Int J Agric Biol. , 17(6)

Khan, Z.U.H., Shah, N.S., Iqbal, J., Khan, A.U., Imran, M., Alshehri, S.M., Muhammad, N., Sayed, M., Ahmad, N., Kousar, A. and Ashfaq, M., 2020. Biomedical and photocatalytic applications of biosynthesized silver nanoparticles: Ecotoxicology study of brilliant green dye and its mechanistic degradation pathways. *Journal of Molecular Liquids*, *319*, p.114114.

Koga, M., Murai, J., Saito, H., Matsumoto, S. and Kasayama, S., 2009. Effects of thyroid hormone on serum glycated albumin levels: study on non-diabetic subjects. Diabetes research and clinical practice, 84(2), pp.163-167.

Koupaie, E. H., Moghaddam, M. A., & Hashemi, S. H. (2012). Investigation of decolorization kinetics and biodegradation of azo dye Acid Red 18 using sequential process of anaerobic sequencing batch reactor/moving bed sequencing batch biofilm reactor. Int Biodeter Biodegr, 71: 43-49.

Leme, D.M. and Marin-Morales, M.A., 2009. Allium cepa test in environmental monitoring: a review on its application. Mutation Research/Reviews in Mutation Research, 682(1), pp.71-81.

Levin, L., Melignani, E., & Ramos, A. M. (2010). Effect of nitrogen sources and vitamins on ligninolytic enzyme production by some white-rot fungi. Dye decolorization by selected culture filtrates. Bioresour. Technol., 101(12), 4554-4563.

Liba, C. M., Ferrara, F. I. S., Manfio, G. P., Fantinatti-Garboggini, F., Albuquerque, R. C., Pavan, C., ... & Barbosa, H. R. (2006). Nitrogen-fixing chemo-organotrophic bacteria

isolated from cyanobacteria-deprived lichens and their ability to solubilize phosphate and to release amino acids and phytohormones. *Journal of applied microbiology*, *101*(5), 1076-1086.

Lin, J.N., Chang, L.L., Lai, C.H., Lin, K.J., Lin, M.F., Yang, C.H., Lin, H.H. and Chen, Y.H., 2015. Development of an animal model for alcoholic liver disease in zebrafish. Zebrafish, 12(4), pp.271-280.

Lin, J.N., Chang, L.L., Lai, C.H., Lin, K.J., Lin, M.F., Yang, C.H., Lin, H.H. and Chen, Y.H., 2015. Development of an animal model for alcoholic liver disease in zebrafish. Zebrafish, 12(4), pp.271-280.

Liu, H., Liao, B. and Lu, S., 2004. Toxicity of surfactant, acid rain and Cd2+ combined pollution to the nucleus of Vicia faba root tip cells. Ying yong sheng tai xue bao= The journal of applied ecology, 15(3), pp.493-496.

Liu, S., Xu, X., Kang, Y., Xiao, Y., & Liu, H. (2020). Degradation and detoxification of azo dyes with recombinant ligninolytic enzymes from Aspergillus sp. with secretory overexpression in Pichia pastoris. *Royal Society open science*, *7*(9), 200688.

Looney, W. J., Narita, M., & Mühlemann, K. (2009). Stenotrophomonas maltophilia: an emerging opportunist human pathogen. *The Lancet infectious diseases*, *9*(5), 312-323.

Lumbaque, E.C., Gomes, M.F., Carvalho, V.D.S., de Freitas, A.M. and Tiburtius, E.R.L., 2017. Degradation and ecotoxicity of dye Reactive Black 5 after reductive-oxidative process. Environmental Science and Pollution Research, 24(7), pp.6126-6134.

Lv, G. Y., Cheng, J. H., Chen, X. Y., Zhang, Z. F., & Fan, L. F. (2013). Biological decolorization of malachite green by Deinococcus radiodurans R1. Bioresour. Technol., 144, 275-280.

Material Safety Data Sheet of Malachite Green Oxalate salt, Sigma-Aldrich, 2014

Modi, H. A., Rajput, G., & Ambasana, C. (2010). Decolorization of water soluble azo dyes by bacterial cultures, isolated from dye house effluent. Bioresour. Technol., 101(16), 6580-6583.

Mukherjee, T. and Das, M., 2014. Degradation of malachite green by Enterobacter asburiae strain XJUHX-4TM. CLEAN–Soil, Air, Water, 42(6), pp.849-856.

Narayanan, M. P., Murugan, S., Eva, A. S., Devina, S. U., & Kalidass, S. (2015). Application of immobilized laccase from Bacillus subtilis MTCC 2414 on decolorization of synthetic dyes. Res J Microbiol, 10(9), 421-432.

National Toxicology Program, 2005. Toxicology and carcinogenesis studies of malachite green chloride and leucomalachite green.(CAS NOS. 569-64-2 and 129-73-7) in F344/N rats and B6C3F1 mice (feed studies). National Toxicology Program technical report series, (527), pp.1-312.

OECD 201 (2011) OECD guideline for testing of chemicals. 'Alga, growth inhibition test'.

OECD 202 (2004) OECD guideline for testing of chemicals. 'Daphnia sp., acute immobilisation test'.

OECD 203 (2019) OECD guideline for testing of chemicals. 'Fish Acute Toxicity Test'.

OECD 207 (1984) OECD guideline for testing of chemicals. 'Earthworm Acute Toxicity Test'.

OECD 221 (2006) OECD guideline for testing of chemicals. 'Lemna sp., growth inhibition test'.

Pages, D., Rose, J., Conrod, S., Cuine, S., Carrier, P., Heulin, T., & Achouak, W. (2008). Heavy metal tolerance in Stenotrophomonas maltophilia. *PLoS One*, *3*(2), e1539.

Parshetti, G., Kalme, S., Saratale, G., & Govindwar, S. (2006). Biodegradation of Malachite Green by *Kocuria rosea* MTCC 1532. Acta Chim. Slov. , *53*(4).

Parshetti, G., Kalme, S., Saratale, G., & Govindwar, S. (2006). Biodegradation of Malachite Green by *Kocuria rosea* MTCC 1532. Acta Chim. Slov. , *53*(4).

Patil, S. N., Aglave, B. A., Pethkar, A. V., & Gaikwad, V. B. (2012). Stenotrophomonas koreensis a novel biosurfactant producer for abatement of heavy metals from the environment. Afr. J. Microbiol. Res., 6(24), 5173-5178

Pham, D.H. and Yin, C., 2019. Zebrafish as a model to study cholestatic liver diseases. In Experimental cholestasis research (pp. 273-289). Humana Press, New York, NY.

Phugare, S., Patil, P., Govindwar, S., & Jadhav, J. (2010). Exploitation of yeast biomass generated as a waste product of distillery industry for remediation of textile industry effluent. Int Biodeter Biodegr, 64(8), 716-726.

Plachtová, P., Medrikova, Z., Zboril, R., Tucek, J., Varma, R.S. and Maršálek, B., 2018. Iron and iron oxide nanoparticles synthesized with green tea extract: differences in ecotoxicological profile and ability to degrade malachite green. ACS sustainable chemistry & engineering, 6(7), pp.8679-8687.

Qiao, M., Wei, K., Ding, J., Liu, Z., Zhang, K. Q., & Huang, X. (2011). Decolorizing activity of malachite green and its mechanisms involved in dye biodegradation by Achromobacter xylosoxidans MG1. *Journal of Molecular Microbiology and Biotechnology*, *20*(4), 220-227.

Rao, J.V. and Kavitha, P., 2004. Toxicity of azodrin on the morphology and acetylcholinesterase activity of the earthworm Eisenia foetida. Environmental research, 96(3), pp.323-327.

Reddy, N.C. and Rao, J.V., 2008. Biological response of earthworm, Eisenia foetida (Savigny) to an organophosphorous pesticide, profenofos. Ecotoxicology and Environmental Safety,

71(2), pp.574-582.

Romano, N., Kumar, V., Yang, G., Kajbaf, K., Rubio, M.B., Overturf, K., Brezas, A. and Hardy, R., 2020. Bile acid metabolism in fish: disturbances caused by fishmeal alternatives and some mitigating effects from dietary bile inclusions. Reviews in Aquaculture, 12(3), pp.1792-1817.

Ryan, R. P., Monchy, S., Cardinale, M., Taghavi, S., Crossman, L., Avison, M. B., & Dow, J.

M. (2009). The versatility and adaptation of bacteria from the genus Stenotrophomonas. *Nature Reviews Microbiology*, *7*(7), 514-525.

Sánchez, M. B. (2015). Antibiotic resistance in the opportunistic pathogen Stenotrophomonas maltophilia. *Frontiers in microbiology*, *6*, 658.

Sari, I. P., & Simarani, K. (2019). Decolorization of selected azo dye by Lysinibacillus fusiformis W1B6: Biodegradation optimization, isotherm, and kinetic study biosorption mechanism. *Adsorption Science & Technology*, *37*(5-6), 492-508.

Sathya, T.N., Deepa, V., Dutt, M. and Murthy, P., 2009. DNA Damage Caused by a Textile Dye (Acid Red) in Coelomocytes of Earthworm,'Eisenia Fetida'. Australasian Journal of Ecotoxicology, 15(2/3), pp.45-50.

Shah, P. D., Dave, S. R., & Rao, M. S. (2012). Enzymatic degradation of textile dye Reactive Orange 13 by newly isolated bacterial strain Alcaligenes faecalis PMS-1. *International Biodeterioration & Biodegradation*, *69*, 41-50

Shah, R. and John, S., 2019. Cholestatic jaundice (cholestasis, cholestatic hepatitis). StatPearls [Internet].

Shanmugam S, Ulaganathan P, Swaminathan K, Sadhasivam S, Wu Y. R. (2017). Enhanced biodegradation and detoxification of malachite green by *Trichoderma asperellum* laccase:

degradation pathway and product analysis. Int Biodeter Biodegr.125: 258-268

Sihag, S., Pathak, H., & Jaroli, D. P. (2014). Factors affecting the rate of biodegradation of polyaromatic hydrocarbons. Int J Pure Appl Biosci., *2*(3), 185-202.

Sinha, R.A., Singh, B.K. and Yen, P.M., 2018. Direct effects of thyroid hormones on hepatic lipid metabolism. Nature Reviews Endocrinology, 14(5), p.259.

Solís, M., Solís, A., Pérez, H.I., Manjarrez, N. and Flores, M., 2012. Microbial decolouration of azo dyes: a review. Process Biochemistry, 47(12), pp.1723-1748.

Song, J., Han, G., Wang, Y., Jiang, X., Zhao, D., Li, M., ... & Mu, Y. (2020). Pathway and kinetics of malachite green biodegradation by Pseudomonas veronii. *Scientific reports*, *10*(1), 1-11.

Suckstorff, I., & Berg, G. (2003). Evidence for dose-dependent effects on plant growth by Stenotrophomonas strains from different origins. *Journal of applied microbiology*, *95*(4), 656-663.

Sutar, S. S., Patil, P. J., Tamboli, A. S., Patil, D. N., Apine, O. A., & Jadhav, J. P. (2019). Biodegradation and detoxification of malachite green by a newly isolated bioluminescent bacterium Photobacterium leiognathi strain MS under RSM optimized culture conditions. *Biocatalysis and Agricultural Biotechnology*, *20*, 101183.

Tachibana, S., Kuba, N., Kawai, F., Duine, J. A., & Yasuda, M. (2003). Involvement of a quinoprotein (PQQ-containing) alcohol dehydrogenase in the degradation of polypropylene glycols by the bacterium Stenotrophomonas maltophilia. *FEMS microbiology letters*, *218*(2), 345-349.

VC, M. and Stephen, J., 1980. Adriamycin induced genetic toxicity as demonstrated by the Allium test. Cytologia, 45(4), pp.769-777.

Vignesh, A., Manigundan, K., Santhoshkumar, J., Shanmugasundaram, T., Gopikrishnan, V., Radhakrishnan, M., Joseph, J., Ayyasamy, P.M., Kumar, G.D., Meganathan, R. and Balagurunathan, R., (2020). Microbial degradation, spectral analysis and toxicological assessment of malachite green by Streptomyces chrestomyceticus S20. *Bioprocess and biosystems engineering*, *43*(8), pp.1457-1468.

Vijayalakshmidevi, S. R., & Muthukumar, K. (2014). Biodegradation of malachite green by Ochrobactrum sp. World Journal of Microbiology and Biotechnology, 30(2), 429-437.

Wanyonyi, W. C., Onyari, J. M., Shiundu, P. M., & Mulaa, F. J. (2017). Biodegradation and detoxification of malachite green dye using novel enzymes from bacillus cereus strain KM201428: kinetic and metabolite analysis. *Energy Procedia*, *119*, 38-51.

Yang, X., Zheng, J., Lu, Y., & Jia, R. (2016). Degradation and detoxification of the triphenylmethane dye malachite green catalyzed by crude manganese peroxidase from Irpex lacteus F17. *Environmental Science and Pollution Research*, *23*(10), 9585-9597.

Yasmin, S. and D'Souza, D., 2010. Effects of pesticides on the growth and reproduction of earthworm: a review. *Applied and Environmental Soil Science*, *2010*.

Zhan, X., Yan, C., Zhang, Y., Rinke, G., Rabsch, G., Klumpp, M., ... & Dittmeyer, R. (2020). Investigation of the reaction kinetics of photocatalytic pollutant degradation under defined conditions with inkjet-printed TiO 2 films–from batch to a novel continuous-flow microreactor. *Reaction chemistry & engineering*, *5*(9), 1658-1670.

Chapter 4
Studies on the Bioadsorption of Remazol Brilliant Blue R by the Strain *Bacillus rigiliprofundi*

INTRODUCTION

Biosorption is the adsorption of dye by biological agents and is gaining popularity to reduce environmental pollution (Johari et al., 2013). Removal of dyes by biosorption can be performed by several agents like bacteria, fungi, algae, agricultural wastes, polysaccharides, etc. Biorenewable materials like cellulose, the most abundantly available natural polymer, have been used as a biosorbent (Thakur, Thakur and Gupta, 2014). Microbial biomass is more effective than macroscopic materials like seaweeds, crab shells, etc., as far as the removal of dyes through adsorption is concerned. This difference in adsorption behavior may be due to the cell wall constituents and the functional groups of the bacteria or fungi (Saravanan et al., 2013). Microorganisms have a high surface-to-volume ratio and thus offer a larger contact area for the interaction of the dye molecules and the cell wall. Again, compared to yeast and fungi, bacteria have been reported more frequently to exhibit faster growth and higher adaptability to extreme conditions of pH, temperature, nutrient availability, etc. (Chen et al., 2007). Biosorption by bacteria is mediated by electrostatic forces and chemical reactions between the dye and the binding sites. Remazol Brilliant Blue R, an anthraquinone dye, is a potent toxic organo-pollutant and is frequently used as the precursor of many other dyes (Mechichi et al., 2006). It is one of the most frequently utilized dyes in the textile industry (Ada et al., 2009). *Dichomitus squalens, Trametes trogii* (Eichlerová et al., 2005), *Pleurotus calyptratus* and *Ischnoderma resinosum* have been reported to degrade RBBR (Saratale et al., 2009).

MATERIALS AND METHODS

Dyes and media

Remazol Brilliant Blue R dye was obtained from Sigma Aldrich. Nutrient Broth (NB) [HM Peptone B (1.5g/L), Yeast extract (1.5g/L), NaCl (5g/L), Peptone (5g/L), pH 7] and nutrient agar [Peptone (10g/L), Meat extract B (10g/L), Sodium chloride (5g/L), Agar (12g/L), pH 7.3], purchased from HiMedia Laboratories were used for the isolation of bacteria. Minimal Salt Medium (MSM) [$(NH_4)_2HPO_4$ (0.72g/L), $MgSO_4.7H_2O$ (0.144g/L), $FeSO_4.7H_2O$ (0.0072g/L), K_2HPO_4 (1.8g/L), KCL (0.144g/L), Sucrose (7.2g/L), $MnSO_4.7H_2O$ (0.00504g/L), Na_2HPO_4 (1.8g/L), pH 7] was used for the screening and other experiments.

Decolorisation experiments

100 ml nutrient broth was inoculated with a loopful of the selected bacterial strains individually and incubated at 37ºC for 48h. After completion of the incubation period, 5ml culture was added to 50 ml MSM amended with 20mg/L RBBR. Flasks were incubated for ten days at 37 °C and pH 7. Aliquots (4ml) were centrifuged at 10,000 rpm for 15 min to pellet out the biomass. The absorbance of the supernatant was measured at 592nm using UV-Vis spectrophotometer (Agilent Cary 60) at regular intervals. Uninoculated MSM amended with 20mg/L RBBR was kept as control.

The following equation was used to determine the decolorisation efficiency in terms of percentage decolorisation as indicated in Chapter 2. For convenience of the readers it is mentioned again here:

$$\textbf{Percentage decolorisation} = \frac{\textbf{Initial absorbance} - \textbf{Final absorbance}}{\textbf{Initial absorbance}} \times \textbf{100}$$

Equation 2.1

Effect of different physical parameters on dye adsorption

The effects of different physical parameters (pH, temperature, initial dye concentration, and biomass concentration) on the adsorption of RBBR by the selected strain P24 were studied.

Initial biomass concentration

The initial biomass required for efficient adsorptive decolorisation of RBBR was evaluated. Biomass (6, 15, 24, 30, 39 and 45 mg) was added to 100mL MSM amended with RBBR (20mg/L) and incubated for 240h at 37 ºC. After completion of the incubation period, the adsorptive dye decolorisation was evaluated by the method explained. The most suitable inoculum size was chosen for all subsequent studies.

Initial dye concentration

To evaluate the effect of initial dye concentration on the adsorptive decolorisation efficiency of the strain, 100ml MSM was amended with varying RBBR concentrations (25, 35, 45, 75 and 100mg/L) and was inoculated with 30mg *B.rigiliprofundi* biomass and incubated at 37 ºC. Adsorptive decolorisation was noted after 240h, according to the procedure mentioned above.

pH

The effect of varying pH on the adsorptive decolorisation of RBBR (25mg/L) was studied by inoculating 100ml dye-amended MSM with 30mg biomass. The range of pH studied varied from acidic (4.5) to alkaline (10.5). Adsorptive decolorisation conditions were the same as mentioned in the above tests.

Temperature

To estimate the effect of temperature, 100 ml MSM amended with 25mg/L RBBR was inoculated with 30mg biomass and incubated at temperatures varying between 10ºC to 60ºC for 240h. Adsorptive decolorisation was estimated after the completion of the incubation period by methods and conditions mentioned in the above experiments.

Effect of RBBR on the growth profile

The growth of the strain was studied in the presence of RBBR (25mg/L) and compared with its growth in dye-less MSM (control). A 24h culture of the strain was inoculated into 200ml media at a 1% level and incubated at 37ºC. Aliquots were extracted and the

viable cell count was determined by counting the number of Colony-Forming-Units on a solid nutrient agar medium at regular intervals.

Kinetics of adsorption

The actual amount of the adsorbed dye can be evaluated only on reaching equilibrium, which is why it is vital to study the kinetics of adsorption and estimate the time required to attain equilibrium (Sahoo & Prelot, 2020). Kinetic studies were performed by mixing 30mg biomass with 100ml MSM amended with RBBR (25 mg/L) at pH 5.5 and temperature 40°C for 264h. Aliquots were withdrawn from the mixture at regular intervals (24h) and centrifuged at 10000rpm for 15min. The rate of dye removal was evaluated by measuring the absorbance of the supernatant at 590nm. The amount of dye adsorbed (q_e) by the bacterial biomass at equilibrium was estimated according to the mass balance equation:

$$q_e = \frac{(C_0 - C_t)V}{M}$$

Equation 4.1

Where C_0 and C_t are the initial and final concentrations of RBBR (mg/L) in the solution, respectively after time t, V is the volume (L) of the solution, and M is the biomass (g) of the bacteria used.

Pseudo-first order and pseudo-second order models were investigated for determining the adsorption kinetics. The pseudo first order kinetics is given by the Lagergren equation (Lagergren, 1898):

$$\frac{dq_t}{dt} = k_1(q_e - q_t)$$

Equation 4.2

Where q_e is the amount of RBBR adsorbed at equilibrium per unit weight of the bacteria (mg g^{-1}),

q_t is the amount of RBBR adsorbed at time t (mg g^{-1}),

k_1 is the pseudo-first order rate constant (hr^{-1})

Integrating Equation 4.2 with the following conditions as q_t=0 to q_t=q_t at t=0 to t=t, the final equation can be expressed as:

$$\log(q_e - q_t) = \log q_e - \frac{k_1 t}{2.303}$$

Equation 4.3

When log (q_e-q_t) versus time t is plotted, the pseudo first order rate constant k_1 can be obtained from the slope of the graph.

The pseudo-second order model is denoted by the following equation (Ho and McKay, 1999):

$$\frac{dq_t}{dt} = k_2(q_e - q_t)^2$$

Equation 4.4

Integrating Equation 4.4 with the conditions, $q_t = 0$ to $q_t = q_e$ and $t = 0$ to $t = t$, the linear form can be obtained as below:

$$\frac{t}{q_t} = \frac{1}{k_2 q_e^2} + t/q_e$$

Equation 4.5

Where k_2 is the pseudo-second order rate constant $(gmg^{-1}hr^{-1})$

When t/q_t is plotted versus time t, the pseudo-second order rate constant can be obtained from the slope of the graph.

Adsorption isotherms

Adsorption isotherm analysis was performed by inoculating 100ml MSM amended with RBBR (5, 10, 25, 45 and 75 mg/L) with 30mg biomass at pH 5.5 and temperature 40ºC. Two types of adsorption isotherms were studied:

a) Langmuir Isotherm (1918):

$$\frac{C_e}{q_e} = \frac{1}{k_l q_m} + \frac{C_e}{q_m}$$

Equation 4.6

Where k_l is the Langmuir isotherm constant $(mLmg^{-1})$ and q_m is the maximum amount of the dye adsorbed (mgg^{-1})

b) Freundlich Isotherm (1906):

$$\ln q_e = \ln k_f + \frac{1}{n}\ln C_e$$

Equation 4.7

Where K_f is the constant of Freundlich isotherm $(mLmg^{-1})$ and n is the adsorption constant.

SEM and FTIR Analysis

Scanning electron microscopy (SEM)

100 ml MSM amended with RBBR (25mg/L) was inoculated with 30mg bacterial biomass and incubated at 40ºC, pH 5.5 for 240h. The biomass was then harvested by centrifugation at 10000rpm for 8min. The pellet was collected and fixed with 4% (v/v) glutaraldehyde and serially dehydrated using ethanol. Dehydrated samples were air-dried and mounted on SEM stubs. The samples were then gold-coated. Bacterial cells without RBBR were prepared likewise and kept as the control for comparison. Morphological and surface changes were studied by scanning electron microscopy (SEM) using Zeiss EVO LS 10.

Fourier transform infrared spectroscopy (FTIR)

30 mg bacterial biomass was added to 100 ml RBBR-amended (25mg/L) MSM under optimized conditions (temperature 40ºC, pH 5.5) for 240h. After incubation, the biomass was separated by centrifugation at 10000 rpm for 8min. The pellets thus obtained were dried before the FTIR studies. Bacterial samples prepared in the same way in the absence of dye were considered as the control. FTIR analysis was performed in the spectral range of 500 to 4500 cm^{-1} before and after RBBR adsorption to identify the functional groups of the dye that were on the bacterial surface. Measurements were carried out using an FTIR spectrophotometer (Bruker Alpha model, USA) in the absorbance mode.

Phytotoxicity study

100mL RBBR dye solution (25mg/L) was inoculated with 30mg bacterial biomass and incubated at 40ºC, pH 5.5 for ten days. Phytotoxicity of the resultant solution was studied. High-yield variety rice seeds (*Oryza sativa* var. IET 4786) were procured from the Rice Research Institute, Chinsurah, West Bengal, India. The seeds were placed equidistantly in sterile Petri plates lined with two Whatman filter papers soaked in the untreated RBBR and the solution obtained after the bacterial treatment. Two essential parameters, i.e., germination percentage and seedling lengths, were considered for evaluating the phytotoxicity. Germination was monitored on the third, fifth, and seventh days. Seeds in which radical emerged were considered germinated. Root lengths and shoot lengths were measured on the 14th day.

Cytotoxicity Study

Peripheral Blood Mononuclear Cells (PBMC) were suspended in RPMI 1640 media supplemented with 10% Fetal Bovine Serum (FBS) and 2% Penicillin-Streptomycin. The cells were cultivated in T-15 flasks until they were 80% confluent. After transferring 2 ml of PBMC suspensions into each tube, 50µL of the untreated RBBR (25 mg/L) and the bacterially treated RBBR were applied. For 24 hours, the tubes were incubated at 37°C in the presence of 5% CO2. The MTT assay was then used to calculate the percentage of live and dead cells in various test samples by measuring absorbance at 590 nm.

$$\% \textbf{ Live Cells} = \frac{\textbf{Absorbance of treated cells}}{\textbf{Absorbance of untreated cells}} \textbf{ x 100}\%$$

Equation 4.8

RESULTS AND DISCUSSION

Decolorization of Remazol Brilliant Blue R by *Bacillus rigiliprofundi*

Remazol Brilliant Blue R solution (20mg/L) in distilled water was subjected to 5mL culture of *B. rigiliprofundi* and decolorization was observed intermittently. Nearly 70% decolorization was recorded at 168h (7days). Decolorization gradually increased to 73% at the end of 264 h (11 days) (Figure 4.1). The decolorisation increased linearly till the seventh day and subsequently reached saturation. No additional supplement had been added in the decolorization medium. This is the first report of *B. rigiliprofundi* decolorizing Remazol Brilliant Blue R.
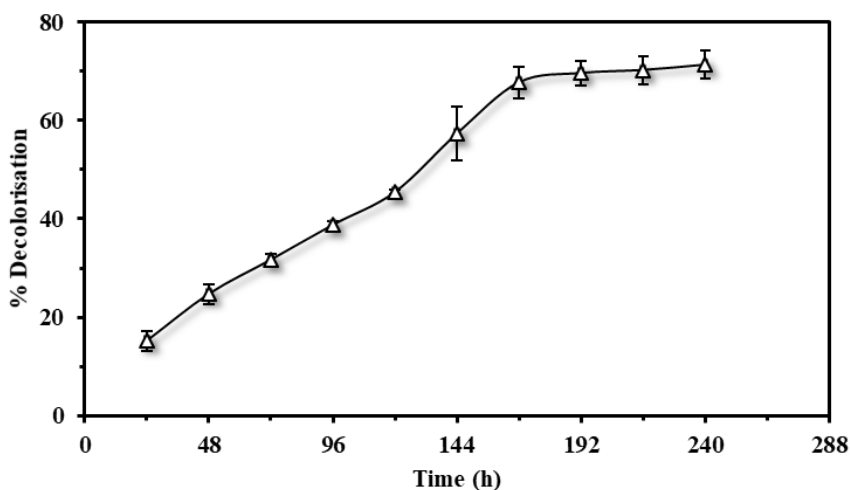
Figure 4.1 Remazol Brilliant Blue R decolorisation profile of *Bacillus rigiliprofundi*

Only a few RBBR degrading strains of fungi have been reported to date, which may be due to the highly recalcitrant nature of the dye. Ligninolytic enzymes from some tropical Brazilian basidiomycetes fungi capable of RBBR decolorisation were reported by Machado et al (2005). *Trametes hirsuta* was reported to decolorise 91% of 25mg/L RBBR, in 15 days (Bibi and Bhatti, 2012). *Trichoderma citriniviridae* and *Pestalotiopsis sp*. perform enzymatic degradation of RBBR (initial dye concentration 50mg/L) to an extent of 80.9% and 87.2% respectively in 14 days under glucose-supplemented conditions. Biological adsorption is a cost-effective method to reduce the presence of water-soluble dyes in textile and tannery effluents. Natural or processed plant parts, fungi and bacteria effectively adsorb and remove dye from the solution. The adsorption

of RBBR on pinang frond-based activated carbon was reported by Ahmad et al (2014). Pomegranate-fruit-peel activated carbon was used for the adsorptive removal of RBBR (81.35% adsorptive decolorisation, initial dye concentration 25mg/L) from synthetic wastewater (Ahmad et al, 2020). Apart from these, watermelon rind, mangosteen peel, etc. have also been used to produce activated carbon for the adsorptive removal of RBBR (Ahmad et al, 2015; Ahmad and Alrozi, 2010). Kulkarni et al (2018) used water hyacinth root powder to adsorb and remove RBBR. Syafiuddin & Fulazzaky (2021) reported adsorptive removal of RBBR by *Trichoderma koningiopsis*. Barreda-Reyes et al (2015) reported the use of yeast biomass to perform adsorptive removal of RBBR. *Scenedesmus quadricauda*, green algae, was immobilized in alginate gel beads and used for adsorptive removal of RBBR by Ergene et al (2009).

Pellets obtained on centrifuging the decolorised medium after bacterial treatment (by methods described earlier) took up the bright blue color of the RBBR dye, indicating that the bacterial biomass had adsorbed the dye (Figure 4.2).

Figure 4.2 Bright blue cell pellets obtained after dye removal from the medium, indicating the adsorption of RBBR on the bacterial biomass

Saputra et al. (2017) report that the adsorptive removal of RBBR using amino-functionalised organosilane. A cross-linked chitosan-glyoxal/kaolin clay composite was used by Jawad et al (2021) for adsorptive removal of RBBR. Diethyl triamine functionalized magnetic macro-reticular hybrid material exhibited sorptive removal of RBBR (Elwakeel et al, 2016). A macroporous polystyrene resin was used to perform adsorptive removal of RBBR by Ozturk and Silah (2020). Borax cross-linked Jhingan gum hydrogel could remove RBBR from water (Mate and Mishra, 2020). Reghioua et al

(2021) synthesized and used a magnetic chitosan-glutaraldehyde/zinc oxide/Fe_3O_4 nanocomposite for adsorptive decolorisation of RBBR.

Effect of different physical parameters on dye adsorption

The key parameters (pH, temperature, inoculum size, and initial biomass) influencing dye adsorption were studied. Biosorption experiments were carried out with six different biomass (6, 15, 24, 30, 39 and 45 mg) at five different pH (4.5, 5.5, 7.5, 8.5 and 10.5) and at five different temperature (10ºC, 30ºC, 40ºC, 50ºC, and 60ºC) for five different initial RBBR concentrations (5, 10, 25, 30, 50 and 75 mg/L).

Effect of biomass on biosorption

Figure 4.3a illustrates the effect of inoculum size in terms of biomass on the adsorption of RBBR by *B.rigiliprofundi*. When 6mg biomass was used, only 28% adsorptive decolorisation was observed. An increase in adsorptive decolorisation was recorded on increasing the biomass upto 30mg (80.5% adsorptive decolorisation). This observation indicates that an increase in biomass increases biosorption of the dye. Further increase in biomass did not affect the biosorption of RBBR by *B.rigiliprofundi*. As a result of the increase in biomass or biosorbent surface area, the number of functional groups involved in the biosorption process effectively increases till saturation is achieved (Hamzeh, 2012). Adsorption improves when the adsorbent's surface area becomes more accessible.

Effect of dye concentration on biosorption

The effect of RBBR concentration on the biosorption ability of the strain is presented in Figure 4.3b. Adsorptive decolorisation decreased with the increase in RBBR concentration. While more than 83.45% adsorptive decolorisation was observed for 25mg/L dye, it was reduced to only about 15.55% for 100mg/L RBBR concentration. This might happen because, at higher dye concentrations, excess dye molecules are present compared to the binding sites available on the bacterial biomass. Similar observations were reported in case of adsorptive removal of the azo dye Remazol Black by *Sarocladium sp.*(Nouri et al, 2020)

Effect of pH on biosorption

pH is one of the most important factors which determines the efficiency of biosorption (Aksu et al., 2005). The impact of pH on biosorption was investigated and an optimum pH for adsorptive decolorisation was selected (Figure 4.3c). Highest adsorptive

decolorisation (82%) was recorded at pH 5.5. At more alkaline pH, adsorptive decolorisation decreased significantly: only about 16% adsorptive decolorisation was observed at pH 10.5. The bacterial cell wall shows variable susceptibility to the pH of the medium which leads to differences in pollutant biosorption (Ozturk et al. 2020). Optimum pH for dye removal varies significantly from species to species and from dye to dye. At low pH, the number of positively charged adsorption sites increases, making binding the anionic dye RBBR more feasible. On the other hand, adsorbent surfaces accumulate negative charges at high pH, reducing adsorption efficacy due to repulsion (Ozcan & Ozcan, 2004; Nouri et al. 2020). *Rhodopseudomonas palustris* 51ATA showed maximum azo dye Fast black K removal at optimal pH 8 (Öztürk et al. 2020). Periphytic biofilms show Methyl orange adsorption in a wide range of pH and optimal dye removal is observed in the pH range 5-9 (Wu 2016). 92.4% bio removal of azo dye direct violet at a highly acidic condition (pH 2) was reported by Abd El-Rahim et al (2009).

Effect of temperature on biosorption

The most favorable temperature range for biosorption of RBBR by *B. rigiliprofundi* was found to be between 30ºC to 40ºC (Figure 4.3d). The highest adsorptive decolorisation (more than 82%) was achieved at 40ºC which reduced to only 18% at 60ºC. Physical biosorption has been more efficient at lower temperatures (Abbas and Trari, 2015). Temperature can affect the stability and configuration of the bacterial cell wall, thereby ionizing the chemical moieties and the binding sites of the cell surfaces (Kalamdhad & Kazmi, 2009). At higher temperatures, the bonds between the cell surface and the dye may break, causing desorption (Asku 2005, Gadd 2009). Several bacterial strains have been reported to exhibit optimal dye adsorption at temperatures ranging from 30ºC to 40ºC. The highest bioremoval of methyl red by *Lysinibacillus fusiformis* was recorded at 30ºC (Sari & Simarani 2019). *Pseudomonas putida* showed maximum dye adsorption at 37ºC.
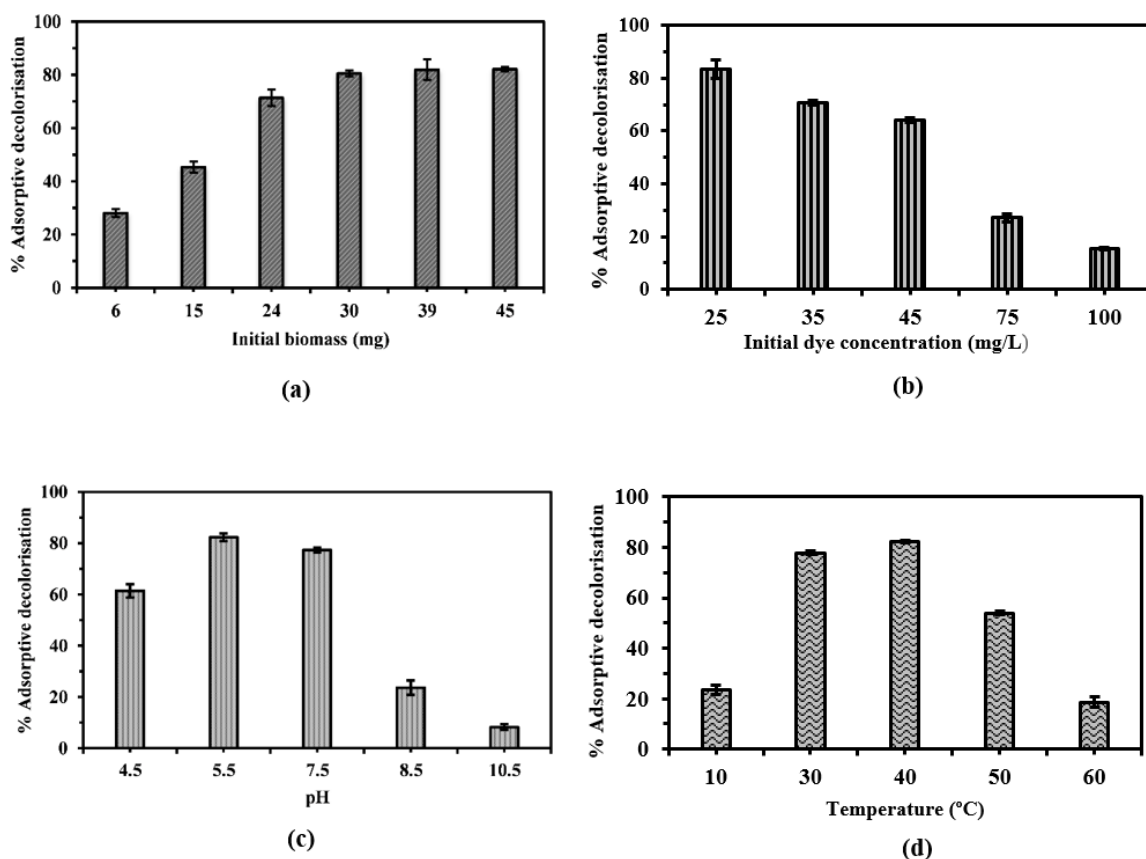
Figure 4.3 Effects of biomass (a), initial dye concentration (b), pH (c), and temperature (d) on adsorptive decolorisation

Growth profile of *B. rigiliprofundi* in presence and absence of RBBR

The growth pattern was investigated by growing the organisms in the presence of dye and comparing them to the dye-less control (Figure 4.4). The presence of 25mg/L RBBR dye in the media extended the lag phase of the bacteria. The bacteria adapt to their environment and prepare for exponential growth during the lag phase. The bacteria required a more prolonged lag phase to adapt to the dye-rich growth media. Exponential growth initiated after 24 hours in the absence of RBBR and 48 hours in the presence of the dye RBBR. The highest viable cell count in the dye-free medium was greater ($Log_{10}(CFU/ml)$=8.9) than in the dye-rich medium ($Log_{10}(CFU/ml)$=8.4). Hence it can be concluded that although the growth was initially slower, *B. rigiliprofundi* could adapt to and overcome the toxicity of the dye.
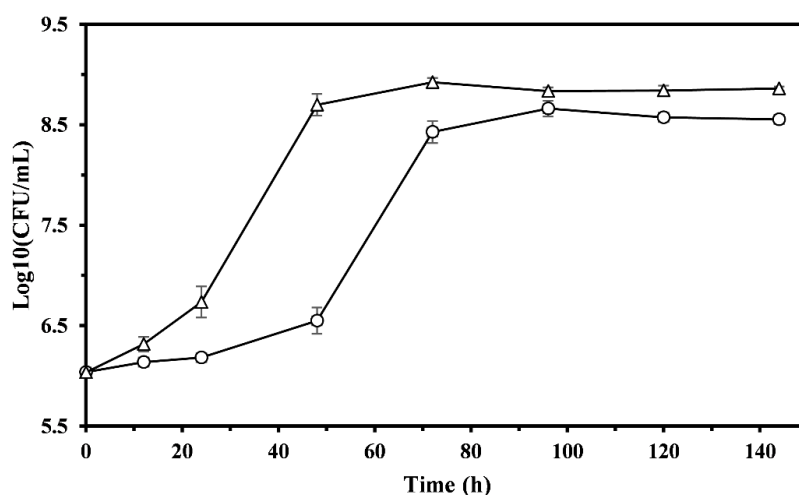
Figure 4.4 Growth profile of *Bacillus rigiliprofundi* in the presence (O) and absence (Δ) of RBBR

Kinetics of adsorption

The term "sorption" refers to attaching a substance to a surface that results in an interaction. Sorption can be classified as physical, chemical, or electrostatic, depending on the type of interaction between the sorbent and the sorbate. The kinetic model followed by a biosorption system can predict the rate of adsorption of dye on the surface of the bacteria and can also provide valuable information on adsorption pathways and the mechanisms that may be involved. Since the R^2 value of pseudo-first order kinetics (0.98) was higher than that of the pseudo-second order kinetics (0.94), it was concluded that the pseudo-first order kinetics is more appropriately applicable. Adsorption is typically reported to occur via physisorption or diffusion through the interface when a biosorption system follows the Lagergren pseudo first-order rate equation (Ferreiro et al. 2019, Sahoo and Prelot, 2020). In physisorption, the adsorbate adheres to the surface via weak van der Waals forces, hydrogen bonding, or electrostatic attraction (Sahoo & Prelot, 2020). The rate of sorption site occupation is proportional to the number of vacant sites for systems that follow the pseudo-first order kinetics (Salam, 2013). This is reflected in the phenomenon that during the initial stages of adsorption, there are abundant vacant sites on the bacterial cells, and thus the dye molecules are rapidly taken up from the media; however, during the later phases, the number of vacant sites for dye adsorption is effectively reduced, resulting in a slower rate of dye-adsorption. The rate constants were calculated and have been presented in Table 4.1. The pseudo-first order kinetics of RBBR adsorption by the bacteria is shown in Figure 4.5.
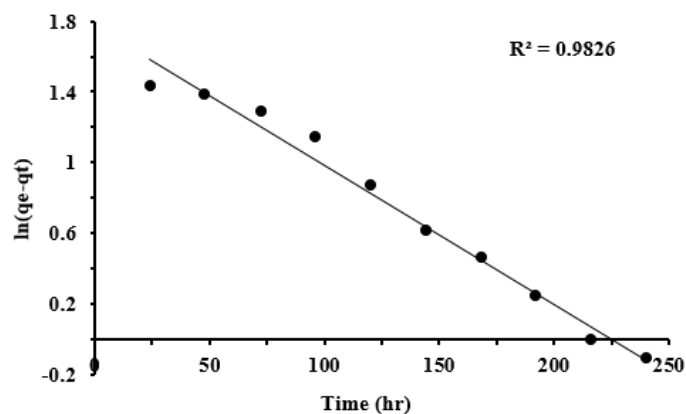
(a)
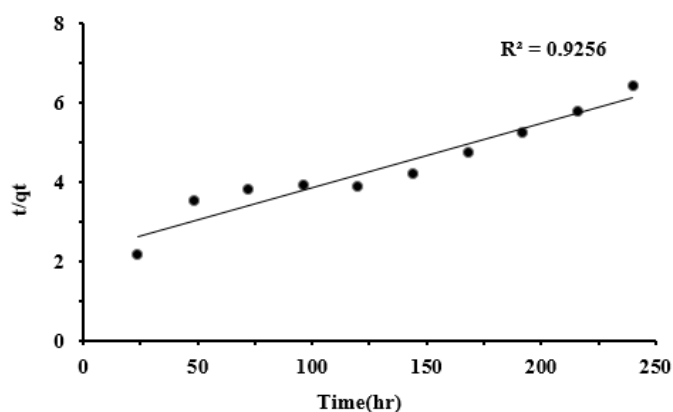
(b)

Figure 4.5 (a) Pseudo-first order kinetics plotted as a function of ln (q_e-q_t) versus time and (b) pseudo-second order kinetics plotted as a function of t/q_t versus time

Table 4.1 Comparison of kinetic parameters of adsorption of the dye on the bacteria

Models	Parameters	Description	Values
Pseudo-first order	k_1	Pseudo-first order rate constant	7.7×10^{-3} h^{-1}
	$q_{e\,(experimental)}$	Quantity of RBBR dye adsorbed at equilibrium (experimental)	53.66 mgg^{-1}
	$q_{e\,(calculated)}$	Quantity of RBBR dye adsorbed at equilibrium (calculated)	64.24 mgg^{-1}
	R^2	Correlation coefficient	0.98
Pseudo-second order	k_2	Pseudo-second order rate constant	1.3×10^{-4} gmg^{-1}h^{-1}
	q_e	Quantity of RBBR dye adsorbed at equilibrium	78.74 mgg^{-1}
	R^2	Correlation coefficient	0.94

Adsorption isotherms

Adsorption isotherms indicate the interaction pathway between the adsorbate and the adsorbent. The Langmuir isotherm model assumes that the surface of the adsorbent is covered by a monolayer of the adsorbate and adsorption takes place at specific homogeneous sites. In contrast to the Langmuir model, the Freundlich model allows multilayer adsorption (Aurich, 1906) and heterogeneous energetic distribution of active sites (Ozturk et al, 2020; Nouri et al, 2020). The Langmuir and Freundlich isotherms of RBBR adsorption on *Bacillus rigiliprofundi* are presented in Table 4.2. The best fit generated following the Langmuir and Freundlich models is shown in Figure 4.6. Results indicate that the biosorption of RBBR on *B. rigiliprofundi* fits the Langmuir isotherm more appropriately since the R^2 value of the Langmuir isotherm model (0.99) was greater than that of the Freundlich model (0.86). The maximum adsorption capacity (q_m) of *B. rigiliprofundi* was 57.803 mgg[-1].

Table 4.2 Comparison of adsorption isotherm models

Models	Parameters	Description	Values
Langmuir isotherm	q_m	Maximum monolayer adsorption capacity	57.803 mgg[-1]
	K_l	Langmuir isotherm constant	1.73 mLmg[-1]
	R^2	Correlation coefficient	0.99
Freundlich isotherm	K_f	Freundlich isotherm constant	32.57 mLmg[-1]
	1/n	Adsorption intensity	0.1485
	R^2	Correlation coefficient	0.84
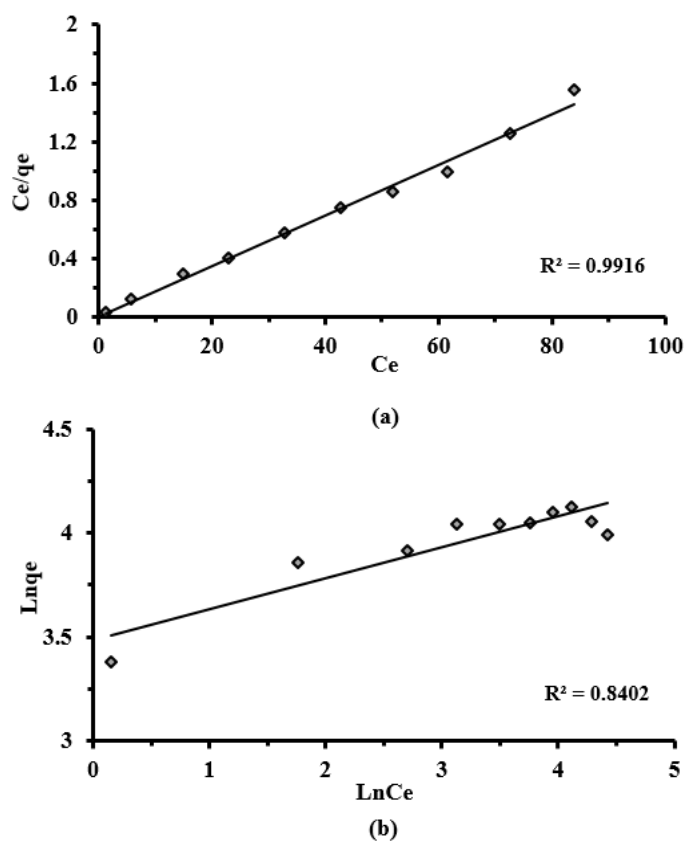
Figure 4.6 The Langmuir (a) and Freundlich (b) adsorption isotherms of RBBR on *Bacillus rigiliprofundi*

FTIR Analysis

Adsorption is a surface phenomenon and hence knowledge about the existing functional groups is essential. This also provides evidence of adsorption of dye on the bacterial surface. FTIR spectrum of the bacterial surface before and after dye adsorption (Figure 4.7) was studied. The enolic OH of quinones causes a peak at 3100 cm^{-1} in the FTIR spectrum of RBRR. It does not appear in the FTIR spectra of bacteria, but a peak at 3100 cm^{-1} in the spectrum of RBRR-bound bacteria confirms the presence of enolic OH of quinones, which could be attributed to the adsorbed RBRR on the bacterial surface. Again a peak at 681 cm^{-1} present in RBRR may be due to the C-S stretching which is absent in the bacteria. After adsorption of RBRR, the dye-bound bacteria gives a peak at 681 cm^{-1} confirming the presence of C-S stretching (Srinivasaraghavan et al., 2017). Similarly, a peak at 913 cm^{-1} indicates SO$_3$ stretching which is very prominent in RBRR but absent in the bacterial surfaces. In RBRR-adsorbed bacteria, this signature peak at 913 cm^{-1} indicates the presence of SO$_3$ due to adsorption of RBRR on to bacterial surface

(Srinivasaraghavan et al., 2017). A peak at 564 cm^{-1} is present in RBRR may be due to the presence of Na in the RBRR structure as aryl halides give peak in this range. This peak is absent in the bacterial FTIR spectrum. However, it appears prominently in RBRR-bound bacteria. Likewise, a peak at 1655 cm^{-1} in the bacterial spectrum may be due to C=O stretching of ester groups present on their surfaces which again is present in RBRR-bound bacteria but absent in the dye itself. In the bacterial spectrum, a small hump can be observed around 3200-3400 cm^{-1}, which may be due to the N-H stretching of amines of proteins present on the bacterial surface. The smaller humps corresponding to reduced intensity around 3400-3600 cm^{-1} may be due to the OH stretching of alcoholic groups on the bacterial surface. A prominent hump in the region of 3200-3600 cm^{-1} in the RBRR spectrum may be due to N-H stretching. In the RBRR-bound bacterial spectrum, the presence of all these groups was confirmed by the presence of similar peak and humps. The peaks at 1000 cm^{-1} and 1200 cm^{-1} designates the N-H stretching of NH$_2$ present in both the dye and the bacteria and these common peaks are also present in the RBRR-bound bacteria (Srinivasaraghavan et al., 2017). Similarly, the peaks around 700-800 cm^{-1} corresponding to aromatic rings and those at 2800 cm^{-1} and 2900 cm^{-1} corresponding to the CH symmetric and asymmetric stretching of CH$_2$, respectively, are present in all three spectra (Fanchiang and Tseng, 2009).
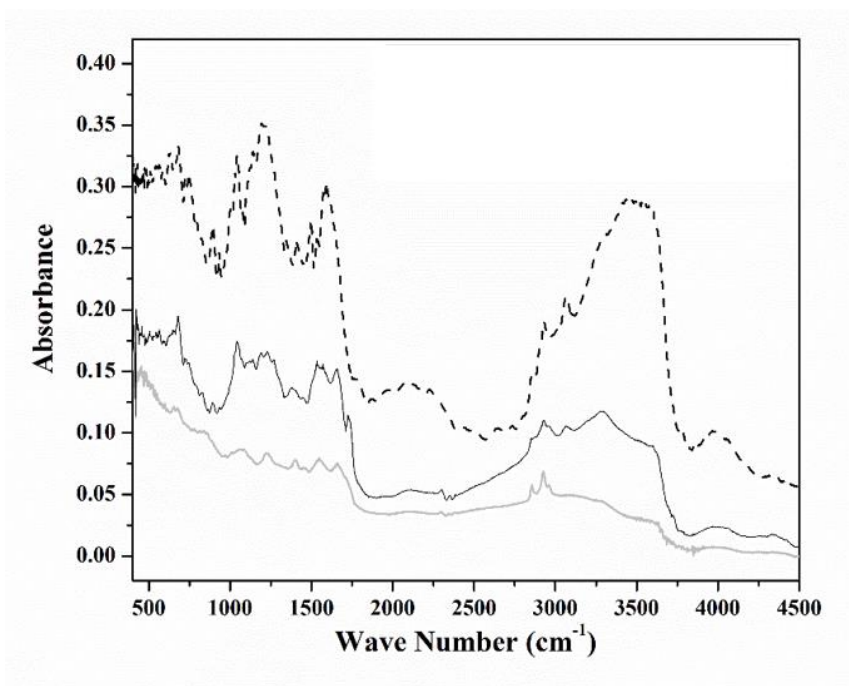
Figure 4.7 FTIR spectra of the bacteria (——) RBBR-bound bacteria (——) and RBBR (-----)

SEM analysis

Scanning electron microscopy is widely used to study the morphological features as well as topological or surface characteristics of adsorbent material. SEM images of the bacteria before and after adsorption of the dye are represented in Figure 4.8. Before adsorption (Figure 4.8a), the bacteria are visible as rod-shaped cells with smooth and regular surfaces. After biosorption of the dye, significant changes in the surface characteristics could be observed. The cell surfaces appeared rough, wrinkled, with a visible coating, indicating the deposition of the dye molecules (Figure 4.8b).
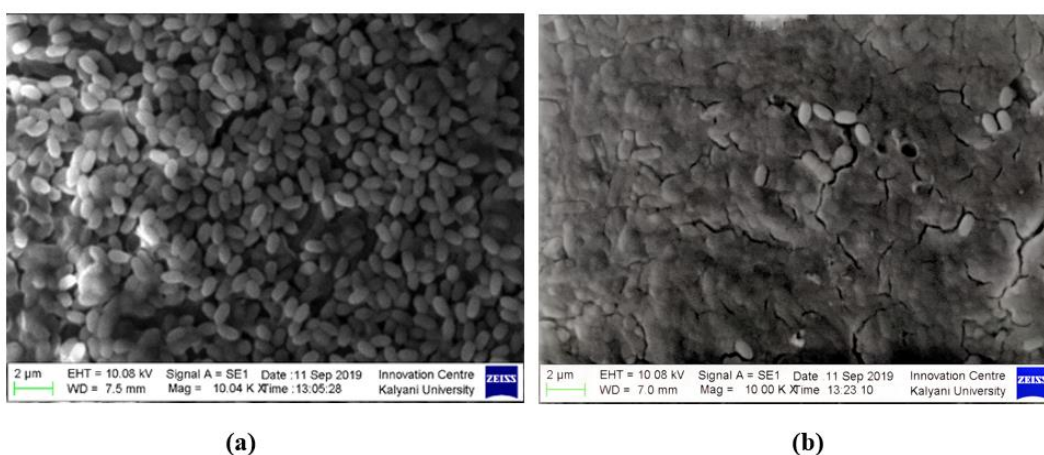
Figure 4.8. Scanning electron micrograph of *Bacillus rigiliprofundi* before (a) and after (b) adsorption of RBBR

Phytotoxicity

Table 4.3 and 4.4 represent germination percentage and root length and shoot length respectively as a measure of phytotoxicity of RBBR before and after treatment on *Oryza sativa* var. IET 4786. It can be observed that at the end of seven days, germination has taken place in very low frequency (about 5%) in the seeds soaked in the untreated RBBR, whereas, higher rate of emergence of radical (about 68%) can be seen in the seeds soaked in the treated dye solution. At the end of fourteen days, the rice seedlings grown in untreated RBBR show shorter root and shoot lengths than those grown in RBBR treated with the bacteria. The RBBR-grown rice seedling is also visibly deficient in chlorophyll pigments (Figure 4.9).
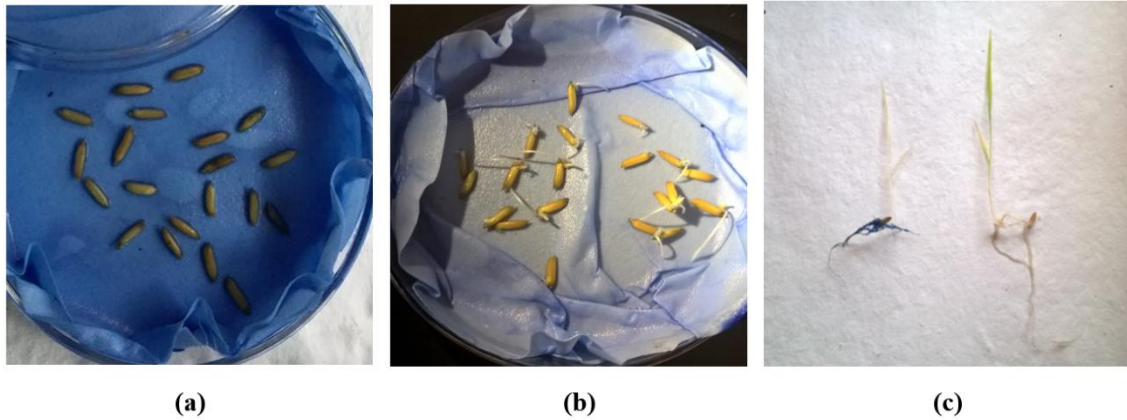
Figure 4.9 Phytotoxicity studies: Germination (a, b) and seedling lengths (c) of *Oryza sativa* **IET 4786 in presence of RBBR dye before and after treatment**

Table 4.3 Germination percentage of Oryza sativa var. IET 4786 in presence of treated and untreated RBBR

Days	Germination percentage		
	Control (water)	Untreated RBBR	Treated RBBR
3th	23.35±0.38	0	15±0.006
5th	46.65±0.05	8.35±0.002	33.35±0.07
7th	83.35±0.66	5.35±0.07	68.35±0.088

Values are represented as mean of three replicates ± standard deviation

Table 4.4 Root length and shoot length of Oryza sativa var. IET 4786 in presence of treated and untreated RBBR on the 14th day of treatment

Treatments	Root length (cm)	Shoot length (cm)
Control (water)	11.14±0.52	13.892±0.39
Untreated RBBR	4.09±0.04	5.86±0.08
Treated RBBR	8.1±0.54	8.531±0.08

Values are represented as mean of three replicates ± standard deviation

RBBR has been reported to show prominent phytotoxicity by many authors. In general, it delays and lowers the rate of germination and results in stunted growth of early seedlings. The concentration of the dye is directly proportional to the phytotoxicity elicited (Velayutham et al., 2018; Osma et al., 2010). The result of the phytotoxicity analysis was in line with the previous works and it was observed that reduction in the

concentration of the dye (brought about by the bacterial treatment) resulted in lowering the phytotoxicity.

Cytotoxicity

Peripheral Blood Mononuclear (PBM) cell lines were used to test the toxicity of dye solutions by MTT assay. In toxicology, the MTT assay is a well-known and well accepted method for studying cellular responses to toxicants. It has the ability to provide data on cell death, survival, and metabolic processes. Reduction of toxicity after bacterial treatment of the dye is clearly indicated by the significantly greater viability of the PBMC from the original dye as (Figure 4.10). More than 80% cells remained viable in presence of the bacterially treated RBBR, indicating its ecological biocompatibility.
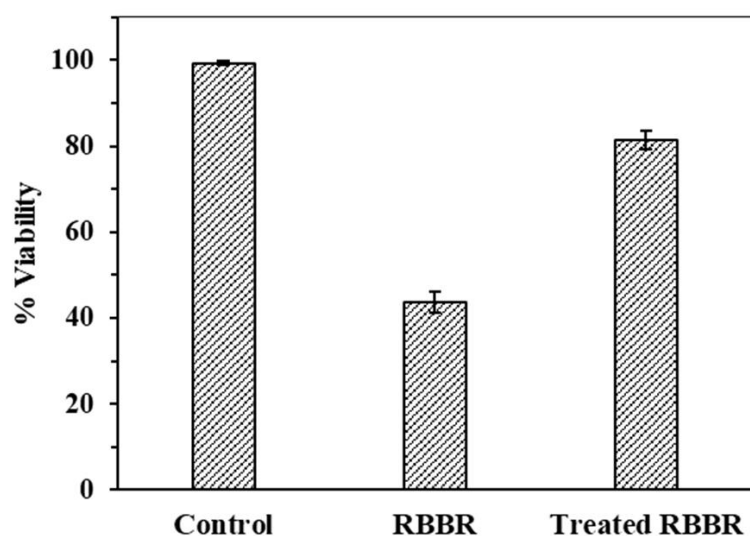
Figure 4.10 % viability of Peripheral Blood Mononuclear Cells after exposure to treated and untreated RBBR

The anthraquinone dye RBBR has significant cytotoxic effect on different animal and human cell lines. RBBR was cytotoxic to the Human Dermal Fibroblast (HDF) cell line (40% cell viability), but treatment with fungus *Trametes hirsuta* significantly reduced the cytotoxicity and the cell viablilty increased to 90%. Other cell lines, such as murine muscle cells (C2C12) and dog kidney cells (MDCK) showed a similar pattern [Alam et al., 2021]. The results of the cytotoxicity investigation were consistent with earlier studies, and it was observed that lowering the dye concentration (due to bacterial treatment) resulted in lower cytotoxicity.

CONCLUSION

Bacterial cell walls include functional groups that interact with the environment and, as a result, can adsorb ions; the type of cell wall components regulates the quantity and exposure of these groups. Although multiple bacteria have been reported to adsorb various dyes, no *Bacillus* strain has yet been identified to remove RBBR via adsorption, making this work the first report of *B.rigiliprofundi* to remove RBBR via adsorption. Since no further processing or supplementation is required, the novel bacterial strain *Bacillus rigiliprofundi* can be considered as a convenient and cost-effective means of adsorptive removal of the hazardous, recalcitrant dye RBBR.

REFERENCES

Abbas, M. and Trari, M., Kinetic, equilibrium and thermodynamic study on the removal of Congo Red from aqueous solutions by adsorption onto apricot stone. Process safety and Environmental protection, 2015, vol. 98, pp.424-436.

Ada, K., Ergene, A., Tan, S. and Yalçın, E., Adsorption of Remazol Brilliant Blue R using ZnO fine powder: Equilibrium, kinetic and thermodynamic modeling studies. J. Hazard. Mater. , 2009, vol. 165, pp.637-644.

Agarry, S.E. and Ayobami, O., Evaluation of microbial systems for biotreatment of textile waste effluents in Nigeria: biodecolourization and biodegradation of textile dye, J. Appl. Sci. Environ. Manag., 2011, vol. 15, pp. 79–86.

Ahmad, M. A., & Alrozi, R., Optimization of preparation conditions for mangosteen peel-based activated carbons for the removal of Remazol Brilliant Blue R using response surface methodology, Chem. Eng. Sci., 2010, vol.165, pp. 883-890.

Ahmad, M. A., Herawan, S. G., & Yusof, A. A.. Equilibrium, kinetics, and thermodynamics of Remazol Brilliant Blue R dye adsorption onto activated carbon prepared from pinang frond. 2014. International Scholarly Research Notices.

Ahmad, M. A., Ahmad, N., & Bello, O. S. Removal of remazol brilliant blue reactive dye from aqueous solutions using watermelon rinds as adsorbent. J Dispers Sci Technol., 2015. vol. 36, pp. 845-858.

Ahmad, M. A., Eusoff, M. A., Oladoye, P. O., Adegoke, K. A., & Bello, O. S. Statistical optimization of remazol brilliant blue R dye adsorption onto activated carbon prepared from pomegranate fruit peel. Chem. Data Collect. 2020. Vol. 28, pp. 100426.

Alam, R., Ardiati, F.C., Solihat, N.N., Alam, M.B., Lee, S.H., Yanto, D.H.Y., Watanabe, T. and Kim, S., 2021. Biodegradation and metabolic pathway of anthraquinone dyes by Trametes hirsuta D7 immobilized in light expanded clay aggregate and cytotoxicity assessment. *Journal of Hazardous Materials*, *405*, p.124176.

Aurich, A.; Hofmann, J.; Oltrogge, R.; Wecks, M.; Gläser, R.; Blömer, L.; Mauersberger, S.; Müller, R.A.; Sicker, D.; Giannis, A. Over the adsorption in solution. J. Phys. Chem. 1906, vol. 57, pp. 1100–1107

Barreda-Reyes, K. L., Ortega-López, J., Ortega-Regules, A. E., Santiago-Santiago, L. A., & Netzahuatl-Muñoz, A. R. Removal of remazol brilliant blue R dye from aqueous solutions using yeast biomass as biosorbent. Rev. cuba. quím. (En línea), 2015. vol. 27(2).

Bibi, I., & Bhatti, H. N. Enhanced biodecolorization of reactive dyes by basidiomycetes under static conditions. Appl. Biochem. Biotechnol., 2012 vol. 166(8), pp. 2078-2090.

Chen CC, Liao HJ, Cheng CY, Yen CY, Chung YC. Biodegradation of crystal violet by Pseudomonas putida. Biotechnol. Lett., 2007, vol. 29, pp.391-6.

Eichlerová, I., Homolka, L., Lisá, L. and Nerud, F., Orange G and Remazol Brilliant Blue R decolorization by white rot fungi *Dichomitus squalens, Ischnoderma resinosum* and *Pleurotus calyptratus.* Chemosphere, 2005, vol. 60, pp.398-404.

Elwakeel, K. Z., El-Bindary, A. A., Ismail, A., & Morshidy, A. M. Sorptive removal of Remazol Brilliant Blue R from aqueous solution by diethylenetriamine functionalized magnetic macro-reticular hybrid material. Rsc Advances, 2016 vol. 6(27), pp.22395-22410.

Ergene, A., Ada, K., Tan, S., & Katırcıoğlu, H.. Removal of Remazol Brilliant Blue R dye from aqueous solutions by adsorption onto immobilized Scenedesmus quadricauda: Equilibrium and kinetic modeling studies. Desalination, 2009 vol. 249(3), pp.1308-1314.

Fanchiang, J.M. and Tseng, D.H., Degradation of anthraquinone dye CI Reactive Blue 19 in aqueous solution by ozonation. Chemosphere, 2009, vol.77, pp.214-221.

Ferreiro, C., Villota, N., Lombraña, J. I., Rivero, M. J., Zúñiga, V., & Rituerto, J. M. Analysis of a hybrid suspended-supported photocatalytic reactor for the treatment of wastewater containing benzothiazole and aniline. Water, 2019. vol. 11, pp. 337.

Freundlich, H. M. F. Over the adsorption in solution. J. Phys. chem, vol. (1906). vol. 57(385471), pp. 1100-1107.

Gadd, G.M.,. Biosorption: critical review of scientific rationale, environmental importance and significance for pollution treatment. J. Chem. Technol. Biotechnol. 2009 vol. 84(1), pp.13-28.

Hamzeh, Y., Ashori, A., Azadeh, E. and Abdulkhani, A.,. Removal of Acid Orange 7 and Remazol Black 5 reactive dyes from aqueous solutions using a novel biosorbentMater. Sci. Eng. C, 2012. Vol. 32(6), pp.1394-1400.

Ho YS, McKay G. Pseudo-second order model for sorption processes. Process Biochem. 1999, vol. 34, pp.451-65.

Jawad, A. H., Abdulhameed, A. S., Kashi, E., Yaseen, Z. M., ALOthman, Z. A., & Khan, M. R.. Cross-linked chitosan-glyoxal/kaolin clay composite: Parametric optimization for color removal and COD reduction of remazol brilliant blue R dye. J Polym Environ., 2021 vol. 1-15.

Johari, I. S., N. A. Yusof, M. J. Haron, and S. M. M. Nor., Preparation and characterization of poly(ethyl hydrazide)- grafted oil palm empty fruit bunch fibre for the removal of Cu(II) Ions from an aqueous environment. Molecules, 2013, vol.18, pp61–8472.

Kalamdhad, A. S., & Kazmi, A. A. Rotary drum composting of different organic waste mixtures. Waste Manag Res., 2009. vol.27 (2), pp129-137.

Kulkarni, M. R., Bhagyalakshmi, C., Anand, D., & Herle, R. N. Removal of remazol brilliant blue dye from aqueous solutions using water hyacinth root powder. Desalination Water Treat., 2018. Vol. 122, pp. 331-338.

Lagergren, S.K., About the theory of so-called adsorption of soluble substances. Sven. Vetenskapsakad. Handingarl, 1898 vol. 24, pp.1-39.

Langmuir, I. (1918). The adsorption of gases on plane surfaces of glass, mica and platinum. J. Am. Chem. Soc, vol. 40(9), pp. 1361-1403.

Machado, K. M., Matheus, D. R., & Bononi, V. L. Ligninolytic enzymes production and Remazol Brilliant Blue R decolorization by tropical Brazilian basidiomycetes fungi. Braz. J. Microbiol., 2005 vol.36, pp. 246-252.

Mate, C. J., & Mishra, S. Synthesis of borax cross-linked Jhingan gum hydrogel for remediation of Remazol Brilliant Blue R (RBBR) dye from water: adsorption isotherm, kinetic, thermodynamic and biodegradation studies. Int. J. Biol. Macromol, 2020 vol.151, pp.677-690.

Mechichi, T., Mhiri, N. and Sayadi, S., Remazol Brilliant Blue R decolourization by the laccase from *Trametes trogii.* Chemosphere, 2006, 64, pp.998-1005.

Natarajan S, Tiruvenkadam K, Basha CA, Veerasamy M. Biosorption of textile dye using immobilized bacterial (Pseudomonas aeruginosa) and fungal (Phanerochate chrysosporium) cells. Am. J. Environ. Sci., 2013, vol. 9, pp: 377-87.

Nouri, H., Azin, E., Kamyabi, A., & Moghimi, H. Biosorption performance and cell surface properties of a fungal-based sorbent in azo dye removal coupled with textile wastewater. Int J Environ Sci Technol., 2020. pp 1-14.

Osma, J.F., Toca-Herrera, J.L. and Rodríguez-Couto, S.,Transformation pathway of Remazol Brilliant Blue R by immobilised laccase. Bioresour. Technol., 2010, vol. 101, pp.8509-8514.

Özcan, A. S., & Özcan, A. (2004). Adsorption of acid dyes from aqueous solutions onto acid-activated bentonite. J. Colloid Interface Sci, vol. 276(1), pp. 39-46.

Öztürk, Ayten, Emel Bayol, and Meysun I. Abdullah. "Characterization of the biosorption of fast black azo dye K salt by the bacterium Rhodopseudomonas palustris 51ATA strain." Electron. J. Biotechnol. 2020, vol. 46, pp 22-29

Ozturk, G., & Silah, H. Adsorptive Removal of Remazol Brilliant Blue R from water by using a macroporous polystyrene resin: isotherm and kinetic studies. Environ. Process, 2020. Vol.7 (2), 479-492

Reghioua, A., Barkat, D., Jawad, A. H., Abdulhameed, A. S., Rangabhashiyam, S., Khan, M. R., & ALOthman, Z. A. Magnetic Chitosan-Glutaraldehyde/Zinc Oxide/Fe 3 O 4 Nanocomposite: Optimization and Adsorptive Mechanism of Remazol Brilliant Blue R Dye Removal. J. Polym. Environ, 2021. pp. 1-16.

Sahoo, T. R., & Prelot, B. (2020). Adsorption processes for the removal of contaminants from wastewater: the perspective role of nanomaterials and nanotechnology. In *Nanomaterials for the Detection and Removal of Wastewater Pollutants* .pp. 161-222. Elsevier.

Salam MA. , Removal of heavy metal ions from aqueous solutions with multi-walled carbon nanotubes: kinetic and thermodynamic studies. Int J Environ Sci Technol, 2013, vol. 10, pp.677–688.

Saputra, O. A., Rachma, A. H., & Handayani, D. S. Adsorption of remazol brilliant blue R using amino-functionalized organosilane in aqueous solution. Indones. J. Chem, 2017 vol. 17(3), 343-350.

Saratale, R.G., Saratale, G.D., Kalyani, D.C., Chang, J.S. and Govindwar, S.P., Enhanced decolorization and biodecolorisation of textile azo dye Scarlet R by using developed microbial consortium-GR.*,* Bioresour. Technol., 2009, vol. 100, pp.2493-2500.

Sari, I. P., & Simarani, K. Decolorization of selected azo dye by Lysinibacillus fusiformis W1B6: Biodegradation optimization, isotherm, and kinetic study biosorption mechanism. Adsorp Sci Technol. ,2019. vol. 37(5-6), pp.492-508

Srinivasaraghavan, R., Seshadri, S., Gnanasambandan, T. and Srinivasan, G., Experimental and Theoretical Spectroscopic Analysis on N-((1-(phenyl-sulfonyl)-1H-indol-3-Yl) methyl) acetamide. Pharmaceut Anal Acta S., 2017, vol.8, pp.2.

Syafiuddin, A., & Fulazzaky, M. A. Decolorization kinetics and mass transfer mechanisms of Remazol Brilliant Blue R dye mediated by different fungi. Biotechnol. Rep. 2021. vol. 29, e00573.

Thakur VK, Thakur MK, Gupta RK. Graft copolymers of natural fibers for green composites. Carbohydr. Polym., 2014, vol.104, pp.87-93.

Velayutham, K., Madhava, A.K., Pushparaj, M., Thanarasu, A., Devaraj, T., Periyasamy, K. and Subramanian, S., Biodegradation of Remazol Brilliant Blue R using isolated bacterial culture (*Staphylococcus* sp. K2204). Environ. Technol., 2018 vol. 39, pp.2900-2907.

Abd El-Rahim, W.M., El-Ardy, O.A.M. and Mohammad, F.H.,. The effect of pH on bioremediation potential for the removal of direct violet textile dye by *Aspergillus niger*. Desalination, 2009 vol. 249(3), pp.1206-1211.

Wu, Y. Chapter 16 - The Removal of Methyl Orange by Periphytic Biofilms: Equilibrium and Kinetic Modeling in Periphyton: functions and application in environmental remediation. 2016 Elsevier.

Chapter 5
Conclusion

The strains *Stenotrophomonas koreensis* and *Bacillus rigiliprofundi* isolated from textile effluents and identified by 16S rDNA sequencing were able to decolorise the toxic industrial dyes Malachite green and Remazol Brilliant Blue by degradation and adsorption respectively.

The strain *Stenotrophomonas koreensis* showed upto 98.78% decolorisation of malachite green under optimised conditions within one hour of inoculation. Decolorisation was caused as a result of degradation of the dye, as confirmed by UV-Vis and FTIR spectrophotometry and TLC and HPLC. *S. koreensis* demonstrated excellent decolorisation (95% in 1hr) of malachite green in plain distilled water in presence of only one nitrogen supplement, peptone or soymeal extract (1g/L), This can be undoubtedly described as one of the fastest decolorisations reported till date. It remains active in presence of some heavy metals and is also capable to decolorise methyl orange, which is an azo dye, obviously having a completely different structure and chemical nature from the triphenylmethane dye malachite green. *S.koreensis* can be immobilised into re-usable PVA-sodium alginate beads to facilitate easier handling. The enzymes responsible for the degradation of malachite green in *S.koreensis* were tyrosinase, MG-reductase and NADH-DCIP reductase. The degradation products were subjected to toxicological testing (according to the OECD guidelines for testing of chemicals) with a wide variety of organisms, ranging from the prokaryotic unicellular bacteria to higher animals like mice and also in human cell lines. From the elaborate ecotoxicological studies performed with the representative organisms of the key levels of the ecosystem, it can be ascertained that the final products of malachite green decolorisation by this strain was significantly safe for release in the environment. Hence, overall, *Stenotrophomonas koreensis* is an extremely promising bioresource which can be utilized to bioremediate malachite green efficiently.

Bacillus rigiliprofiundi was able to bioadsorb more than 80% of the toxic dye Remazol Brilliant blue. No chemical treatment or complex procedure needed to be followed for the adsorptive removal of the dye, however, optimisation of some physical parameters could lead to better results.

In this quest, it was established that bacteria can be an ideal solution for combating the dye pollution globally, replacing the expensive, and hazardous conventional treatment procedures.

LIST OF PUBLICATIONS

	A. FULL PAPERS
2022	**Biswas, S.**, Banerjee, N, and Basak, P., (2022) 'Adverse Effects of the Toxic Industrial Dye Malachite Green on the Antioxidant and Antimicrobial Properties of *Allium cepa*', ***Plant Science Today***. **Horizon e-Publishing** Group *https://doi.org/10.14719/pst.1339*
2021	**Biswas, S.** and Basak, P., (2021) 'Biosorption of the Industrial Dye Remazol Brilliant Blue R by *Bacillus rigiliprofundi*.' ***Microbiology,*** **Springer** *90*(6), pp.816-828.
	Basak, P., Adhikary, T., Das, P., Shee, M., Dutta, T., **Biswas, S.**, Paul, S. & Manna, S., (2021) 'Cellulases in paper and pulp, brewing and food industries: Principles associated with its diverse applications', ***Current Status and Future Scope of Microbial Cellulases,*** **Elsevier,** (pp. 275-293). *https://doi.org/10.1016/B978-0-12-821882-2.00003-X n*
2019	Guha Ray, P., **Biswas, S.**, Roy, T., Ghosh, S., Majumder, D., Basak, P., and Dhara, S. (2019). 'Sonication assisted Hierarchical decoration of Ag-NP on Zinc Oxide Nanoflowers impregnated Eggshell Membrane: Evaluation of Antibacterial Activity and in vitro Cytocompatibility', ***ACS Sustainable Chemistry & Engineering*** ISSN: 2168-0485 *doi: 10.1021/10.1021/acssuschemeng.9b01185*
	Biswas S., and Basak, P., (2019) 'Biodecolourization of Azo Dyes by Microbes', ***Textile Industry and Research in 2030: Challenges and Opportunities'.*** Publisher: **Shree Vaishnav Institute of Textile Technology.** ISBN : 978-93-5351-406-8
	Biswas S., Basak, P., Jasu, A., (2019) 'Exploring different sources for Malachite decolorising bacteria**'** ***Journal of the Indian Chemical Society***, **Elsevier,** 96 (4), ISSN: 0019-4522
	Basak, P., Adhikary, T., Das, **Biswas, S.,** (2018) 'Phytochemical Analysis and comparative study of Antibacterial Effect of Turmeric Extracts Using Different Solvents',*IOP Conf. Series: Materials Science and Engineering* 410ISSN 17578981 *doi:10.1088/1757-899X/410/1/012018*
	Basak, P., Paul, S., **Biswas, S.,** Jasu, A., Majumder, R., (2018) 'Potential

2018	Therapeutic Activity of Bio-Synthesized Silver Nanoparticles as Anticancer and Antimicrobial Agent', *IOP Conf. Series: Materials Science and Engineering,* 410ISSN 17578981 *doi:10.1088/1757-899X/410/1/012020*
	Basak.P., Das, P., **Biswas, S.** , Biswas, N. C., Mahapatra, G.C., (2018) 'Green Synthesis and Characterization of Gelatin-PVA Silver Nanocomposite Films for Improved Antimicrobial Activity' , *IOP Conf. Series: Materials Science and Engineering* 410ISSN 17578981 *doi:10.1088/1757-899X/410/1/012019*
	Biswas, S., Bhattacharjee, A., Basak. P., (2018) 'Effect of Tannery Effluent on Germination and Early Seedling Growth of *Oryza sativa* var. IET 4786' *Utilisation and Management of Bioresources*, **Springer** ISBN 978-981-10-5349-8 *doi: 10.1007/978-981-10-5349-8_23*

B. INTERNATIONAL / NATIONAL CONFERENCE ABSTRACTS	
2021	Ghosal, D., Das, P., Adhikary, P., Manna, S., Roy, A., Mukherjee, A., **Biswas, S.**, Basak, P., (2021) 'Synthesis And Characterization of Poly Ester Urethane Film For Biomedical Application', *Bioactive Glass, Ceramics & Composites in healthcare: Current Technological Trends*, *2021* Organized by **Bioceramics & Coating Division, CSIR-Central Glass & Ceramic Research Institute, Kolkata, India** 27.05.2012 to 28.05.2021
2020	Manna, S., Das, P., **Biswas, S.**, Paul, S., Das, P., and Basak.P., (2020) 'Synthesis of Novel Graphene Oxide Based Nanocomposites for Multiple Pollutants Separation', *2nd International conference on Advances in Bioprocess Engineering and Technology* **Organized by Heritage Institute of Technology, Kolkata, India** 20.01.2020 to 22.01.2020
2019	Santra, T., **Biswas, S.,** and Basak,P., (2019) 'A Cytotoxicity assay of *Aegle marmelos* aqueous leaf extract and it's Green-Synthesized Silver Nanocomposites (AgNCs) on Human PBMCs and MCF-7 cell line; along with the Synthesis and Characterization of PVA-Gelatin based composite hydrogel membrane as a potential delivery system for the synthesized AgNCs in vivo', *National Conference on Recent Developments in Nanoscience and Nanotechnology*, **Jadavpur University, Kolkata, India** 29-01-2019 to 31-01-2019

2018	**Biswas, S.**, Kahali,T., and Basak, P., (2018) 'Investigating the potential of bacteria isolated from different sources for the biodegradation of Remazol Brilliant Blue Present in Industrial Waste', *National Conference On Innovative Structural Materials* **, Bhubaneswar, Odisha, India** 24-12-2018 to 25-12-2018
	Banerjee, N., Basak, P., Hossain,C.M.., **Biswas, S.,** (2018) 'Analysis of Phytochemical Properties of Ethanolic Extract of *Allium cepa* L. and Evaluation of its Antioxidant and Antibacterial Effects', *2nd International Conference on Biotechnology and Biological Sciences*, **University of Engineering & Management, Kolkata, India** 27-07-2018 to 28-07-2018
2017	**Biswas, S.**, Bhattacharjee, A., and Basak, P., (2017) 'Effect of Remazol Brilliant Blue Dye on Germination and Early Seedling Growth of *Oryza sativa* var. IET 4786' Book of Papers for *International Conference on Textile and Clothing: Present and Future Trends*, ISBN: 978-93-84923-15-0 **.organized by Centre for Research in Nanoscience & Nanotechnology at the University of Calcutta, Kolkata, India** 03-01-2017 to 05-01-2017
2016	Guha Ray, P., **Biswas, S.**, Basak, P., Roy, S., (2016) 'Surface Modification of Eggshell Membrane for Immobilization and Detection of Oligonucleotide', *International Conference on Functional Nanomaterials 2016*, **Indian Institute of Engineering Science & Technology, Shibpur, Howrah, India** 28-09-2016 to 29-09-2016

LIST OF FIGURES

LIST OF TABLES

Report

9%

SIMILARITY INDEX

PRIMARY SOURCES

1	www.hindawi.com Internet	110 words — < 1%
2	hdl.handle.net Internet	75 words — < 1%
3	shodhganga.inflibnet.ac.in Internet	72 words — < 1%
4	pubs.rsc.org Internet	71 words — < 1%
5	Wicaksana, F.. "Microfiltration of algae (Chlorella sorokiniana): Critical flux, fouling and transmission", Journal of Membrane Science, 20120101 Crossref	65 words — < 1%
6	documents.mx Internet	65 words — < 1%
7	Joydeep Dutta, Aijaz Ahmad, Joginder Singh. " Study of industrial effluents induced genotoxicity on L ", Caryologia, 2018 Crossref	62 words — < 1%
8	mltgeeks.com Internet	61 words — < 1%

9	eprints.soton.ac.uk Internet	56 words — < 1%
10	cyberleninka.org Internet	53 words — < 1%
11	aquaticbiosystems.biomedcentral.com Internet	48 words — < 1%
12	J. P. Jadhav, S. P. Govindwar. "Biotransformation of malachite green bySaccharomyces cerevisiae MTCC 463", Yeast, 2006 Crossref	47 words — < 1%
13	pubs.sciepub.com Internet	46 words — < 1%
14	daneshyari.com Internet	44 words — < 1%
15	repositorio.unesp.br Internet	40 words — < 1%
16	www.iq.ufrgs.br Internet	38 words — < 1%
17	www.ijcmas.com Internet	36 words — < 1%
18	eur-lex.europa.eu Internet	34 words — < 1%
19	www.thaimoodle.net Internet	34 words — < 1%
20	www.scribd.com Internet	32 words — < 1%

21 D. C. Kalyani, A. A. Telke, S. N. Surwase, S. B. Jadhav, J.-K. Lee, J. P. Jadhav. "Effectual decolorization and detoxification of triphenylmethane dye malachite green (MG) by Pseudomonas aeruginosa NCIM 2074 and its enzyme system", Clean Technologies and Environmental Policy, 2012
Crossref

31 words — < 1%

22 "Advances in Bioprocess Engineering and Technology", Springer Science and Business Media LLC, 2021
Crossref

30 words — < 1%

23 assets.researchsquare.com
Internet

30 words — < 1%

24 krishikosh.egranth.ac.in
Internet

29 words — < 1%

25 www.ideals.illinois.edu
Internet

28 words — < 1%

26 Tamer Akar, Sema Celik. "Efficient biosorption of a reactive dye from contaminated media by Neurospora sitophila cells-Zea mays silk tissue biomass system", Journal of Chemical Technology & Biotechnology, 2011
Crossref

27 words — < 1%

27 acta.chem-soc.si
Internet

27 words — < 1%

28 horizonepublishing.com
Internet

27 words — < 1%

29 bnrc.springeropen.com
Internet

26 words — < 1%

30 dns2.asia.edu.tw
Internet

26 words — < 1%

31 www.slideshare.net
Internet

26 words — < 1%

32 www.chemmethod.com
Internet

25 words — < 1%

33 Abdallah Reghioua, Djamel Barkat, Ali H. Jawad, Ahmed Saud Abdulhameed, Mohammad Rizwan Khan. "Synthesis of Schiff's base magnetic crosslinked chitosan-glyoxal/ZnO/Fe3O4 nanoparticles for enhanced adsorption of organic dye: Modeling and mechanism study", Sustainable Chemistry and Pharmacy, 2021
Crossref

24 words — < 1%

34 ethesis.nitrkl.ac.in
Internet

24 words — < 1%

35 Said Galai. "A New Stenotrophomonas maltophilia Strain Producing Laccase. Use in Decolorization of Synthetics Dyes", Applied Biochemistry and Biotechnology, 10/17/2008
Crossref

23 words — < 1%

36 aem.asm.org
Internet

23 words — < 1%

37 dspace.stir.ac.uk
Internet

23 words — < 1%

38 repository.up.ac.za
Internet

22 words — < 1%

39 www.jaduniv.edu.in
Internet

22 words — < 1%

40 Sushama S Gomare, Ganesh K Parshetti, Sanjay P Govindwar. "Biodegradation of Malachite Green by <I>Brevibacillus laterosporus</I> MTCC 2298", Water Environment Research, 2009
Crossref

21 words — < 1%

41 Yogita Prabhakar, Anshu Gupta, Anubha Kaushik. "Using indigenous bacterial isolate Nesterenkonia lacusekhoensis for removal of azo dyes: A low-cost ecofriendly approach for bioremediation of textile wastewaters", Environment, Development and Sustainability, 2021
Crossref

21 words — < 1%

42 www.1717mc.com
Internet

21 words — < 1%

43 www.frontiersin.org
Internet

21 words — < 1%

44 epdf.pub
Internet

20 words — < 1%

45 gyan.iitg.ac.in
Internet

20 words — < 1%

46 repository.tudelft.nl
Internet

20 words — < 1%

47 www.degruyter.com
Internet

20 words — < 1%

48 Balvindra Singh, Neelima Garg, Priti Mathur, Supriya Vaish, Sanjay Kumar. "Microbial production of multienzyme preparation from mosambi peel using Trichoderma asperellum", Research Square Platform LLC, 2022
Crossref Posted Content

18 words — < 1%

49 Jadhav, J.P.. "Decolourization of azo dye methyl red by Saccharomyces cerevisiae MTCC 463", Chemosphere, 200706
Crossref

50 cdr.lib.unc.edu
Internet

51 tel.archives-ouvertes.fr
Internet

52 Shilpa Gupte, Haresh Keharia, Akshaya Gupte. " Toxicity analysis of azo Red BS and Methyl Red dye solutions on earthworm ( ), micro-organisms, and plants ", Desalination and Water Treatment, 2013
Crossref

53 www.jesc.ac.cn
Internet

54 "Methods in Actinobacteriology", Springer Science and Business Media LLC, 2022
Crossref

55 Lamia Ayed. "Biodegradation of triphenylmethane dye Malachite Green by Sphingomonas paucimobilis", World Journal of Microbiology and Biotechnology, 04/2009
Crossref

56 sustainenvironres.biomedcentral.com
Internet

57 zfin.org
Internet

18 words — < 1%

18 words — < 1%

18 words — < 1%

17 words — < 1%

17 words — < 1%

16 words — < 1%

16 words — < 1%

16 words — < 1%

16 words — < 1%

58 Saurabh Mishra, Abhijit Maiti. "Chapter 6 Biological Methodologies for Treatment of Textile Wastewater", Springer Science and Business Media LLC, 2020
Crossref
15 words — < 1%

59 coek.info
Internet
15 words — < 1%

60 Siqi Liu, Xiaolin Xu, Yanshun Kang, Yingtian Xiao, Huan Liu. " Degradation and detoxification of azo dyes with recombinant ligninolytic enzymes from sp. with secretory overexpression in ", Royal Society Open Science, 2020
Crossref
14 words — < 1%

61 edoc.site
Internet
14 words — < 1%

62 ijrdo.org
Internet
14 words — < 1%

63 journals.sagepub.com
Internet
14 words — < 1%

64 nopr.niscair.res.in
Internet
14 words — < 1%

65 royalsocietypublishing.org
Internet
14 words — < 1%

66 worldwidescience.org
Internet
14 words — < 1%

67 www.jairjp.com
Internet
14 words — < 1%

68 www.spandidos-publications.com
Internet
14 words — < 1%

69 www.ukm.my
Internet
14 words — < 1%

70 Jadhav, J.P.. "Evaluation of the efficacy of a bacterial consortium for the removal of color, reduction of heavy metals, and toxicity from textile dye effluent", Bioresource Technology, 201001
Crossref
13 words — < 1%

71 Li Gan, Fengfei Zhou, Gary Owens, Zuliang Chen. "Burkholderia cepacia immobilized on eucalyptus leaves used to simultaneously remove malachite green (MG) and Cr(VI)", Colloids and Surfaces B: Biointerfaces, 2018
Crossref
13 words — < 1%

72 Qayyum Husain. "Peroxidases as a Potential Tool for the Decolorization and Removal of Synthetic Dyes from Polluted Water", Environmental Protection Strategies for Sustainable Development, 2012
Crossref
13 words — < 1%

73 Research-Repository.griffith.edu.au
Internet
13 words — < 1%

74 Sabarathinam Shanmugam, Priyadharshini Ulaganathan, Krishnaswamy Swaminathan, Subramaniam Sadhasivam, Yi-Rui Wu. "Enhanced biodegradation and detoxification of malachite green by Trichoderma asperellum laccase: Degradation pathway and product analysis", International Biodeterioration & Biodegradation, 2017
Crossref
13 words — < 1%

75 core.ac.uk
Internet
13 words — < 1%

digital.library.txstate.edu

76   Internet

13 words — < 1%

77   imagesurfer.cs.unc.edu
Internet

13 words — < 1%

78   ir.uiowa.edu
Internet

13 words — < 1%

79   mdpi.com
Internet

13 words — < 1%

80   www.freepatentsonline.com
Internet

13 words — < 1%

81   www.medrxiv.org
Internet

13 words — < 1%

82   www.sigmaaldrich.com
Internet

13 words — < 1%

83   Jyoti Tolia, Mousumi Chakraborty, Z. Murthy. "Photocatalytic degradation of malachite green dye using doped and undoped ZnS nanoparticles", Polish Journal of Chemical Technology, 2012
Crossref

12 words — < 1%

84   Purbasha Saha, Sonal Madliya, Anmol Khare, Ikshita Subudhi, Kokati Venkata Bhaskara Rao. " Enzymatic Biodegradation, Kinetic study, and Detoxification of Reactive Red-195 by Isolated from Marine Sediments of Andaman Sea, India ", Environmental Technology, 2022
Crossref

12 words — < 1%

85   Swati Sambita Mohanty, Arvind Kumar. " Response surface methodology mediated

12 words — < 1%

optimization of Indanthrene Blue RS by a novel isolated bacterial strain TS8 ", Water Environment Research, 2019
Crossref

86 Tessa Acar, Sandra Moreau, Olivier Coen, Frédéric De Meyer, Olivier Leroux, Marine Beaumel, Paul Wilkin, Aurélien Carlier. "Distinct within-host bacterial populations ensure function, colonization and transmission in leaf symbiosis", Cold Spring Harbor Laboratory, 2021   12 words — < 1%
Crossref Posted Content

87 Zelal Isik, Mohammed Saleh, Zeynep Bilici, Nadir Dizge. "Remazol brilliant blue R (RBBR) dye and phosphate adsorption by calcium alginate beads modified with polyethyleneimine", Water Environment Research, 2021   12 words — < 1%
Crossref

88 opus.bibliothek.uni-wuerzburg.de   12 words — < 1%
Internet

89 publikationen.uni-tuebingen.de   12 words — < 1%
Internet

90 researchrepository.murdoch.edu.au   12 words — < 1%
Internet

91 studentsrepo.um.edu.my   12 words — < 1%
Internet

92 www.hrpub.org   12 words — < 1%
Internet

93 "Microbial Rejuvenation of Polluted Environment", Springer Science and Business Media LLC, 2021   11 words — < 1%
Crossref

94 Anuprita D. Watharkar, Rahul V. Khandare, Apurva A. Kamble, Asma Y. Mulla, Sanjay P. Govindwar, Jyoti P. Jadhav. "Phytoremediation potential of Petunia grandiflora Juss., an ornamental plant to degrade a disperse, disulfonated triphenylmethane textile dye Brilliant Blue G", Environmental Science and Pollution Research, 2012
Crossref

11 words — < 1%

95 C. Femina Carolin, P. Senthil Kumar, G. Janet Joshiba. "Sustainable approach to decolourize methyl orange dye from aqueous solution using novel bacterial strain and its metabolites characterization", Clean Technologies and Environmental Policy, 2020
Crossref

11 words — < 1%

96 Lin-Na Du, Sheng Wang, Gang Li, Bing Wang, Xiao-Ming Jia, Yu-Hua Zhao, Yun-Long Chen. "Biodegradation of malachite green by Pseudomonas sp. strain DY1 under aerobic condition: characteristics, degradation products, enzyme analysis and phytotoxicity", Ecotoxicology, 2011
Crossref

11 words — < 1%

97 Olugbenga Solomon Bello, Mohd Azmier Ahmad. "Response Surface Modeling and Optimization of Remazol Brilliant Blue Reactive Dye Removal Using Periwinkle Shell-Based Activated Carbon", Separation Science and Technology, 2011
Crossref

11 words — < 1%

98 S.S. Gomare. "*Brevibacillus laterosporus* MTCC 2298: a potential azo dye degrader", Journal of Applied Microbiology, 03/2009
Crossref

11 words — < 1%

99 Sabarathinam Shanmugam, Swaminathan Krishnaswamy, Rejeeth Chandrababu,

11 words — < 1%

Udhayakumar Veerabagu et al. "Optimal immobilization of Trichoderma asperellum laccase on polymer coated Fe3O4@SiO2 nanoparticles for enhanced biohydrogen production from delignified lignocellulosic biomass", Fuel, 2020
Crossref

100   Srivastava, S.. "Toxicological effects of malachite green", Aquatic Toxicology, 20040225   11 words — < 1%
Crossref

101   Swarnkumar Reddy, Jabez W. Osborne. " Biodegradation and biosorption of Reactive Red 120 dye by immobilized Kinetic and toxicity study ", Water Environment Research, 2020   11 words — < 1%
Crossref

102   Venkatesh Chaturvedi, Khushboo Bhange, Renu Bhatt, Pradeep Verma. "Biodetoxification of high amounts of malachite green by a multifunctional strain of Pseudomonas mendocina and its ability to metabolize dye adsorbed chicken feathers", Journal of Environmental Chemical Engineering, 2013   11 words — < 1%
Crossref

103   dokumen.pub
Internet   11 words — < 1%

104   hl-128-171-57-22.library.manoa.hawaii.edu
Internet   11 words — < 1%

105   ijsr.in
Internet   11 words — < 1%

106   ir.library.ui.edu.ng:8080
Internet   11 words — < 1%

107   iwaponline.com
Internet

119 "Recent Trends in Mycological Research", Springer Science and Business Media LLC, 2021
Crossref

10 words — < 1%

120 Agnieszka Agas, Arun Reddy Ravula, Xiaotang Ma, Yiming Cheng, Kevin D. Belfield, James Haorah. "Hemolytic Iron Regulation in Traumatic Brain Injury and Alcohol Use", Research Square Platform LLC, 2021
Crossref Posted Content

10 words — < 1%

121 Amar A. Telke, Seon-Won Kim, Sanjay P. Govindwar. "Significant reduction in toxicity, BOD, and COD of textile dyes and textile industry effluent by a novel bacterium Pseudomonas sp. LBC1", Folia Microbiologica, 2012
Crossref

10 words — < 1%

122 Anna Jasińska, Sylwia Różalska, Przemysław Bernat, Katarzyna Paraszkiewicz, Jerzy Długoński. "Malachite green decolorization by non-basidiomycete filamentous fungi of Penicillium pinophilum and Myrothecium roridum", International Biodeterioration & Biodegradation, 2012
Crossref

10 words — < 1%

123 Bobo Wang, Jing Lu, Junfang Zheng, Zhisheng Yu. "iTRAQ-facilitated proteomic analysis of Bacillus cereus via degradation of malachite green", Journal of Microbiology, 2021
Crossref

10 words — < 1%

124 Chimezie Jason Ogugbue, Thomas Sawidis, Nathaniel A. Oranusi. "Bioremoval of chemically different synthetic dyes by Aeromonas hydrophila in simulated wastewater containing dyeing auxiliaries", Annals of Microbiology, 2011
Crossref

10 words — < 1%

125 Craita Maria Rosu, Mihaela Avadanei, Daniela Gherghel, Marius Mihasan et al. "Biodegradation and Detoxification Efficiency of Azo-Dye Reactive Orange 16 by Pichia kudriavzevii CR-Y103", Water, Air, & Soil Pollution, 2017
Crossref

10 words — < 1%

126 Deborah Gnana Selvam Alexander, A. Joseph Thatheyus. "Fungal bioremediation of toxic textile dye effluents", Elsevier BV, 2021
Crossref

10 words — < 1%

127 Gajanan Ghodake, Umesh Jadhav, Dhawal Tamboli, Anuradha Kagalkar, Sanjay Govindwar. "Decolorization of Textile Dyes and Degradation of Mono-Azo Dye Amaranth by Acinetobacter calcoaceticus NCIM 2890", Indian Journal of Microbiology, 2011
Crossref

10 words — < 1%

128 Lin-Na Du, Gang Li, Yu-Hua Zhao, He-Kun Xu, Yang Wang, Ying Zhou, Liang Wang. "Efficient metabolism of the azo dye methyl orange by Aeromonas sp. strain DH-6: Characteristics and partial mechanism", International Biodeterioration & Biodegradation, 2015
Crossref

10 words — < 1%

129 M. Danouche, H. El Arroussi, W. Bahafid, N. El Ghachtouli. "An overview of the biosorption mechanism for the bioremediation of synthetic dyes using yeast cells", Environmental Technology Reviews, 2021
Crossref

10 words — < 1%

130 Navneet Joshi, Uma Bhardwaj, Shellina Khan, Hafiz M.N. Iqbal. "Synergistic role of bacterial consortium to biodegrade toxic dyes containing wastewater and its simultaneous reuse as an added value", Chemosphere, 2021
Crossref

10 words — < 1%

131 S.U. Jadhav, S.D. Kalme, S.P. Govindwar. "Biodegradation of Methyl red by Galactomyces geotrichum MTCC 1360", International Biodeterioration & Biodegradation, 2008
Crossref

10 words — < 1%

132 Sujit Roy, Lalit Mohan Kundu, Gobinda Chandra Roy, Manabendu Barmana et al. "Deciphering colchicine like actions of clerodin in terms of microtubule destabilization based mitotic abnormalities, G2/M-phase arrest, and plant polyploidy", Cold Spring Harbor Laboratory, 2020
Crossref Posted Content

10 words — < 1%

133 Umesh U. Jadhav. "Decolorization of Direct Blue GLL with enhanced lignin peroxidase enzyme production in <i>Comamonas</i> sp UVS", Journal of Chemical Technology & Biotechnology, 01/2009
Crossref

10 words — < 1%

134 Xueting Yang, Jinzhao Zheng, Yongming Lu, Rong Jia. "Degradation and detoxification of the triphenylmethane dye malachite green catalyzed by crude manganese peroxidase from Irpex lacteus F17", Environmental Science and Pollution Research, 2016
Crossref

10 words — < 1%

135 apps.who.int
Internet

10 words — < 1%

136 baadalsg.inflibnet.ac.in
Internet

10 words — < 1%

137 bbrc.in
Internet

10 words — < 1%

138 eprints.fbme.utm.my
Internet

10 words — < 1%